

**ROLE OF FUNCTIONAL MAGNETIC RESONANCE IMAGING (fMRI),
DIFFUSION TENSOR IMAGING (DTI) AND VOXEL BASED MORPHOMETRY
(VBM) FOR PRESURGICAL LATERALIZATION OF LANGUAGE IN PATIENTS
WITH EPILEPSY**

A THESIS PRESENTED BY

JIJA S JAMES

TO

SREE CHITRA TIRUNAL INSTITUTE FOR
MEDICAL SCIENCES AND TECHNOLOGY (SCTIMST)
THIRUVANANTHAPURAM

IN PARTIAL FULFILMENT OF THE REQUIREMENTS

FOR THE AWARD OF

DOCTOR OF PHILOSOPHY

2016

DECLARATION

I, **Jija S James**, hereby declare that I had personally carried out the work depicted in the thesis entitled “**Role of functional magnetic resonance imaging (fMRI), diffusion tensor imaging (DTI) and voxel based morphometry (VBM) for presurgical lateralization of language in patients with epilepsy**”. No part of the thesis has been submitted for award of any other degree or diploma prior to this date.

Signature: 

Date: 29/04/2016

Dr. C.KESAVADAS, MD

Professor

Imaging Science and Interventional Radiology

Department of Imaging Science and Interventional Radiology

Sree Chitra Tirunal Institute for Medical Sciences & Technology,

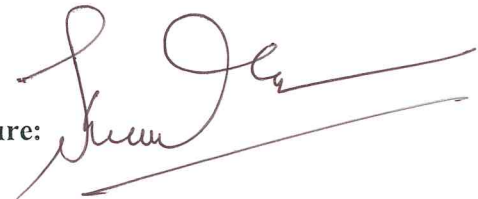
Medical College P.O, Trivandrum,

Kerala, India- 695 011

CERTIFICATE

This is to certify that **Mrs. Jija S James**, in the Department of Imaging Science and Interventional Radiology of this institute, has fulfilled the requirements prescribed for the Ph.D degree of the Sree Chitra Tirunal Institute for Medical Sciences and Technology, Trivandrum, India. The thesis entitled “**Role of functional Magnetic Resonance Imaging (fMRI), Diffusion Tensor Imaging (DTI) and Voxel Based Morphometry (VBM) for presurgical lateralization of language in patients with epilepsy**” was carried out under my direct supervision. No part of thesis was submitted for the award of any degree or diploma prior to this date. Clearance was obtained from the Institutional Ethics Committee for carrying out the study.

Signature:



Date:

29/4/2016

The thesis entitled

**Role of functional Magnetic Resonance Imaging (fMRI),
Diffusion Tensor Imaging (DTI) and Voxel Based
Morphometry (VBM) for presurgical lateralization of language
in patients with epilepsy**

Submitted by


J I J A S J A M E S

for the degree of
Doctor of Philosophy
of

SREE CHITRA TIRUNAL INSTITUTE
FOR

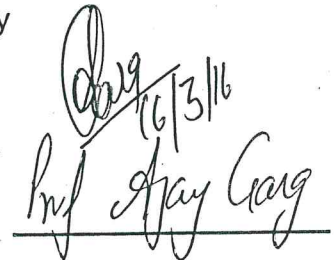
MEDICAL SCIENCES AND TECHNOLOGY, TRIVANDRUM
Thiruvananthapuram

Is evaluated and approved by



[Handwritten signature]
Dr. C. Kesavadas

Name of guide



[Handwritten signature]
16/3/16
Prof. Jay Gang

Name of thesis examiner

ACKNOWLEDGEMENTS

It's my immense pleasure to thank all those people who made this thesis possible.

I am greatly indebted to my Ph.D. supervisor **Dr. C. Kesavadas**, Professor of Radiology, SCTIMST, for his constant encouragement and enthusiastic guidance for the entire duration of my study. I am fortunate to have had him as my mentor for it was he who taught me the scientific experimentation.

I express my sincere gratitude to my Doctoral Advisory Committee members, **Dr. Bejoy Thomas**, Additional Professor, Department of Imaging Science and Interventional Radiology, SCTIMST, **Dr. Sanjeev Thomas**, Professor, Department of Neurology, SCTIMST, **Dr. P.S Mathuranath**, Additional Professor of Neurology, NIMHANS, Bangalore for their valuable suggestions and constant encouragement.

I express my special thanks to **Dr Ashalatha Radhakrishnan**, Associate professor, Department of Neurology for her great contributions, immense support and for helping me to recruit the study subjects.

I am thankful to all Radiographers and DAMITS of the Dept. of Imaging Science and Interventional Radiology of SCTIMST for helping me to collect the MRI data at any time all throughout the duration of my research.

I express my sincere gratitude to **KSCSTE (Kerala State Council for Science, Technology and Environment)** for granting me the financial assistance to conduct this research study.

Special thanks to my dearest colleagues, Dr.Ruma Madhu Sreedhar, Smitha K.A, Sheela Nair, Tinu Varghese, Anuvida Chandran, Rajesh P.G, Mini Madhusoodanan ,Arun K.M, Diljith Singh, Subramaniom and Anu Sundar for their timely help and good company.

Thank you my dear parents for unwavering love and supports! Special thanks my sister, Jeena S James and brother Reejan Soman, for their encouragements and take caring.

Finally, thanks to my wonderful husband, Rejimon Soman, for his valuable care, support and suggestions.

JJA S JAMES

TABLE OF CONTENTS

List of Figures.....	xi
List of Tables.....	xv
List of Abbreviations.....	xvi
SYNOPSIS.....	xviii
INTRODUCTION.....	1

CHAPTER 1

1. INTRODUCTION TO NEUROIMAGING TECHNIQUES.....	8
1.1 functional Magnetic Resonance Imaging (fMRI).....	8
1.1.1 Introduction	
1.1.2 The neurophysiology of BOLD signal	
1.1.3 fMRI: Brief history	
1.1.4 fMRI: Temporal and spatial characteristics	
1.1.5 fMRI: Scanning Methodologies	
1.1.6 fMRI Paradigm Design	
1.1.7 BOLD fMRI- limitations and considerations	
1.2 Diffusion Tensor Imaging (DTI) and Tractography.....	26
1.2.1 Introduction	
1.2.2 Diffusion of water molecules	
1.2.3 Anisotropic Diffusion in Biological Tissues	
1.2.4 Diffusion measurement using Nuclear Magnetic Resonance (NMR)	
1.2.5 The diffusion tensor	
1.2.6 Quantification and Visualization of Tensor-derived Parameters	
1.2.7 White matter fibre Tractography	
1.2.8 DTI- limitations and technical considerations	
1.3 Voxel Based Morphometry (VBM).....	44
1.3.1 Introduction	
1.3.2 Steps in VBM analysis	

- 1.3.2.1 Spatial Normalization
- 1.3.2.2 Segmentation
- 1.3.2.3 Smoothing
- 1.3.2.4 Statistical Analysis
- 1.3.3 VBM limitations and technical considerations

CHAPTER 2

2 LITERATURE REVIEW.....51

- 2.1 Introduction
 - 2.1.1 Epilepsy and Epilepsy Surgery
 - 2.1.2 Presurgical evaluation in epilepsy
- 2.2 Mesial Temporal Sclerosis (MTS)
 - 2.2.1 Anterior Temporal Lobe Resection (ATLR)
 - 2.2.2 Techniques used for Temporal Lobe Resection (TLR)
 - 2.2.3 Language lateralization in TLE
 - 2.2.4 Neuroimaging in TLE
 - 2.2.5 Advanced Neuroimaging techniques for presurgical evaluation in TLE
 - 2.2.5.1 fMRI
 - 2.2.5.2 Diffusion Tensor Imaging (DTI) and Tractography
 - 2.2.5.3 Structural neuroimaging based VBM analysis

CHAPTER 3

3 DESIGN OF THE STUDY.....76

- 3.1 Materials and Methods
 - 3.1.1 Subject details
 - 3.1.2 Inclusion criteria
 - 3.1.2.1 Patients
 - 3.1.2.2 Healthy controls
 - 3.1.3 Exclusion criteria
 - 3.1.3.1 Patients
 - 3.1.3.2 Healthy controls
 - 3.1.4 Ethics Approval
 - 3.1.5 Data Acquisition

3.1.6 fMRI Language paradigms	
3.1.6.1 Visual Verb Generation task	
3.1.6.2 Syntactic task	
3.1.6.3 Semantic task	
3.1.6.4 Word pair task	
3.1.7 Data Analysis	
3.1.7.1 fMRI Data Analysis	
3.1.7.1.1 Pre-processing of fMRI data-preparing data for analysis	
3.1.7.1.1.1 Realignment	
3.1.7.1.1.2 Co-registration – within subject registration	
3.1.7.1.1.3 Normalization – between subject registration	
3.1.7.1.1.4 Smoothing	
3.1.7.1.1.5 Statistical Analysis – using General Linear Model (GLM)	
3.1.7.1.1.6 Inference and Interpretation of results	
3.1.7.2 Diffusion fiber Tractography for white matter tract reconstruction	
3.1.7.2.1 Dorsal Language pathways	
3.1.7.2.1.1 Superior Longitudinal Fasciculus (SLF) / Arcuate Fasciculus (ArcF)	
3.1.7.2.2 Ventral Language Pathways	
3.1.7.2.2.1 Uncinate Fasciculus (UF)	
3.1.7.2.2.2 Inferior Longitudinal fasciculus (ILF)	
3.1.7.2.2.3 Inferior fronto-occipito Fasciculus (IFOF)	
3.1.7.3 VBM based volumetric analysis	
3.5 Statistical Analysis	98

CHAPTER 4

4 RESULTS	100
4.1 Major findings of fMRI experiment	
4.1.1 Control subjects	
4.1.2 TLE subjects	
4.1.3 Hemodynamic response functions in controls and TLE	
4.1.4 Variability in language localization by measuring laterality Indices	
4.2 Reconstruction of white matter language pathways using Deterministic Tractography.	

- 4.2.1 Tract specific measurements in controls and TLE subjects
- 4.2.2 fMRI- DTI correlation for language lateralization
- 4.3 VBM based volumetric measurements in controls and TLE
- 4.3.1 Correlation between grey matter volumetry and white matter structural integrity

CHAPTER 5

5. DISCUSSION.....	128
5.1 Functional hemispheric language lateralization in TLE by fMRI	
5.2 Functional hemispheric language lateralization in TLE by DTI and fibre tractography	
5.3 Functional hemispheric language lateralization in TLE by VBM	

CHAPTER 6

6 SUMMARY AND CONCLUSIONS.....	144
6.1 Major findings	
6.2 Major implications of these findings	
6.3 Conclusion	
6.4 Future directions	
Bibliography.....	149
List of Publications.....	173

LIST OF FIGURES

Figure No.	Caption	Page No.
1	Basic concept of fMRI data processing	10
2	The proposed Neurovascular coupling	13
3	The Hemodynamic Response Function	14
4	Temporal and spatial characteristics of different imaging modalities	18
5	Echo Planar Imaging (EPI) sequence	20
6	The effect of Echo time on T2* signal	20
7	Random walk of water molecules over time (t)	27
8	The origin of diffusion anisotropy in biological tissues	29
9	The Stejskal-Tanner Pulsed Gradient Spin-echo (PGSE) sequence	33
10	The geometrical representation of the diffusion tensor as an ellipsoid	36
11	Degree of diffusion anisotropy	36
12	Quantitative maps derived from a DTI experiment	37
13	Color coded FA map indicating the orientation of white matter tracts.	39
14	The concept of fibre assignment by continuous tracking (FACT) used for deterministic diffusion tensor tractography	42
15	Steps involved in standard and optimized VBM	46

16	Normalization by 12-parameter affine transformation for linear registration	47
17	Segmentation of spatially smoothed images to Grey matter, White matter and CSF	48
18	Eloquent cortical language areas	53
19	(a) Patient with right Hippocampal Sclerosis	56
	(b) Anterior Temporal Lobectomy	56
20	Classical Model on language processing	61
21	Dual stream model for language processing	63
22	Axial MR image of TLE patient showing a right anterior temporal lobe lesion.	66
23	Schematic representation of fMRI setup	80
24	Blocked Design paradigm for stimulus presentation and predicted BOLD signal pattern	81
25	Work flow of Statistical Parametric Mapping software.	82
26	Realignment of fMRI datasets	84
27	Group level activations overlaid on a standard template image	85
28	Smoothing by convoluting with Gaussian kernel of varying size of FWHM	86
29	General Linear Modelling	87
30	Glass brain view for group level analysis	88
31	Final interpretation of statistical parametric map	90
32	Procedure for selecting the desired white matter	

	tract using Boolean operators.	92
33	Work flow of Deterministic fibre tractography	92
34	The trajectory of Superior Longitudinal Fasciculus and its identification in color FA maps	94
35	The trajectory of the uncinate fasciculus and its Identification in color maps	95
36	The trajectory of the Inferior Longitudinal fasciculus and its identification in color maps	96
37	The trajectory of the Inferior fronto-occipito fasciculus and its identification in color maps	97
38	Segmentation of grey matter structures	98
39	3D overlay of grey matter structures	98
40	Plot showing Hemodynamic response functions in control subjects	103
41	Bar diagram showing LI of right and left TLE patients	106
42	Plots showing hemodynamic response functions in TLE subjects	107
43	Group level average activation SPM t maps	110
44	Tractography of dorsal and ventral language pathways in control subjects	112
45	Fibre tractography in TLE patients	114
46	Positive correlation between fibre tract symmetry index and fMRI laterality in TLE subjects	116

47	Negative correlation between UF and IFOF Asymmetry index and fMRI laterality in TLE subjects	117
48	Segmentation and volume calculation of subcortical grey matter structures using VBM technique	120
49	Box plot showing HG, PT and insular volume differences in control subjects	121
50	Box plot showing HG, PT and insular volume differences in TLE subjects	122
51	Correlation between ArcF FA and grey matter volume in LTLE	123
52	Correlation between ILF FA and grey matter volume in LTLE	124
53	Negative correlation between FA (ArcF, ILF) and insula volume in RTLE	125

LIST OF TABLES

Table No.	Title	Page No.
1	Patient Demographics	76
2	BOLD fMRI activation results in healthy controls	104
3	BOLD fMRI activation results in RTLE and LTLE patients	109
4	Tract based statistics results of white matter tracts	111
5	Correlation between fMRI, DTI and VBM parameters	127

LIST OF ABBREVIATIONS

TLE	Temporal Lobe Epilepsy
MTS	Mesial Temporal Sclerosis
ATL	Anterior Temporal Lobectomy
fMRI	functional Magnetic Resonance Imaging
DTI	Diffusion Tensor Imaging
DFT	Diffusion Fibre Tractography
VBM	Voxel Based Morphometry
EPI	Echo Planar Imaging
FA	Fractional Anisotropy
MD	Mean Diffusivity
ArcF	Arcuate Fasciculus
ILF	Inferior Longitudinal Fasciculus
IFOF	Inferior FrontoOccipito Fasciculus
UF	Uncinate Fasciculus
IFG	Inferior Frontal Gyrus
HG	Heschl'sgyrus
PT	PlanumTemporale
STG	Superior Temporal Gyrus
RTLE	Right Temporal Lobe Epilepsy
LTLE	Left Temporal Lobe Epilepsy
VG	Verb Generation
Syn	Synatx
SeT	Semantic Task

WP	Word Pair
AED	Anti Epileptic Drug
EEG	Electroencephalography
MEG	Magneto encephalography
PET	Positron Emission Tomography
SPECT	Single-Photon Emission Computed Tomography
DWI	Diffusion weighted Imaging
HS	Hippocampal Sclerosis
MATL	Modified Anterior Temporal Lobe Resection
FCD	Focal Cortical Dysplasia
SPM	Statistical Parametric Mapping
ROI	Region of Interest
BOLD	Blood Oxygen Level Dependent
ATP	Adenosine Tri Phosphate
HRF	Hemodynamic Response Function
GE	Gradient Echo
SE	Spin Echo
EPI	Echo planar imaging
TE	Time of Echo
ADC	Apparent Diffusion Coefficient
SNR	Signal to Noise Ratio

SYNOPSIS

Study background

Temporal lobe epilepsy (TLE) is the most common form of localization-related epileptic disorder and it is generally refractory to medical treatment. Mesial temporal sclerosis (MTS) is the frequent abnormality usually found in these patients and is characterized by neuronal loss and gliosis of the mesial temporal structures. Anterior Temporal lobectomy (ATL) is an effective remedial measure for patients who suffer from medically intractable epilepsy, but it carries risk of disruption of lateralization of language function in brain. In order to reduce cognitive deficits after surgery, it is important to determine the brain locus of seizure origin and its relation to various functionally active areas, especially language and memory functions.

Presurgical evaluation in patients with intractable epilepsy mainly focuses on the identification of cortical area capable of generating seizures, so that removal or disconnection of that particular area will result in seizure freedom. An important part of preoperative evaluation is the determination of hemisphere dominance for language, because the procedure should be planned to avoid resecting cortex essential for language function. Traditional way for presurgical functional mapping includes Intracarotid amobarbital (Wada test) but it is invasive and involves potential risks. Compared with this test, advanced non-invasive technique, fMRI offers a promising tool for localizing language functions preoperatively so as to reduce language deficits after ATL. Using fMRI it is possible to, (a) localize eloquent brain areas with respect to the envisaged site of surgery, (b) detect the dominant hemisphere

for specific brain functions, (c) localize epileptic zones and lateralization of epileptic activity, (d) delineate neuroplastic changes of brain activity.

As language function relies on a system of intercommunicating neuronal network, it is possible that organization depends on the integrity of connecting white matter tracts. Structural brain asymmetries in the brain white matter could be related to functional asymmetries such as Handedness or Hemispheric language dominance. The white matter tracts can be studied by means of Diffusion Tensor Imaging Tractography (DTIT), which is nowadays accepted as an intact neuroimaging technique for understanding microstructural architecture of white matter pathways in the human brain. Additionally, the anatomical correlates of language function can be identified with an automated voxel based volumetric technique, Voxel Based Morphometry (VBM). Morphological asymmetries favouring the left hemisphere in the Planum Temporale (PT), Insula and Heschl's Gyrus (HG) have been presumed to relate to the typical left-hemisphere dominance for language functions.

The proposed study was to reveal the efficacy of Diffusion Tensor Imaging and Voxel Based Morphometry for lateralizing language in comparison to fMRI to noninvasively assess hemispheric language specialization as part of the presurgical work-up in temporal lobe epilepsy (TLE).

Objectives

In this research work, fMRI and DFT techniques were used to explore structure/function relationships, particularly language dysfunction often associated with intractable epilepsy and results were compared with volumetric measurements of grey matter structures calculated by means of VBM. The main objective was to evaluate the concordance

of language lateralization obtained by DTI & VBM to fMRI and thus to see whether there exists an anatomical correlate for language lateralization result obtained using fMRI.

Hypothesis

It was assumed that the combination of fMRI, DTI and VBM together can give better information of the language lateralization in intractable TLE patients than using a single technique alone. Considering fMRI as a non-invasive gold standard for language lateralization, we wanted to test our hypothesis that DTI and VBM are as sensitive as fMRI in language lateralization.

Materials and methods

MR imaging data were acquired using 1.5 Tesla Magnetic Resonance scanner (Avanto SQ engine, Siemens, Erlangen, Germany) with Echo Planar Imaging (EPI) capabilities. Sixty (42 males; 18 females) age (20-38 years) matched normal healthy controls and fifty seven intractable Temporal lobe epilepsy cases (39 males, 18 females; age range: 15-40 years; 41 = Right MTS, 16 = Left MTS) underwent fMRI of language function using four different language paradigms. 30 directions DTI was performed with $2 \times 2 \times 2$ isotropic voxel and 2mm slice thickness. A high resolution T1 weighted 3D MPRAGE (Magnetization Prepared Rapid Gradient Echo), with excellent grey matter- white matter contrast was used for VBM based volumetric analysis and coregistration of fMRI data. The fMRI data analysis was done using Statistical Parametric Mapping software (SPM5, Wellcome Trust Department of Cognitive Neurology, London, UK, www.fil.ion.ucl.ac.uk/spm).

DTI post processing was done by the method of tract based statistical analysis using DTI studio (<http://Ibam.med.jhmi.edu>) software. Fractional anisotropy (FA), Mean Diffusivity (MD) and Relative fiber density (RFD) of arcuate fasciculus (ArcF), inferior longitudinal fasciculus (ILF), inferior fronto- occipital fasciculus (IFOF) and uncinate fasciculus (UF) was calculated in both hemispheres.

Volumes of different sub cortical structures (planum temporale, heschl's gyrus and insula) were calculated by VBM based volumetry approach using SPM. Using a combined fMRI, Diffusion based tractography and voxel based morphometry approach, I investigated the relation of microstructural asymmetries in language-relevant white matter pathways and functional activation asymmetries during visual verb generation, syntax, semantics and word pair tasks in concordance with Planum Temporale, Insula and Heschl's gyrus volumetry. Tractography - based statistics revealed that inferior frontal and superior temporal activation asymmetries during visual verb generation and semantic decision making tasks were positively related to the strength of specific microstructural white matter asymmetries in the ArcF and ILF. The scientist who performed the DTI & VBM processing was blinded to the results of fMRI processing. Concordance between the results obtained in fMRI processing with DTI & VBM processing for language lateralization was measured using Cohen's kappa coefficient.

Major findings

- a) First, I optimized the protocols for various fMRI language paradigms (Visual verb generation –VG; Syntax –Syn; Semantics-SeT and Word pair –WP) by studying the fMRI blood oxygen level dependent (BOLD) activation results in healthy controls. Visual verb generation and semantic decision making tasks generated significant

- ($p < 0.05$) BOLD fMRI activations in classic language processing areas (IFG and Posterior STG).
- b) Significant differences in BOLD activity pattern were found between the TLE group and the controls, more specifically in Inferior parietal language (Geschwind's area) and Superior Temporal Gyrus (STG). LTLE patients were found to have significantly reduced activation in the right inferior -parietal language areas during VG ($t = -3.551$, $p = 0.002$) and SeT tasks ($t = -2.035$, $p = 0.052$) and RTLE patients showed a trend for reduced left temporal activations during VG ($t = -1.897$, $p = 0.069$) but not during SeT task ($t = -0.717$, $p = 0.48$). Inferior frontal area activations were found to be not reduced relative to controls on either task ($t = 1.752$, $p = 0.094$ for VG and $t = 0.429$, $p = 0.675$ for SeT).
- c) No significant differences were observed between LTLE and RTLE patients in percent signal intensity change for either task.
- d) Significant differences ($p = 0.004$) were also found in the values of the fMRI language laterality indices between the TLE and control group. In order to check the possibility of intra-hemispheric variability in lateralization of language-related activation in LTLE cases, the ratio of inferior frontal activated clusters to left temporal activations were compared between LTLE patients and controls. No significant difference was observed on this measurements between LTLE patients and healthy controls either during verbal fluency task ($t = 0.584$, $p = 0.566$) or semantic decision task ($t = -0.096$, $p = 0.925$); however a tendency was seen for reduced left-lateralised activation widely in LTLE.
- e) The TLE group showed considerable diffusion abnormalities in DTI parameters when compared to the control group. Particularly an increased Mean Diffusivity (MD- 961-

1243.34 mm²/sec) and reduced Fractional Anisotropy (FA- 126.33 – 130.47) was found in patients with mesial temporal sclerosis , in the zones of seizure foci.

- f) Tractography of white matter pathways demonstrated abnormalities in brain's connectivity network that are specific to TLE and MTS. This study showed more bilateral involvement of ArcF and unilateral involvement of ILF with significantly increased MD and decreased FA in both right and left TLE patients. Specifically, in the left TLE group, FA values in the entire left and right AF tract were comparable to controls; however MD values and fiber density were elevated bilaterally. The right TLE group demonstrated higher MD values and lower FA values in right and left ArcF and right ILF compared to controls.
- g) A good correlation was found in TLE group between language fMRI laterality index and fibre tract laterality index, more specifically for Arcuate fasciculus (ArcF), ($r_2=0.2120$, $P < 0.004$) and Inferior longitudinal fasciculus (ILF), ($r_2=0.2330$, $P < 0.007$) and less correlation was found for fMRI laterality index and asymmetry indices of UF and IFOF.
- h) Volumetric studies demonstrated a significant reduction in left HG ($p=0.021$), PT($p=0.020$) and insular volume($p=0.023$) in LTLE cases compared to controls and RTLE demonstrated significant volume reduction only in HG ($p=0.002$) and PT($p=0.034$), no differences was found in insular volume ($p=0.421$).
- i) There exists a strong one to one correlation between fMRI lateralization index, DTI tractography measures & VBM based volumetric measurements of PT, Insula and HG for determining language lateralization. Loss of fibre pathway integrity and functional activation patterns were correlated with changes in cortical grey matter volume. There exist a strong correlation between atrophied ArcF and ILF in LTLE patients with volumetric measurements of left PT ($r_2 = 0.2110$, $P < 0.005$), HG ($r_2 = 0.2130$, $P < 0.022$) and insula ($r_2 = 0.214$, $P < 0.241$) relative to healthy controls. In RTLE a good correlation was found for HG ($r_2 =$

0.2231, $P < 0.002$) and PT ($r_2 = 0.231, P < 0.020$) and no significant correlation ($r_2 = 0.465, P = 0.741$) was found for insular volume and atrophied white matter.

Implication of findings

- The study provided an opportunity to study the relationship between brain structure and function involved in language processing.
- In patients especially small children who fail to perform the fMRI language tasks, the presurgical lateralization of language function may be done using diffusion tractography & volumetry of specific cortical structures.
- A strong degree of asymmetry was specifically found for major language tracts, ArcF and ILF. This data reflects that regional brain function indeed corresponds to higher connectivity.
- Even though no obvious changes in inter- or intrahemispheric laterality of language-related activation were seen in TLE cases during any of the fMRI language paradigms, the study provided evidence that, temporal lobe pathology in MTS patients was strongly related to subtle changes in the language connectivity network and corresponding volume changes in cortical grey matter structures.
- The findings of this study highlights how fMRI technique can be coupled with tractography and morphometric findings to assist neurosurgeons in the surgical planning of intractable TLE patients who are at risk of developing post-operative language deficits.
- From the observed results, we concluded that a combination of functional Magnetic Resonance Imaging (fMRI), Diffusion Tensor Imaging (DTI) and

Voxel Based Morphometry (VBM) used together can give better information of the language lateralization than using a single technique alone.

INTRODUCTION

This thesis describes the utilization of three advanced neuroimaging techniques (fMRI, DTI and VBM) for lateralization of one of the major human cognitive function, language, in medically refractory epilepsy patients as a part of their presurgical evaluation in a non-invasive and reproducible manner. The study also underline the importance of using different fMRI language experimental paradigms eliciting frontal and temporal lobe activations, when studying left and right TLE patients with MTS.

The research study was based on the following assumptions:

(1) Larger density of white matter pathways in the cerebral hemisphere could provide a structural basis for greater intrahemispheric connectivity and dominance. The role of white matter in hemispheric language specialization is supported by the use of Diffusion Tensor Imaging Tractography (DTIT).

(2) Axonal white matter fibres connecting cortical regions involved in speech, language, and reading may demonstrate asymmetry in their microstructural organization. Imaging the white matter tracts using diffusion fibre tractography can be combined with fMRI using blood oxygenated level dependent signal changes, to non-invasively explore the in vivo structure-function relationship of language function in TLE subjects.

(3) VBM of cortical grey matter structures along with fMRI and DTI can provide regional morphological differences in grey matter intensity and concentration between two groups of subjects.

Based on these assumptions we hypothesized that the combined analysis of the fMRI, DTI and VBM provides more significant evidence on functional-structural correlation of language function than using single modality, and corresponding grey matter concentration differences associated with language laterality might also represent morphological changes

underlying functional reorganisation of the language connections in patients with MTS. The present study was to validate DTIT results and test the hypothesis that cortical language areas determined by fMRI activation serve as seed points for the white matter tractography of dorsal and ventral language pathways.

Temporal Lobe epilepsy (TLE) is the most frequent form of focal epilepsy. About 20– 30% of the TLE patients develop resistance to Antiepileptic Drugs (AEDs) and may benefit from a surgical management (Wiebe et al., 2001). For medically refractory TLE patients, surgical excision of the affected temporal lobe, Anterior Temporal Lobectomy (ATL) is an alternative approach to the treatment of this disorder. However, ATL may cause language impairments, as anterior-middle temporal areas are involved in language processing and specifically, naming ability (Hamberger and Seidel, 2009, Baldo et al., 2012). After ATL, approximately 30% of left TLE (LTLE) patients show a significant decline in naming abilities persisting for up to one year (Rosazza et al., 2013). Verbal fluency impairment has also been reported in 12–17% of LTLE patients (Helmstaedter et al., 2004). Postoperative language deficits have been occasionally reported also in right TLE (RTLE) patients (Bonelli et al., 2012, Schwarz and Pauli, 2009).

The successful surgical outcome depends not only on an accurate localization of the epileptogenic zone, but also on the ability to map and preserve the “eloquent brain areas.” In particular, the lateralization and localization of cognitive functional areas, predominantly language processing cortical areas are important for ATL in the dominant hemisphere (Binder et al., 1997). The distance from the language cortex to the resection margin is the most significant predictor of developing postoperative language deficits (Ojemann, 2003).

Language lateralisation in epilepsy patients differs from what is known in the normal subjects (Springer et al., 1999). Bilateral or right-sided representations (atypical) of language function are more frequently found in patients with epilepsy and seemed to be coupled with

left-sided seizure origin, an early age of onset, left handedness, and a lesion in the area of primary language areas of Broca and Wernicke (Woermann et al., 2003) functional Magnetic Resonance Imaging (fMRI) is widely used to map language activation patterns and assess hemisphere dominance for language function prior to epilepsy surgery (Sabsevitz et al.,2003). fMRI technique may further reduce the need for invasive procedures like Intracarotid Amobarbital Procedure (IAP, also called the Wada test) and Electrocortical Stimulation Mapping (ESM).fMRI is helpful in determining language lateralization and estimating the risk of postoperative decline (Richardson et al., 2004, Bell et al., 2009), and is widely considered to be a valid noninvasive gold standard approach. Furthermore, fMRI can be integrated with other MR imaging modalities like DTI to improve surgical strategies adapted to individual epilepsy patients with regard to functional outcome, by virtue of definition of epileptic brain areas that need to be resected and eloquent areas that need to be spared. Language fMRI is a well established technique which is widely used nowadays in many centres and is often applied to identify the language dominant hemisphere on an individual basis.

The complex functional language systems not only depends on localized brain areas or functions but also on their structural connectivity network. Structurally, the interaction between inferior frontal and temporal areas must be based either on direct cortico-cortical pathways or thalamocortical reciprocal pathways, which can be explored by means of DTI based tractography technique. Diffusion Tensor Imaging Tractography (DTIT) is also a non invasive neuroimaging technique that allows tracing of microstructural architecture of white matter tracts in vivo in brain based on the anisotropic diffusion of water molecules. It would be clinically useful, if one can determine any structural changes within the white matter pathways involved in language function in TLE patients, which provides important insights into the mechanisms underlying language plasticity within cerebral networks. There are

recent studies using DTI methods which have explored fibre tracts connecting the language-processing areas in the inferior frontal and the temporal cortex in vivo (Friederici AD, 2002). These studies report two pathways: a ventral pathway connecting the ventral part of the inferior frontal gyrus (IFG) to the anterior-to-mid portion of the superior temporal gyrus (STG) via the uncinate fasciculus and/or the extreme capsule fibre system, and a dorsal pathway connecting the dorsal part of the IFG to the posterior portion of the STG and sulcus (STG/STS) via the superior longitudinal fasciculus and the arcuate fasciculus (Catani et al, 2007, A.Bizzi, 2009).

The most widely used DTI parameters are Mean Diffusivity (MD), a measure of the average motion of water molecules independent of tissue directionality, radial diffusivity (Dr) and axial diffusivity (Da) that demonstrate more specific relationships to white matter pathology. The Dr appears to be modulated by myelin in white matter, whereas the Da is more specific to axonal degeneration (Alexander AL et al, 2007). In order to maximize the specificity, it is recommended to use multiple diffusion tensor measures to better characterize the tissue microstructure. Another important DTI parameter is Fractional Anisotropy (FA), which reflects the degree of alignment of cellular structures within fibre tracts, as well as their structural integrity. MD is supposed to be mainly affected by cellular size, integrity and myelination, whereas FA is indicative of fibre integrity and alignment. In normal fibre tracts, water diffusion is directional (high FA), whereas in degenerated tracts, FA decreases substantially. The tractography analysis can be used to measure connectivity between primary language brain regions such as between Broca's area and Wernicke's area or other language-related functional areas like angular gyrus, supramarginal gyrus, occipital areas, Geschwind's area (inferior parietal lobule), orbitofrontal cortex etc. The strength and asymmetry of language white matter connectivity can be measured in terms of mean fibre length, fibre volume and mean FA within the fibre tract Moreover the anatomical correlates of language

function can be assessed by morphological examination of structural asymmetries of language related cortical grey matter structures such as Planum temporale (PT), Heschl's gyrus (HG) and Insula (Geschwind N and Levitsky, 1968, Wada JA et al., 1975). Quantification of these subcortical grey matter volume and interpretation of their structural asymmetry is possible by means of voxel based statistical approach called VBM (Ashburner & Friston, 2000), which is fully automated, time efficient and analysis in large group of subjects also possible.

Prior studies have tried to relate structural differences in cortical regions between the hemispheres to language lateralization, and have provided mixed results. Two early investigations suggested that planum temporale (PT) area asymmetry correlated with results of Wada testing (Foundas et al., 1994), and that area asymmetry of pars triangularis (the anterior portion of Broca's area) also predicted Wada outcome (Foundas et al., 1996). However, another group concluded that leftward structural asymmetry of the planum temporale and Heschl's gyrus (HG) did not correlate with language lateralization, but that grey matter concentration in the posterior part of inferior frontal gyrus (pars opercularis, the posterior portion of Broca's area) did predict language function in a group of left and right Wada patients (Dorsaint-Pierre et al., 2006). Some authors investigated language lateralization as a part of presurgical evaluation in TLE cases separately by means of language fMRI paradigms (Mahdavi et al., 2011) and related connectivity assessment of language associated white matter pathways by DTIT (Powel et al., 2007). Some other groups studied the morphological correlates of language function in TLE subjects by detecting regional grey matter morphological differences by means of VBM (Keller & Roberts, 2008). VBM can estimate the amount of reduction in the concentration or volume of cerebral grey matter structures ipsilateral and contralateral to the seizure focus (Mueller et al., 2006). Labudda et al., 2012 combined fMRI and VBM techniques to study the atypical language

lateralisation in left-sided Mesial Temporal Lobe Epilepsy (MTLE) patients. Till now there have been no similar combined fMRI, DTI and VBM studies on lateralization of language in epilepsy patients.

Aims and Objectives

The main objective of the present study was to evaluate the concordance of language lateralization obtained by DTI & VBM to fMRI and thus to see whether there exists an anatomical correlate for language lateralization result obtained using fMRI. Based on the previous observations and studies on language laterality, we assumed that the combination of fMRI, DTI and VBM together can give better information of the language lateralization in intractable TLE patients than using a single technique alone. Considering fMRI as a non-invasive gold standard for language

Using a combined fMRI, Diffusion based tractography and VBM, I tried to investigate the relation of microstructural asymmetries in language-relevant white matter pathways and functional activation asymmetries during visual verb generation, syntax, semantics and word pair tasks in concordance with Planum Temporale, Insula and Heschl's gyrus volumetry.

This dissertation describes and discusses the studies performed to estimate the degree of lateralization of language function in medically refractory TLE patients by comparing the results obtained from healthy human volunteers. It is organized in five chapters. In Chapter I, introduces the “**Advanced neuroimaging techniques**” used in this research study for language presurgical lateralization. Chapter II, **Literature review**, brief reviews are presented, necessary to understand the concept of research work. The chapter also explains some clinical applications of fMRI, DTI and VBM in TLE patients that highlights the importance of proper examination procedures relevant to the present study. The chapter III, **Design of the Study**, describes and justifies the materials and methods used to conduct the

study to answer the specific research questions raised. This section also describes different statistical tests and methods employed to examine the significance of major research findings. Chapter IV, **Results** describes the main observations of the study and its statistical significance. The achieved results are represented as tables, graphs and figures. The Chapter V, **Discussion**, interpret the observations obtained from the study and also discuss the implications of major findings and chapter VI, **Summary and Conclusion** summarizes the key observations and findings and conclude by giving most important statement that highlights the major outcome of the study.

CHAPTER 1

INTRODUCTION TO NEUROIMAGING

TECHNIQUES

The research work is mainly focussed on three advanced non-invasive Magnetic Resonance Imaging (MRI) techniques capable of understanding the anatomy and physiology of complex brain functions such as language, memory, emotions, and behaviour. This chapter explains the basic concepts of these techniques, their physics, technical considerations and limitations.

1.1 functional Magnetic Resonance Imaging (fMRI)

1.1.1 Introduction

The primary goal of functional neuroimaging is to create images sensitive to neuronal activity. fMRI extends the use of MRI to provide information about human brain functions in addition to the anatomical information. Dr. Sieji Ogawa and colleagues (1990) at AT&T Bell Laboratories reported that functional brain mapping is possible by using the blood oxygenation level-dependent MRI contrast. Using electrophysiological methods, it is possible to make a whole –brain image of neuronal activity but one would need to place closely spaced electrodes throughout the brain, which is neither practical nor ethical in humans. The other techniques like Electroencephalography (EEG) and Magneto encephalography (MEG) relies on sensors placed outside of brain , which can be applied to humans but provide only indefinite spatial resolution which is insufficient for measuring brain functions. The optical imaging measures the neuronal activity by using voltage sensitive dyes and it has high spatial

and temporal resolution. But the changes in the optical properties of dye in response to changes in the neuronal membrane potential occur within milliseconds of neuronal activity.

fMRI is one of the most promising tools in the field of neuroimaging, enabling the investigation of cognitive brain functions, with an excellent spatial resolution in a non-invasive manner. It creates brain images during physiological activity that can be correlated with neuronal activity. The fMRI data acquisition was originally based on the technique that measures the BOLD signal intensity changes. The advancement of the BOLD contrast based fMRI technique represents a substantial innovation in the area of cognitive neuroscience. As a brain imaging technique, fMRI has several major advantages; (a) It is non-invasive and doesn't involve radiation, making it safe for the subject, (b) It has excellent spatial and good temporal resolution, and (c) It is easy for the experimenter to use.

The basic concept of fMRI technique is to perform a series of experimental tasks (Paradigms) lying inside the MRI scanner. The paradigm contains blocks or events of interest with active and baseline conditions, whilst T2* weighted BOLD images are collected (Le Bihan et al., 1995). A statistical model of expected BOLD response is designed to compare the signal intensity of each voxel within the brain image and considered as significant if any signal intensity changes detected. Using fMRI, detection of any small increases in the signal of the brain areas can be correlated with the behaviour. An fMRI experiment depends upon various techniques and parameters, making it intrinsically multidisciplinary. It is great challenge to neuroscientist to make the best use of this technique.

The three main components of fMRI are; (a) Acquisition of BOLD time –series data, (b) Experimental paradigms (tasks), (c) Preprocessing of fMRI data and statistical analysis (**Figure 1**). For fMRI data acquisition, pre-processing and analysis of experimental designs, one requires good knowledge on all concepts of fMRI experiment, especially on paradigm designing and statistical principles. The following section will present an overview of the “BOLD fMRI: physical principles, neurophysiology and Techniques”.

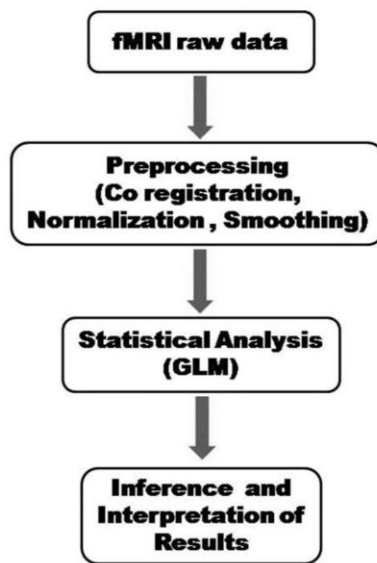


Figure 1: Basic concept of fMRI data processing

1.1.2 The neurophysiology of BOLD signal

BOLD imaging relies on sensitivity to oxygen level changes within the circulating blood. The human brain utilizes about 20% of the oxygen required by the body even though it makes up less than 2% of total body mass. Cerebral blood flow (CBF) delivers glucose and O₂ to the brain, so it is natural to suppose that local CBF varies with neural activity (James, 1890). The change in CBF with a change in neural activity is the principal signal used for mapping brain activity with functional neuroimaging.

The basic information processing of central nervous system is neuron. It has estimated that the brain has about 100 billion neurons. The neuronal activity can be categorized as either integrative activity or signalling activity. The integrative activity involves collection of inputs from other neurons through dendritic connections while signalling activity results from axonal activity, which transmits the outcome of integrative process to one or more other neurons. The information transfer between neurons occurs at specialized locations called synapses. In most synapses, the presynaptic (ending of an axonal process from one neuron) and post synaptic elements are separated by synaptic cleft, where the chemical

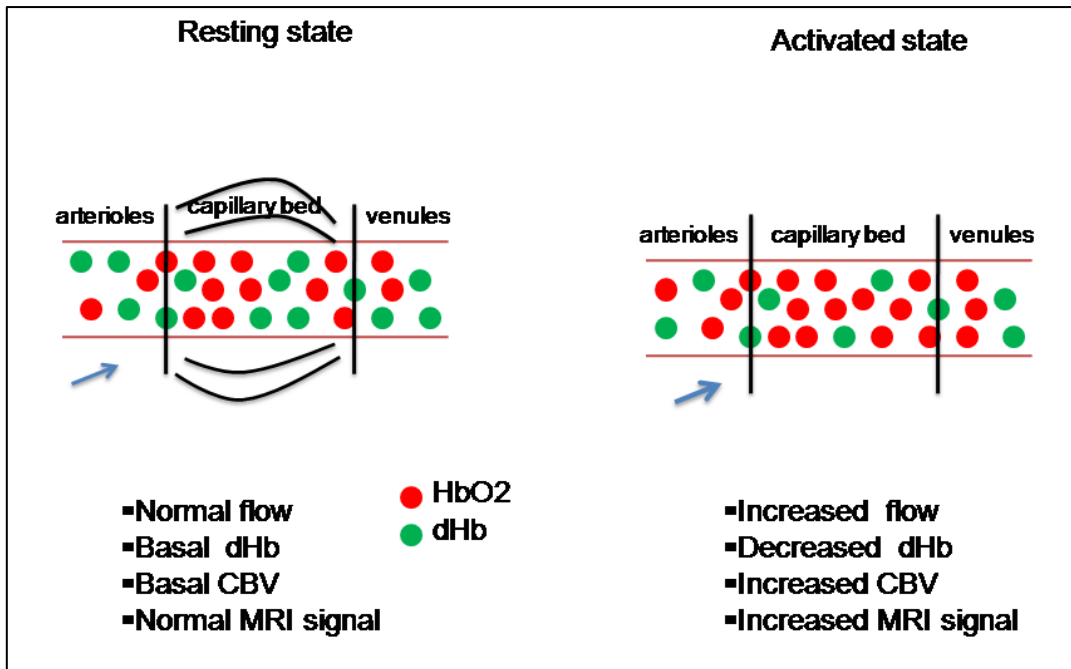
(neurotransmitters like GABA, Glutamate etc) released from the presynaptic elements influence activity in the postsynaptic membrane of the dendrite or soma of another neuron.

Neuronal activity increases metabolic demands. To meet these requirements, the energy is supplied by the vascular system by means of two fuel sources, glucose and oxygen. Because the brain does not store energy, it must create ATP (Adenosine Tri Phosphate) through the oxidation of glucose. Both glucose and oxygen are supplied through increased blood flow. However, blood flow and glucose consumption far exceed the increases in oxygen consumption. The arterial part of the vascular system transports oxygenated blood through network of blood vessels until it reaches the capillary bed where the chemically stored energy is transferred to the neurons. The venous part transports the less oxygenated blood away from the capillary bed (**Figure 2a**). While the arterial network contains only oxygenated haemoglobin (HbO₂), the capillary bed and venous network contains both oxygenated and deoxygenated haemoglobin. An increase of neuronal activity leads to an increased oxygen extraction rate in the capillary bed and thus results in an increase in the concentration of deoxygenated haemoglobin (dHb). The haemoglobin in the blood was strongly paramagnetic in its deoxygenated state, therefore deoxygenated haemoglobin can be treated as a naturally occurring endogenous contrast agent and introduces an inhomogeneity into the nearby magnetic field, whereas oxyhaemoglobin is diamagnetic and produces only little effect on magnetic field.

The fMRI technique works on the principle of magnetic susceptibility between oxygenated and deoxygenated haemoglobin. An increased concentration of deoxyhaemoglobin would result in decreased image intensity, and decreased deoxyhaemoglobin would result in increased image intensity (**Figure 2.b**). Thus, during neuronal activation, a local increase in blood flow increases the blood oxygenation and consequently reduces deoxygenated haemoglobin,

causing increased MR signal intensity. It is assumed that this local increase in blood oxygenation results in increase neuronal activity, which is called Hemodynamic Response Function (HRF). This Blood-Oxygenation-Level Dependent (BOLD) imaging technique eliminates the requirement of exogenous contrast agents, such as radioactive isotopes (Ogawa et al 1990; Turner et al 1998).

a)



b)

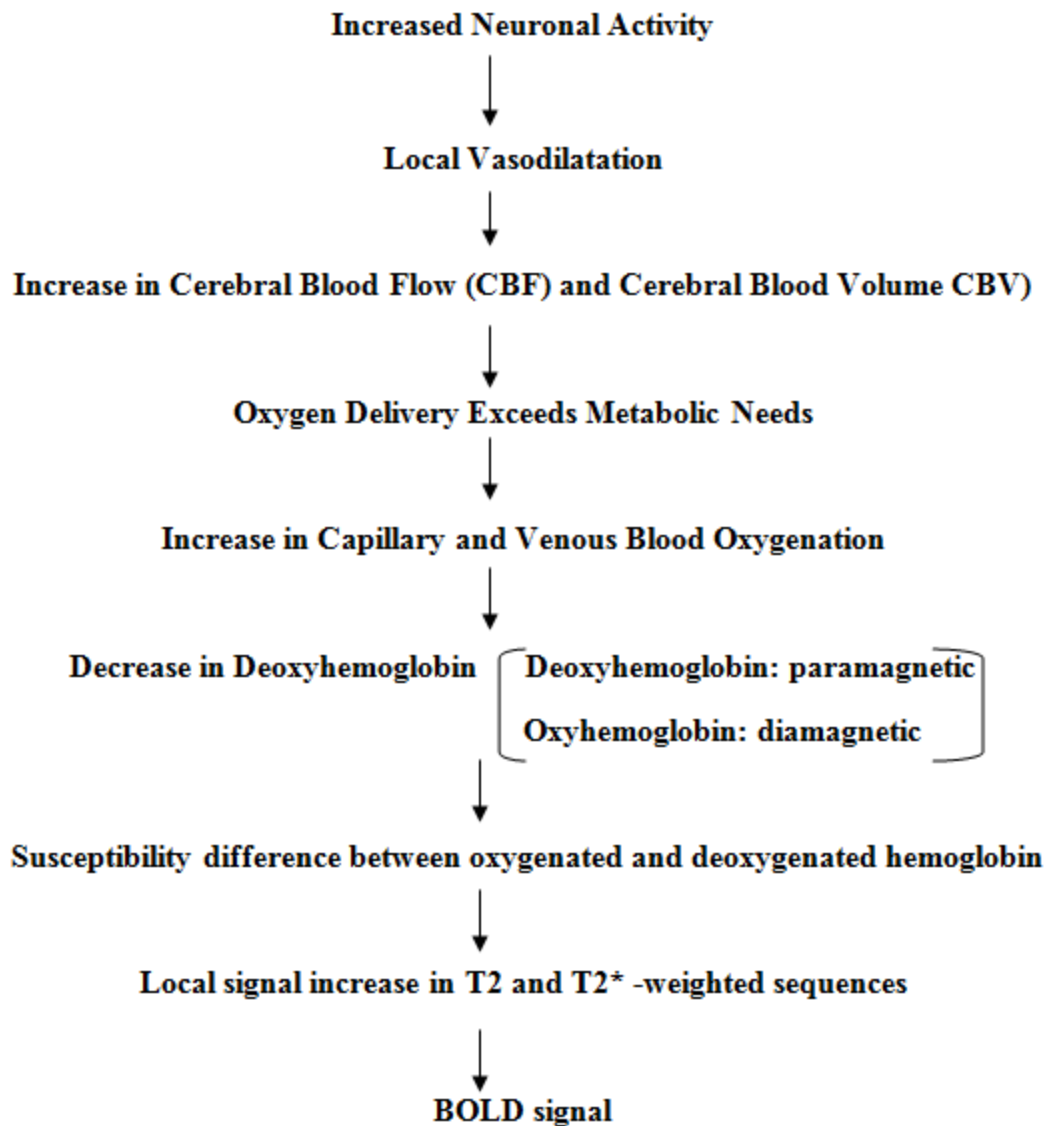


Figure 2: The proposed Neurovascular coupling (a), neurotransmitter recycling and metabolic demand. The effects of deoxyhaemoglobin on the MRI signal (b).

The main three phases of the BOLD fMRI response (HRF) to neuronal activity: (a) An initial dip in neuronal activity below baseline (during the initial period of oxygen consumption), (b) followed by a high increase above baseline (an oversupply of oxygenated blood, which is only moderately compensated for by an increase in deoxygenated blood), and

(c) then by a reduction back to below baseline again (after the oversupply of oxygenated blood has decreased, it still takes some time for the blood volume to return back to baseline (Figure 3).

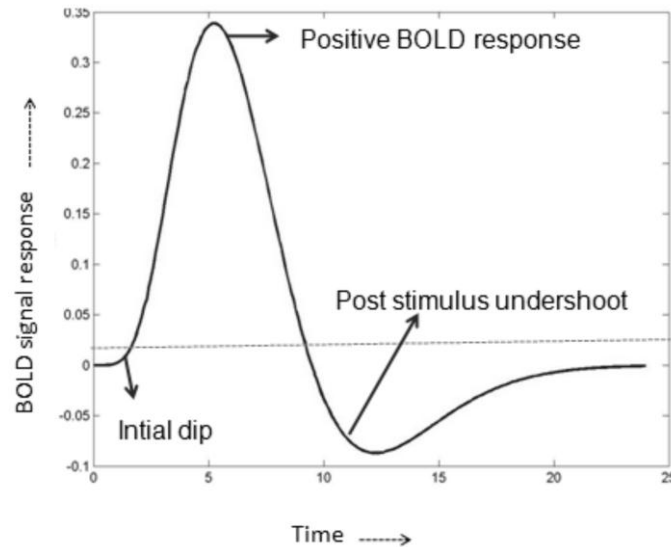


Figure 3: The Hemodynamic Response Function.

1.1.3 fMRI - Brief history

The concept of the relation between cerebral blood flow and neuronal activity is not so recent, and it was first detected by an Italian physiologist of the 19th century, Angelo Mosso. He recorded the pulsations of the human cerebral cortex in patients with skull defects. Mosso observed that these pulsations increased locally (Mosso, 1881) during mental activity. Later, the concept that regional cerebral blood flow (CBF) could reflect neuronal activity began with experiments of Roy & Sherrington in 1890. This idea forms the basis for all hemodynamic-based neuroimaging techniques being used today. Since the glucose metabolism and CBF changes are closely related, the focal increase in CBF can be considered to relate directly to neuronal activity. Thus, for mapping brain functions, it is important to assess the CBF change induced by stimulation. Because cerebral metabolic rate of glucose

(CMRglu) and CBF changes are also related, it is supposed that cerebral metabolic rate of oxygen (CMRO₂) and CBF changes are also coupled.

The first quantitative assessment of regional cerebral blood flow and oxygen consumption in humans were done by using the radiotracer techniques developed by Ter Pogossian et al., 1970 and Raichle,1976. However, based on positron emission tomographic measurements of CBF and CMRO₂ in humans during somatosensory and visual stimulation, Fox and colleagues reported that an increase in CBF surpassed an increase in CMRO₂. Consequently, a mismatch between CBF and CMRO₂ changes results in an increase in the capillary and venous oxygenation level, opening a new physiological parameter (in addition to CBF change) for functional brain mapping.

During the late 1980's, Dr. Seiji Ogawa, a scientist at Bell Laboratories investigated the possibility of examining brain physiology using MRI. Ogawa and Colleagues (1990b) hypothesized that manipulating the proportion of blood oxygen would affect the visibility of blood vessels on T₂* weighted images. They tested their hypothesis by scanning anesthetized rodents using high field 7 (Tesla or greater) MRI. Ogawa et al explained that the deoxygenated haemoglobin in venous blood is a naturally occurring endogenous contrast agent (i.e. depends on intrinsic property of the biological tissue) for magnetic resonance imaging (Ogawa et al., 1990a). This discovery was a major step in the field of functional brain mapping, yielding indirect measurement of neuronal activity. Regarding his experiments, Ogawa, stated that BOLD fMRI technique could be used for in vivo measurement of real time blood oxygenation under normal physiological conditions, adding a new feature to MRI in terms of the functional brain mapping. Since then, fMRI has accepted as a promising method used in neuroimaging and this technique is most commonly used in human brain imaging, because of its non-invasive nature and therefore usually referred as “ Gold standard technique” (Stippich, 2007).

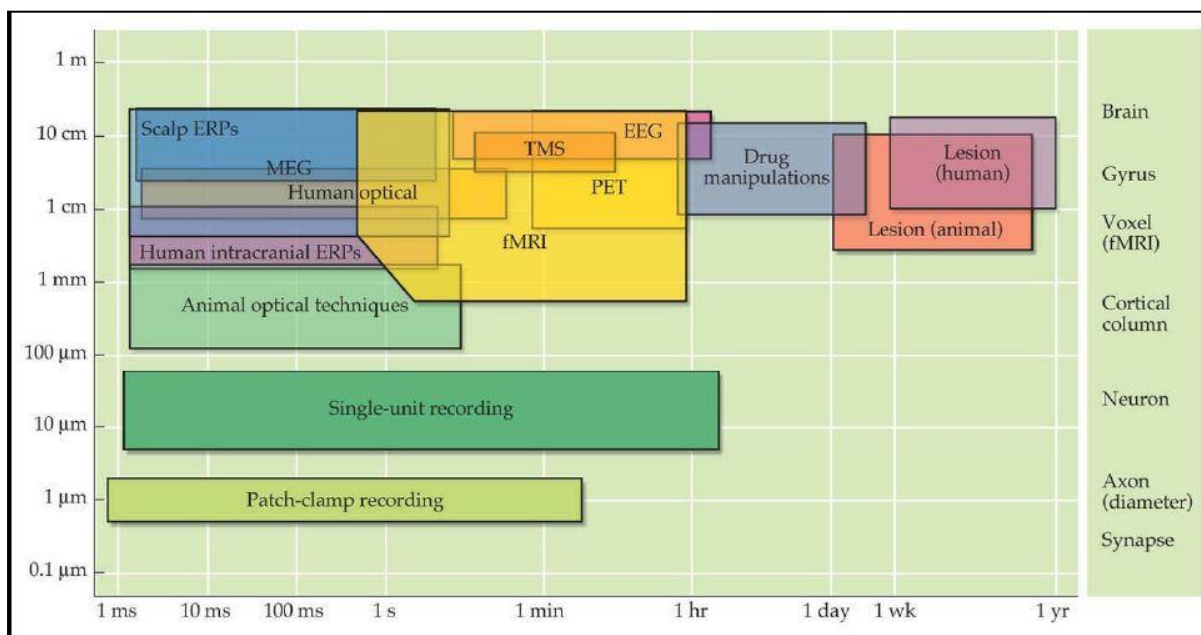
1.1.4 fMRI: Temporal and spatial characteristics

fMRI has exacting spatial and temporal properties over other neuroimaging modalities. One important reason for the success of fMRI experiments to detect human brain functions is that the fMRI response is relatively robust at low spatial resolution in cases where the increases in neural activity take place on a similar spatial scale. However, the major challenge of fMRI is to explore the brain functions at sub millimetre resolution. In order to attain a high spatial resolution with fMRI, there are number of factors to be considered. It is not possible to distinguish the excitatory or inhibitory neural activity, even if the fMRI response is localized to the site of neural activity, since they are both energy-consuming. Some studies (Waldvogel et al., 2000) suggest that inhibitory activity will not result in a BOLD activation at the site of inhibition. In that situation, one perhaps needs to look proximal to the site of inhibition or distal to the inhibited neurones to see a decrease in synaptic activity in the region where the inhibited neurones project to. This implies that the brain needs to be considered as a network or, one has to be familiar with something about the functional connectivity (Friston 1997).

Furthermore, the contributions of spiking and sub-threshold action potentials to the fMRI signal within a brain region are unknown. This could potentially be important for spatial localization, because sub threshold activity often extends further in space than the active spiking. The hemodynamic response that provide the observed fMRI signal changes originate from a number of sources on both the supply from (arterial) side and the draining (venous) side. On the arterial side, there exist heavy increases in blood flow to the cortical region of increased neuronal activity, but these blood flow increases are synchronized by arterial vessels that can be a centimetre or further away from the active site. Because most fMRI experiment is not done in a complete T1 relaxed NMR state, there exists the potential that the in-flow effects in these arterioles brought about by an increased supply of unsaturated

magnetization which may result in signal increases that pretend to be as activation changes but which are not co-localized to the neural activity. Engel et al. (1997) showed that the fMRI signal could be localized to within 1.1 mm at 1.5 Tesla. Gati et al (1997) suggested that in order to increase microvascular contributions to the BOLD signal a high static magnetic field strength (at least 3 or 4 Tesla) should be used.

The spatial resolution of fMRI technique is typically on the order of 3 to 4 mm inplane, which is better than most functional neuroimaging methods such as positron emission tomography (PET) and single photon emission computerized tomography (SPECT) **(Figure4)**. When a neuronal activity occurs in response to the presentation of a stimulus, the fMRI signal begins to increase after a few seconds and does not rise for approximately 5 to 6 seconds and further when the stimulus presentation is turned off,the signal takes approximately 10 to 12 seconds to return to baseline. This relatively extensive hemodynamic response was actually considered as the reason for limited temporal resolution of fMRI studies. Generally the fMRI signal reflects the flow of information processing across different brain regions as a sequence of shifted response profiles. The estimates of temporal resolution with respect to onset delays are more in the order of hundreds of milliseconds than in the order of seconds (Formisano & Goebel, 2003). The BOLD fMRI signal will be influenced by the type of stimulus presented, its duration and frequency.



Adapted from Huettel, Song, & McCarthy (2004). Functional Magnetic Resonance Imaging

Figure 4: Temporal and spatial characteristics of different imaging modalities

1.1.5 fMRI: Scanning Methodologies

An MRI study designed to examine a specific brain function or a number of brain functions involved in a particular physiological or behavioural event depend on variety of parameters and factors arranged in a form of MRI pulse sequences. The MR imaging pulse sequence is a set of instructions given by an expert to the MR scanner's data acquisition system on how to collect the MR signal and sensitize it to a particular property of the target, which could be of a morphological, functional, or chemical origin. To this end, selectivity of an image acquisition protocol usually is accomplished by temporal adjustments of suitable manipulations with magnitude and phase of the sample's bulk magnetization during the data acquisition process.

To examine the brain function using fMRI scanning, it is necessary to repetitively image the brain, while the subject lying inside the MRI scanner is presented with a stimulus or required to carry out some experimental tasks. The success of the experiment is dependent

on three major aspects; (a) the type of imaging sequence used, (b) the design of the experimental paradigm, and (c) the way in which the data is statistically analysed. The magnitude of the static field used is crucial to the percentage signal intensity change obtained on activation. This is because susceptibility differences have a higher signal dephasing effect at greater fields. As field strength increases the magnitude of the BOLD contrast also increases more quickly than system noise, so it would show that higher field strengths are desirable (P.Mansfield,1982;R.Turner et al, 1993), however the quality of the image will be reduced at higher field strength. The most important aspect of the fMRI imaging sequence is that it must generate T2* weighted images. This means that a gradient echo (GE) sequences is most commonly used, though spin echo (SE) sequences still show fMRI

BOLD contrast because of diffusion effects. Most of the fMRI scanning session utilize GEEPI sequence (**Figure 5**) since its fast acquisition rate permits the activation response to short stimuli to be detected. EPI also has the advantage of reduced artefact due subject motion. The amount of T2* weighting in the image is highly dependent on the echo time (TE). If TE is too short, there will be little difference in the T2* curves for the activated state and the baseline state, on the other hand if TE is too long then there will be no signal from either state (**Figure 6**). In order to obtain the maximum BOLD signal change for a specific region with a particular value of T2*, the optimal value of TE can be shown to be equal to the T2* value of that tissue.

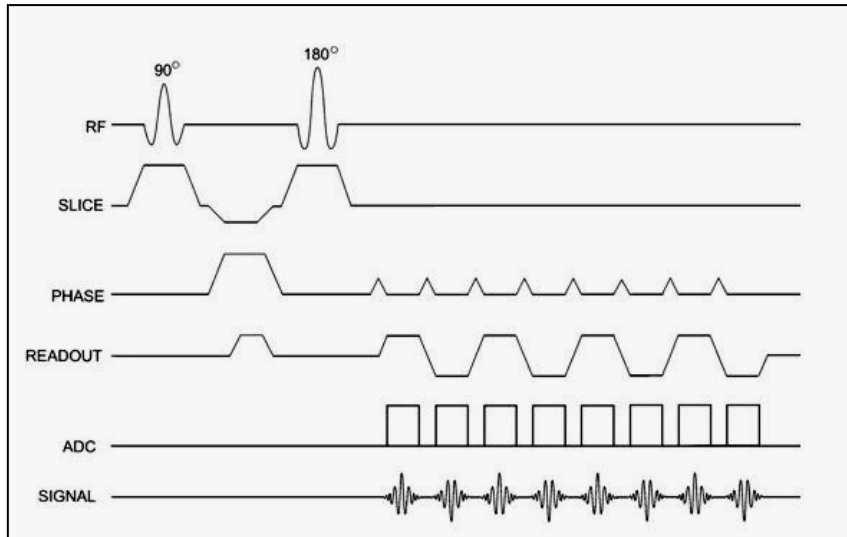


Figure 5: Echo Planar Imaging (EPI) sequence

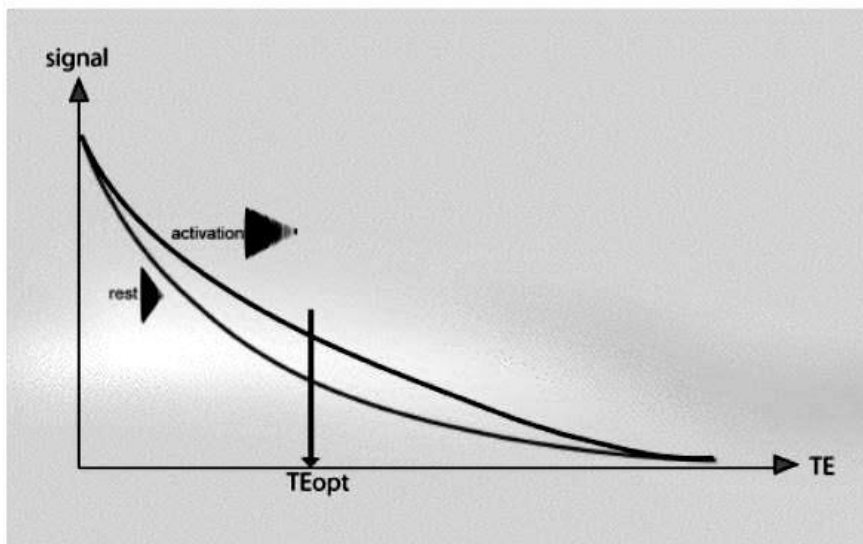


Figure 6: The effect of Echo time on T2* signal

The T2 *-weighted sequence used for fMRI is very sensitive to inhomogeneities in the magnetic field, resulting in signal distortions. This is especially a problem in brain areas where there is crossing between tissues (e.g. air filled sinuses) and metal shavings from prior surgeries. There exist strategies for overcoming these consequences, e.g. alternative MRI-pulse sequences, such as “spin echo BOLD fMRI” or “arterial spin labelling”, and also methods for mapping of B0-field variations to warp distortions after acquisition (Sumanaweera T. S et al, 1993). The degree of these inhomogeneities varies with the

strength of the static magnetic field, which also affects the BOLD fMRI signal intensity. It has been shown that an increased proportion of the BOLD signal arises from the brain tissue (and thus the active neurons) rather than draining veins at higher field strengths. Furthermore, the contrast-to-noise ratio also increases with higher field strength, giving a higher BOLD signal.

After fMRI scanning session, these images need to be pre-processed before further statistical analysis, in order to produce statistical parametric activation maps (t maps). This Statistical parametric mapping activation maps further needs to be interpreted for inference of results. Obviously the process from data acquisition to result interpretation consists of several steps (**explained in chapter 3, section 3.1.7.1.1.6.**) each susceptible to different sources of error. Thus, an expertise in fMRI data acquisition, statistical analysis and functional neuroanatomy is required to perform these investigations accurately

1.1.6 fMRI Paradigm Design

Most commonly during BOLD fMRI experiments, subjects have to perform certain tasks inside the scanner, and the difference in the BOLD signal during performance of the active phase and baseline phase, or task A and task B, can subsequently be analyzed. In task dependent fMRI the experimental designs are often called paradigms (e.g. hand movements, or cognitive tasks, such as language, planning, memory or spatial navigation).

The tasks are usually presented and stimulus collected using a software program like Eprime, or in-house designed programs. The participants view the task on an LCD screen or via a projector mounted outside the scanner bore. The subjects can view the screen through a mirror placed on the head coil or in goggles. The commonly the stimuli are presented according to an blocked design paradigm inspired by earlier works on PET (Raichle 1987), or event-related design inspired by ElectroEncephaloGraphy (EEG) and MagnetoEncephaloGraphy (MEG) studies.

The blocked design paradigm is easy to implement and analyze and have a high signal-to-noise ratio (SNR). Each individual task stimulus usually lasts 14-50 seconds and they are interleaved with control conditions of varying length. The event-related design is more complicated to implement and analyze and have a lower SNR. Each individual task stimulus usually lasts 1-10 seconds spaced apart with active and/or baseline task periods of varying length. Compared to blocked design, event-related design yields higher specificity in the neural correlates of the cognitive task being investigated, but with lower SNR. It is also possible to implement self-paced tasks, in which duration of each stimulus is not predetermined.

Furthermore, predetermined timing of each task condition can be avoided by employing alternative model free analysis methods such as individual component analysis (ICA). It should be noted that there is also task independent fMRI, i.e. resting state fMRI, where the person is resting during fMRI scanning.

1.1.7 BOLD fMRI- limitations and considerations

BOLD fMRI has rapidly become a standard method for studying brain activity. Still, the method has several limitations and shortcomings that must be taken into consideration to properly interpret results. In the following text, methodological issues will be discussed.

- a) The measured BOLD signal changes are not a direct reflection of neural activity. Instead it depicts regions with increased blood flow presumed to be caused by increased neural activity. The maximum signal is delayed from the onset of stimulus due to the time required for production and diffusion of vascular signal substances which dilates the vascular bed and causes a washout of deoxygenated haemoglobin. Therefore, temporal resolution in BOLD fMRI is inferior compared to EEG and MEG. On the other side BOLD fMRI has better spatial localization than EEG and MEG, thus being a complementary brain studying technique.

- b) Patterns of neural activity derived from BOLD fMRI experiments only show the relative differences in neural activity between task conditions. When an active condition is compared to a baseline condition, the results describe the neural activity that is statistically different from the latter. The baseline condition reflects resting state neural activity.
- c) Another confounding phenomenon is the underlying task-independent differences in measured BOLD signal among different subject groups. These differences can be caused by cerebrovascular disease, white matter inflammation, age-related changes in cerebrovasculature and autoregulatory mechanisms (D'Esposito, Zarahn et al. 1999), pharmacological effects and psychostimulant drug use (Turner et al. 2008). These BOLD signal differences might make group-wise comparisons between patients and healthy subjects inaccurate since an intrinsic signal differences are already present independent of the task.
- d) The ability to detect BOLD signal changes is often measured using signal to noise ratio (SNR) which is the relationship or power ratio between the signal and the background noise. The magnitude of BOLD signal changes induced by brain activity is weak usually in the range of 1-6% of the total signal. It is more robust for primary visual, motor and sensory functions than in higher cognitive functions such as memory, planning etc. (Huettel and Song 2004).
- e) BOLD sequence is based on a T2*-weighted gradient echo imaging sequence which is vulnerable to distortions and artifacts caused by several factors. First susceptibility artifacts may arise in regions close to airfilled spaces or sinuses. These regions include orbitofrontal cortex, parahippocampal/hippocampal cortices and the temporal lobes. Second, motion or physiology related artifacts can be caused by subject motion, cardiac pulsation or respiration. Third artifacts or distortions may be the results of

field inhomogeneity of the scanner. During data analysis, the ability to detect BOLD signal related to neural activity can be improved by several means. Motion correction can partially remove the effects of subject motion and the associated signal variability. Spatial smoothing with a Gaussian filter can facilitate the detection of true BOLD signal in statistical analysis by reducing noise (Rahman et al., 2008) and improves the fit of the data to the general linear model. High and low-pass filter (Poline et al., 1995) can remove noise in temporal domain such as physiological noise.

- f) Alternatively, cardiac pulsation and respiration can be monitored and modelled as effects of non-interest during data analysis. The ability to detect BOLD signal is further affected by statistical analysis method. Activation maps calculated from single-voxel based analysis are inherently limited by the SNR of the individual voxel. In ROI based approach some of the low SNR can be overcome, but at the cost of possible overlooking activities in other brain regions than those pre-defined. Also, it is essential to ensure adequate normalization of brains during group-wise comparisons using single-voxel based analyze methods.

Considering the paradigm design, the performance of any tasks inside the scanner should not involve movement of large muscle since any excessive motion will lead to head motion and motion related artifacts. The difficulty of the paradigm has to be adapted to suit the cognitive and motor ability of the test subjects to ensure adequate success rate. The duration of each paradigm should be kept short to prevent subject fatigue. Lengthy experiments can be divided into separate sessions to allow proper restoration in-between. The equipment required for task completion such as response buttons and screen for viewing the task has to be MRI compatible in order to function efficiently, safely and without disturbing the MRI signal significantly. In

term of sensory modalities, it is easiest to present visual stimuli and difficult to receive oral response from the test subject. In an fMRI paradigm, the stimuli or task is the independent variable and the measured BOLD signal is the dependent variable. Additional variables might be present in the paradigm and may correlate with the dependent and independent variable. These variables are called confounding factors and might cause incorrect data interpretation. Methods to minimize these effects include counter balancing and randomization. In counterbalanced experiments, the confounding factors are present in all conditions and will cancel each other out during comparison. For example during visual experiments which involve pictures in task conditions, a scrambled version of the same picture containing the exact same number of pixels of each color can be presented during the rest conditions. In randomized experiments, individual conditions are presented randomly to alleviate the effect of habituation, a psychological process in which psychological and behavioural response decreases as a result of repeated exposure to same or similar task condition over long time.

In BOLD fMRI experiments containing task conditions of varying difficulties, it might be favourable to perform the most challenging task first to avoid fatigue or if the result of that first task condition serves as the input of the next one. Particular attention should be paid to patients with brain disorders who often experiences difficulties in understanding and following instructions. Another factor that needs consideration during paradigm design is the timing of individual task and rest conditions. In epoch based and event related paradigm designs, timing is predetermined and therefore remains constant across subjects. Timing in epoch based paradigms can also be allowed to vary between subjects by terminating the task conditions automatically upon completion thus making the conditions self-paced. By doing so, the onset of the conditions will vary with TR and data sampling will

be distributed in time contributing to reduced bias and increased sensitivity in the final results (Veltman, Mechelli et al. 2002). Also self-pacing reduces neuropsychological effects such as fatigue and habituation by making individual task conditions more different and perhaps more interesting.

1.2 Diffusion Tensor Imaging (DTI) and Tractography

1.2.1 Introduction

DTI is an advanced MR imaging technique that can be used to illustrate the orientational properties of the diffusivity of water molecules (Basser P.J et al.1994, Beaulieu C, 2002). Usually, the information is contracted to two important diffusion parameters: (a) diffusion anisotropy, which represents the amount of directionality of water molecules, and (b) orientation of the axis along which water molecules travel preferentially. Application of this technique to the brain has been demonstrated to provide outstanding information on architecture of white matter pathways (Moseley ME et al, 1990; Pierpaoli C et al, 1996; Beaulieu C, 2002). Because now a days, there are no other imaging modalities that can provide comparable information. DTI is expected to become a sufficient tool for the assessment of brain anatomy and the diagnosis of various abnormalities of white matter tracts. The developments in post processing algorithms for DTI images also allow study of the three dimensional (3D) architecture of major white matter tracts, for which good agreement with postmortem anatomic studies has been reported (Mori S, 1999; Basser PJ, 1994).This section provides more detailed descriptions about the diffusion imaging technique, which was developed to achieve more accurate detections of anisotropic diffusion dominant in biological tissues, as well as a brief discussion of technique underlying white matter tractography in the human brain.

1.2.2 Diffusion of water molecules

All molecules with a temperature higher than absolute zero (i.e., $>-273.15\text{ }^{\circ}\text{C}$) are in constant motion. This phenomenon was first postulated by Robert Brown in 1828 (Brown .R, 1828) based upon the examination of random motion of pollen grains suspended in water. Although pollen grains are significantly larger than individual molecules, the behaviour explained by Brown is similar to that seen in molecules and thus, the molecular phenomenon is generally referred to as Brownian motion. Diffusion is thermally driven and in the simplest case is fully stochastic, with each molecule describing a “random walk” over time.

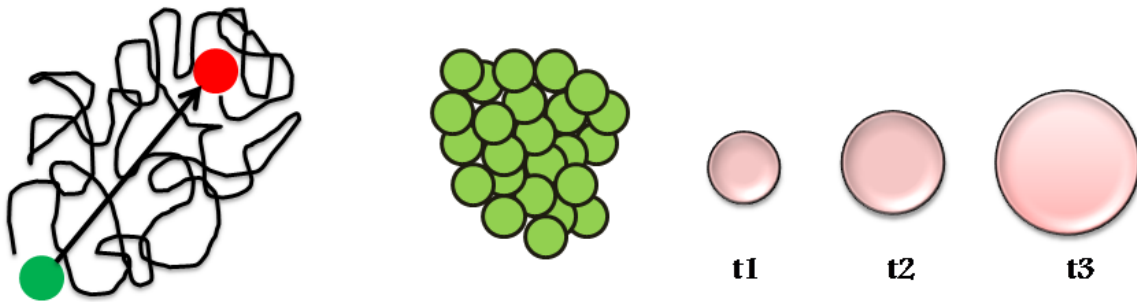


Figure 7: Random walk of water molecules over time (t)

Albert Einstein mathematically solved Brown’s findings (Einstein A., 1905). Let us assume several water molecules diffusing freely, each one with an initial location r at time, $t = 0$. If we allow them to diffuse for a time period T , each water molecule will then be in position r' . The diffusion coefficient D can be found by:

$$D = 1/6T \{ R^T R \}$$

where $R = r' - r$. The spin displacement in time is considered over the spin assembly. The root mean square displacement over time t is given by the equation:

$$r_{ms_n} = \sqrt{2nDt}$$

where n is the number of dimensions. The one dimensional displacement of water molecules is explained in **Figure 7**.

Diffusion is a random (i.e., isotropic) process and, therefore, D is directionally independent. The magnitude of D is dependent on the viscosity and temperature of the medium, and the size of the molecule. D of water at 37 °C is around $3.04 \times 10^{-3} \text{ mm}^2/\text{s}$. In the case of water molecules, the solute and the solvent are the same molecule, and the phenomenon is defined as self-diffusion, for which the simple random walk model can properly predict its behaviour.

1.2.3 Anisotropic Diffusion in Biological Tissues

Evidence from early studies has shown that diffusion of water protons in most biological tissues is anisotropic, i.e., signal attenuation due to diffusion is orientation dependent. Empirical results have shown that signal attenuation along the direction parallel to the white matter fibres is around four times that measured perpendicular to fibres (Le Bihan et al, 1995). Experimental observations (R.Turner et al, 1990) also indicate that diffusion coefficients measured for the three major brain compartments, white matter (WM), grey matter (GM) and cortical spinal fluid (CSF), are quite different. An isotropic diffusion with a diffusion coefficient similar to pure water at body temperature ($3 \times 10^{-3} \text{ mm}^2/\text{s}$) was observed only within CSF. Although nearly isotropic, the diffusion measured from GM was on average 2.5 times smaller than that of pure water. More signal attenuation, up to 10 times less than those of CSF, with high anisotropic diffusion characteristics was observed in different WM structures.

The origin of diffusion anisotropy in the brain is an active research field and controversies still remain. One hypothesis suggests that anisotropic diffusion in neural fibres may come from restrictions of the myelin sheath that becomes the major barrier of water diffusion (Hajnal JV et al, 1991). According to this hypothesis, within a very short time,

water diffusion does not reach physical boundaries and therefore its behaviour is a free, homogenous diffusion. With an increase of diffusion time, impermeable boundaries will restrict the diffusion and the measured diffusion coefficient will decrease. However, this restricted diffusion (**Figure 8**) failed to explain why there is still diffusion anisotropy, although to a less extent, before fibres are myelinated in the infant brain (Neil JJ et al, 1998). Moreover, experimental results also showed that measured diffusion coefficients did not change in WM/GM/CSF with increasing diffusion time (Le Bihan et al, 1995).

Another hypothesis suggests that diffusion in biological tissues is indeed hindered by structural organizations within tissues such as membranes and neural organelles. Instead of being prohibited from moving perpendicular to fibre bundles or the myelin sheath, water diffusion may take tortuous pathways to wander.

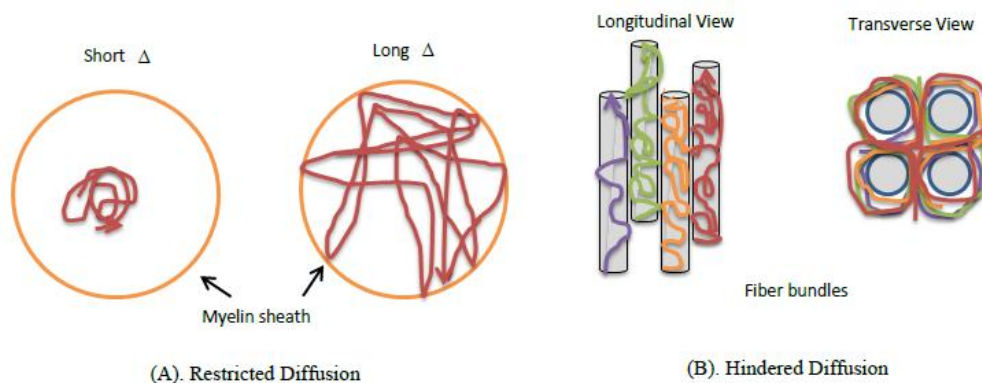


Figure 8: The origin of diffusion anisotropy in biological tissues. (A).The myelin sheath is thought to be the main barrier for water diffusion. Within a very short diffusion time, the displacement of water diffusion is much smaller than the dimension of structures in tissues and the diffusion is free. With increase of diffusion time, water begins to encounter with barriers and diffusion is restricted (B). In the hindered diffusion, the organization of structures in tissue no longer prohibits water to diffuse across them but instead creates more

torturous pathways for water diffusion perpendicular to the orientation of well-organized structures like neural fibre bundles.

1.2.4 Diffusion measurement using Nuclear Magnetic Resonance (NMR)

The effects of diffusion on the NMR signal have been known since the 1950s, when the spin-echo was described by Hahn (1950). A few years later, Carr and Purcell (1954) published their findings on quantitative T2 measurements, in which they recognize the significance of diffusion and even measure D of a water sample. These first attempts to measure D were based on the use of a constant perturbation of the main magnetic field which, among other problems, made the distinction of D-related effects from transverse relaxation difficult. However, it was the work of Stejskal and Tanner that facilitated the quantitative assessment of molecular diffusion coefficients by the use of a Pulsed Gradient Spin Echo Sequence (PGSE). The basic idea is to encode the spatial position of water molecules (spins) at $t = 0$, invert the spin phase with a π -pulse, and decode the spin position after time t . The spin position is encoded and decoded with the use of magnetic field gradients.

More specifically, after the application of $\pi/2$ radio-frequency pulse that places the net magnetization in the x, y plane with zero-phase, a magnetic field gradient with amplitude G and duration δ is turned on, which imparts a phase to the spins according to their spatial position. A π radio-frequency pulse then reverses the spins' phase. A second magnetic field gradient with the same characteristics as the first one (with a separation of time $=\Delta$) causes non-moving spins to retain their original phase. The NMR signal (echo) is acquired at this point. If the spins move during the time between the two magnetic field gradients (due to diffusion or any other cause), the spins will not rephase completely, which causes less NMR signal to be acquired. Note that the field gradients are applied linearly in one dimension, providing diffusion sensitization only to spins moving in that particular direction. That is, if a spin moves perpendicularly to the field gradient direction, it will not contribute to the loss of

NMR signal. The signal can be acquired through a spin-echo, as described above, or through a stimulated echo (Tanner J, 1970). The latter approach, being profoundly T1-weighted, minimizes the signal loss through transverse relaxation, even though its very nature translates into a 50% reduction of the original available signal. By modifying the characteristics of the PGSE sequence, one can increase or decrease the sensitivity to diffusion. If the amplitude of the gradients is increased (G), spins will require less motion to experience a different magnetic field, thus increasing phase change.

Alternatively, one can allow the spins to diffuse for a longer period of time, increasing the probability of the spins to dephase. The diffusion time is expressed as $\Delta - \delta/3$, where the $\delta/3$ correction accounts for the diffusion which occurs during the time in which the gradients are turned on (Stejskal & Tanner, 1965). The sensitivity to diffusion is expressed as

$$b = \gamma^2 G^2 \delta^2 (\Delta - \delta/3)$$

where γ is the gyromagnetic ratio of hydrogen protons (42.58 MHz/T). The above equation assumes that the local magnetic field gradients (independent of the diffusion-sensitizing gradients) are negligible in the sample. In areas of large magnetic field susceptibility differences, local magnetic field gradients are induced. Local gradients would impart further phase shifts to the spin that would not be fully recovered by the second gradient pulse, confounding the measurement of D. Any other magnetic field gradients or inhomogeneities there during the PGSE sequence must be present and equal during both diffusion sensitizing gradient pulses in order to precisely infer D. The tissue boundary between air and tissue is an example of this crisis. The amount of NMR signal available in a diffusion-sensitive experiment exponentially decays according to D, and it is expressed as:

$$S/S_0 = e^{-bD}$$

where S is the intensity of the signal obtained with the diffusion gradient on, and S_0 is the parallel signal intensity obtained without the use of diffusion sensitizing gradients, b is diffusion weighting and D is the “Apparent Diffusion Coefficient”. While originally developed for measuring D in samples (example: for grey matter, $D = 0.7 \times 10^{-3} \text{mm}^2/\text{s}$) and freely diffusing water at 37°C ($D = 3 \times 10^{-3} \text{mm}^2/\text{s}$), the PGSE and its variants can be used in MRI.

In this case, the volume of interest is divided into number of pixels (picture elements, in the two-dimensional case) or voxels (volume elements, in the three-dimensional case), and the diffusion coefficient can be calculated in each individual pixel or voxel. This approach is known as diffusion-weighted imaging (DWI) (Wesbey et al, 1984) and is routinely used in the recognition of ischemic brain injury (Sotak et al, 2002).

The diffusion-sensitizing gradients, as well as the radio-frequency pulses, must be turned on during a certain time, providing an effective diffusion time, $\Delta - \delta/3$ that is around 50-100 milliseconds. In biological tissues, the diffusion of water molecules depends not only on viscosity and temperature, but also on semi-permeable barriers such as cellular membranes. In order to measure viscosity, the diffusion time must be very small, limiting the interactions between the water molecules and semi-permeable membranes. Such short diffusion times are difficult to attain, as they require very strong gradients to be applied for a short period of time (δ). Tanner and Stejskal recognized the effect of diffusion barriers and were the first to propose the idea of measuring restricted diffusion of water molecules by varying the delay between the gradient pulses (Tanner&Stejskal, 1968). In this sequence the unique constant gradient field was split into two matched pulse, one placed on each side of the 180 degree RF pulse (Stejskal and Tanner, 1965) (**Figure 9**). This revision solved the bandwidth and slice-selection problem and also separated the diffusion encoding time (δ , the

duration of the gradient) and diffusion time (Δ , the time interval of the application of the first and second gradient) so that the mathematical expression was much simpler.

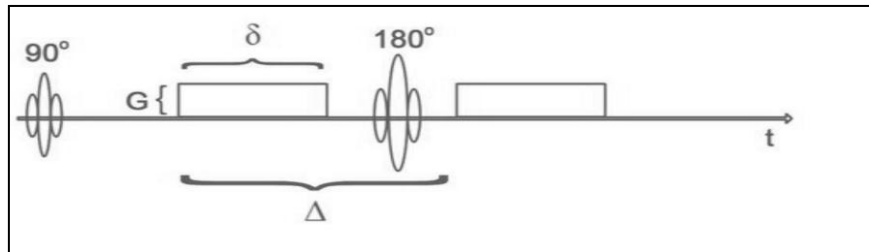


Figure 9: The Stejskal-Tanner pulsed gradient spin-echo (PGSE) sequence. Two matched gradients of strength G and duration δ separated by time Δ are placed on each side of the 180 degree RF pulse.

The diffusion of water molecules is not completely free in biological systems, due to the presence of cellular membranes and organelles, as well as due to the distinguishing tissue architecture. These features cause barriers to diffusion and cause anisotropy (i.e., diffusion is not equal in all directions). The white matter in the brain, which consists of several axonal bundles interconnecting distant discrete portions of the brain, shows a varying degree of architectural coherence. It therefore also shows the greatest degree of anisotropy in the brain.

Axons with similar trajectories are bundled together to form fascicule (also referred to as tracts or fiber bundles). Each axon can be surrounded several times by lipid-rich myelin sheaths, manufactured by oligodendrocytes. The myelin sheaths are periodically interrupted along the axon in the nodes of Ranvier, forcing the propagation of action potentials to be salutatory and therefore faster. Diameter of axons varies from <1 micro meter to approximately 15 micro meter.

Given the diffusion coefficient of water molecules at body temperature, a single water molecule can show a displacement of around 10 micro meter in 50-100 milli seconds (Le

Bihan et al,2002), certainly enough for it to encounter several axonal membranes and other barriers. The longitudinally-oriented microtubules within axons and rapid axonal transport appear to be minimally concerned in the generation of diffusion anisotropy (Beaulieu & Allen, 1994). When axons are structured coherently and strongly packed, as in fasciculi or bundles, the impermeable effects of the myelin sheaths and the axonal membranes merge, causing the overall diffusion measurements of white matter to be anisotropic (Pierpaoli et al, 1996; Beaulieu C, 2002). The grey matter, being structured in layers and functional columns, does not show the same degree of architectural consistency as the white matter. Because of this reason, water diffusion in the cortex does not show a high degree of anisotropy. The CSF, being basically water, shows fast diffusion that is almost isotropic.

1.2.5 The diffusion tensor

Given the diffusion in organized tissues being anisotropic, a scalar quantity such as D is not enough to represent the three-dimensional outline of the movement of water molecules. It is possible to quantify anisotropic diffusion by measuring the Apparent Diffusion Coefficient (ADC) using diffusion-sensitizing gradients oriented both parallel and perpendicular to the tissue, and obtaining the ratio between the two ($\text{anisotropy} = \text{ADC}_{\parallel} / \text{ADC}_{\perp}$). The orientation of the tissue, however, is classically not known in advance, as is the case of the white matter.

In 1994, Basser and colleagues introduced the formalism of the diffusion tensor (Basser PJ, 1994a; 1994b), which permits the quantification of ADC in any direction. Most importantly, the diffusion tensor provides important information on the micro-structure architecture and organization of tissue. The result from the DWI acquisitions is a set of volume images. The individual three dimensional (3D) images correspond to a scan along a certain diffusion encoding gradient direction. Each 3D-image is divided into voxels where each voxel corresponds to a volume in the scanned space. Thus, the measured ADC-value is

the average diffusion coefficient within a specified volume. At the voxel level, the diffusion process is sampled by the ADC values and the encoding directions pairs. The most common mathematical formalism for extracting quantitative data from the diffusion process is the diffusion tensor (Basser et al, 2002).The tensor inherits the properties of the covariance matrix. Thus, it is a 3×3 matrix that is symmetric and positive-definite.

$$D = \begin{bmatrix} D_{xx} & D_{xy} & D_{xz} \\ D_{yx} & D_{yy} & D_{yz} \\ D_{zx} & D_{zy} & D_{zz} \end{bmatrix}$$

The eigenvectors and eigenvalues ($\lambda_1, \lambda_2, \lambda_3$) of the tensor describes the three perpendicular axes in an ellipsoid with the longest axes (λ_1) in parallel with the main diffusion direction of the underlying voxel. Due to the symmetry, dual off-diagonal elements are equal (e.g., $D_{xy} = D_{yx}$). Thus, six parameters need to be estimated in order to completely describe the diffusion process. These are the three diagonal elements and the three upper (or lower) off diagonal elements (**figure 10**). The calculation of the six individual elements of the diffusion tensors requires at least six diffusion weighted images acquired along six non collinear directions. In addition, a non-diffusion weighted image is necessary to compute the MRI-signal reduction.

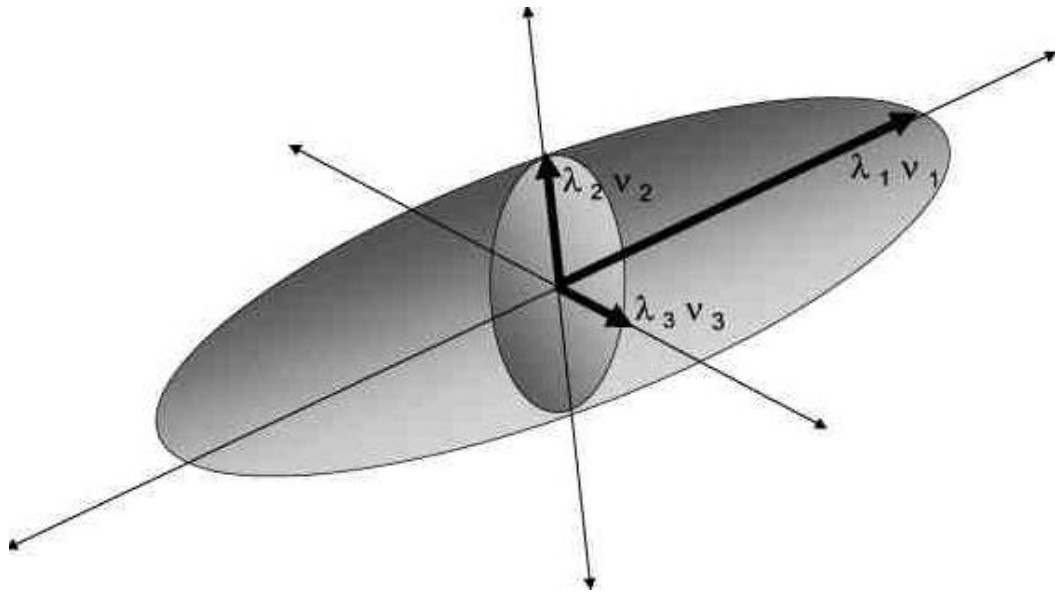


Figure 10: The geometrical representation of the diffusion tensor as an ellipsoid. The spectral components of the diffusion tensor are shown by the three eigen values (λ_1 , λ_2 and λ_3) and eigen vectors (v_1 , v_2 and v_3).

In highly organized white matter structures, the diffusion tensor has a cigar like shape. This structure reflects a higher diffusion along the predominant fibre orientation and, so, the diffusion ellipsoid elongates with the extreme at $\lambda_1 > 0$ and $\lambda_2 = \lambda_3 = 0$. In the absence of bounding structures, the molecules are free to diffuse in any direction leading to diffusion processing an iso-surface with a spherical shape as demonstrated in **Figure 11**. This corresponds to $\lambda_1 = \lambda_2 = \lambda_3$ at the perfectly isotropic diffusion case.

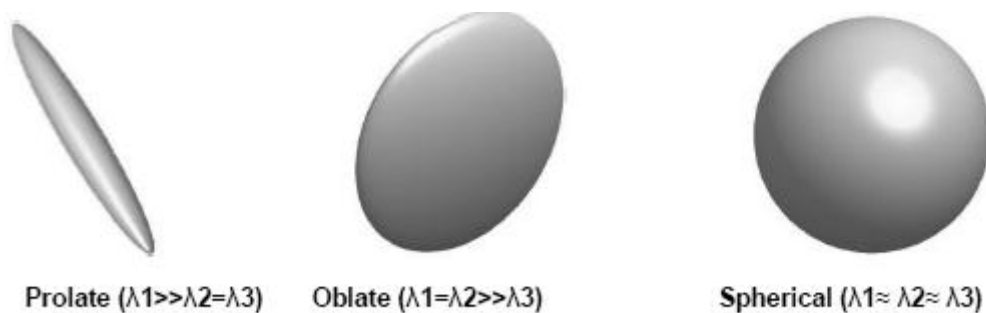


Figure 11: Degree of diffusion anisotropy ranging from highly anisotropic (linear tensors) in coherent medium to isotropic (spherical tensors) in fluid medium.

1.2.6 Quantification and Visualization of Tensor-derived Parameters

Several scalar parameters expressed as the function of the three tensor eigenvalues have been proposed to quantitatively describe the diffusion profile and emphasize different tensor properties. Among these scalar measures, mean diffusivity (MD) and fractional anisotropy (FA) along with the principal eigenvector (PEV) are most commonly used DTI-derived parameters to illustrate tissue microstructure and organization for each voxel within the image volume in DTI applications. **Figure 12** illustrates examples of parametric maps of these DTI-derived parameters along with T1-weighted (T1W) and T2-weighted (T2W) images of the same slice for better identification of different brain tissues.

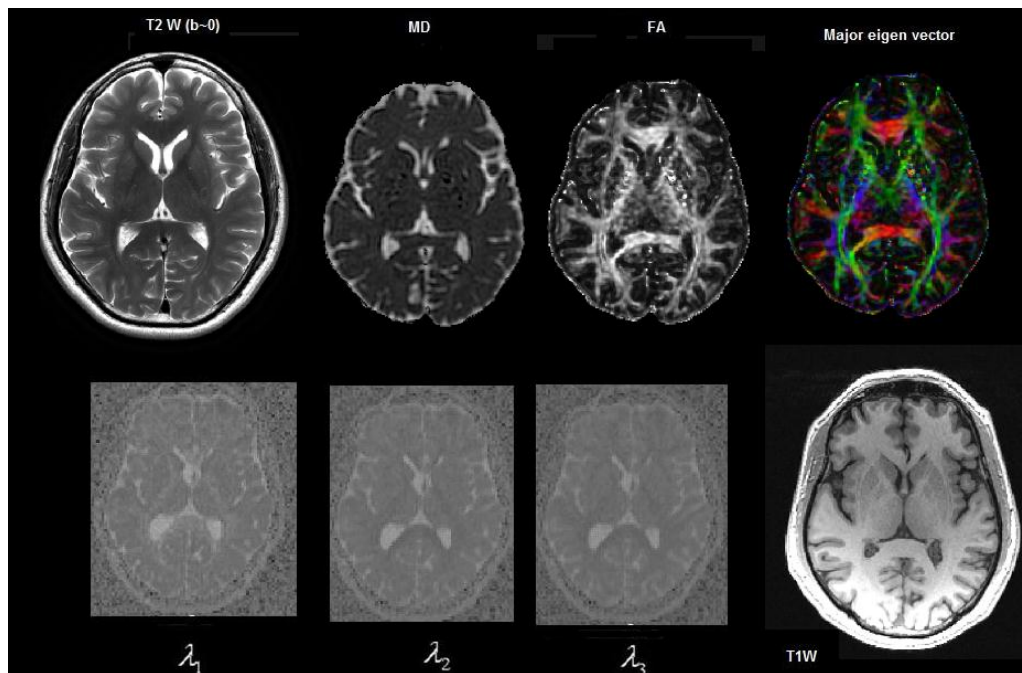


Figure 12: Quantitative maps derived from a DTI experiment. The images include the T2-weighted (T2W) “reference” (or $b=0$) image from DTI data; the mean diffusivity (MD note similar contrast to T2W image with CSF appearing hyper intense); fractional anisotropy (FA - hyper intense in white matter); the major eigenvector direction indicated by color (red = Right-left, green = Anterior-posterior, blue = Superior -inferior) weighted by the FA (note that specific tract groups can be readily identified); the major, medium and minor

eigenvectors (λ_1 , λ_2 , and λ_3 , respectively). A conventional T1-weighted at the same anatomical location is also displayed.

Both MD and FA are functions of the three eigen values and therefore are rotationally invariant. Mean diffusivity is defined as the mean value of the three eigen values and explained by the equation;

$$\text{MD} = \frac{(\lambda_1 + \lambda_2 + \lambda_3)}{3}$$

It provides a quantitative measure of the overall presence of obstacles to water diffusion in vivo in comparison with pure water. MD values are similar for both healthy WM and GM tissues (Pierpaoli C et al, 1996) in brain (MD $\approx 0.7 \times 10^{-3}$ mm²/sec) and therefore the image contrast is uniform for both WM/GM regions in a typical MD map. The most successful application of MD is to detect acute brain ischemia (Moseley ME et al, 1990) where MD is significantly decreased. FA, on the other hand, provides quantitative measures of the eccentricity of the diffusion ellipsoid (or the degree of anisotropy in terms of diffusion displacements) and is related to the geometric organization of structures within tissues, such as highly oriented white matter fibre bundles. FA is defined as below;

$$FA = \frac{\sqrt{(\lambda_1 - \langle \lambda \rangle)^2 + (\lambda_2 - \langle \lambda \rangle)^2 + (\lambda_3 - \langle \lambda \rangle)^2}}{\sqrt{\lambda_1^2 + \lambda_2^2 + \lambda_3^2}} \times \sqrt{\frac{3}{2}}$$

It quantifies the level to which the diffusion tensor deviates from being isotropic and is a dimensionless measure with a range from 0 (completely isotropic) to 1 (completely

anisotropic). FA provides the best contrast between GM and WM. PEV coincides with the long principal axis of the diffusion ellipsoid and defines the spatial orientation of the ellipsoid. It represents the most preferable diffusion direction within the in vivo environment consisting of unique anatomical arrangements of structures. Therefore, it is linked to the orientation of structures. The 3D PEV space can be visualized by assigning each component of PEV to a component in RGB color space. A useful way to illustrate 2D white matter fiber architecture is to generate a color encoded FA map (**Figure 13**) by combining the FA map and PEV.

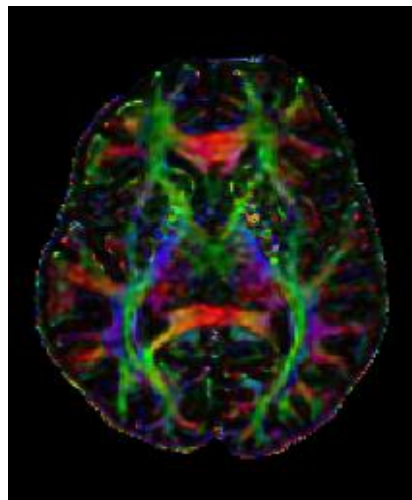


Figure 13: Color coded FA map indicating the orientation of white matter tracts. Red = Right-left, Green = Anterior-posterior, Blue = Superior –inferior.

The intensity of each pixel in a color FA map represents the level of anisotropy and the color indicates the orientation of white matter fibre bundles. By convention, red is associated with fibres running in the left-right direction, green with the anterior-posterior direction and blue with the superior-inferior direction. Moreover, PEV provides the key information for constructing the so-called white matter fibre tractography. Both ADC and FA

are frequently used as parameters for probing white matter properties such as restriction, hindrance, tortuosity and multiple compartments (Le Bihan 1995).

In healthy white matter DTI can be used to follow cerebral maturation in children and adolescence as increment in FA (Mabbott et al. 2009). In pathologic conditions structural barriers to water diffusion in white matter might be subjected to alterations of permeability or geometry, as a result ADC and FA might be changed when compared to unaffected and healthy white matter. After traumatic brain injury, diffuse axonal injury might occur and cause lower FA and higher ADC. These measurements may indicate histological abnormalities such as cytoskeletal misalignment, lobulation and axonal disconnection (Arfanakis, Haughton et al. 2002). Higher ADC and lower FA values are also seen in multiple sclerosis caused by edema, demyelination, inflammation and axonal loss and in Alzheimer's disease which is likely caused by Wallerian degeneration and gliosis.

1.2.7 White matter fibre Tractography

Fibre Tractography is a visualization technique for cerebral axonal bundles based on DTI measurements (Bihan, Mangin et al. 2001; Mori, Frederiksen et al. 2002). By sequentially piecing together discrete and connecting estimates of the principal eigenvectors, the white matter axonal bundles may be visualized. In recent years, several fibre tracking algorithms have been developed such as probabilistic tractography (Behrens, Woolrich et al. 2003; Parker, Haroon et al. 2003) and deterministic tractography (Mori, Crain et al. 1999).

The objective of probabilistic tractography is to obtain a connectivity index along white matter pathways that reflects fibre organization giving a statistical likelihood for the connection from a certain area in the brain to another predetermined region. In probabilistic tractography, the direction is drawn from a distribution of possible orientations. Instead of

reconstructing just a single trajectory in deterministic tractography, probabilistic tractography propagates a large number of pathways from a given seed point. The result of probabilistic tractography is a set of multiple pathways passing through the seed point, and the direction is drawn from a distribution of possible orientations.

Deterministic tractography, on the other hand, follows the direction of the largest eigenvector in each voxel, and virtually reconstructs a tract. The assumption is that the principal eigenvector is parallel to the underlying dominant fibre orientation in each voxel and forms a tangent to the space curve traced out by the white matter tract. The path is propagated from a region of interest (seed point) which is manually placed. It propagates from here, parallel to the principal eigenvector until the boundary of the voxel is encountered, at which point the algorithm traverses the next voxel in a direction parallel to the eigenvector at the center of the new voxel. One of the most commonly used deterministic tracking algorithms is the Fibre Assignment By Continuous Tracking (FACT) algorithm (Mori, Crain et al. 1999) (**Figure 14**). It utilizes a method called fast marching tractography (Basser and Pierpaoli 1996) to find the axonal bundles in the brain. FACT initiates tracking in all voxels in a given data set at once and does not require a seed point to proceed. The reconstructed tracts can be used as a mask to select a region of white matter for analysis. In this dissertation, a deterministic tractographic approach (Muthusami et al., 2013) was used to track the language white matter tracts.

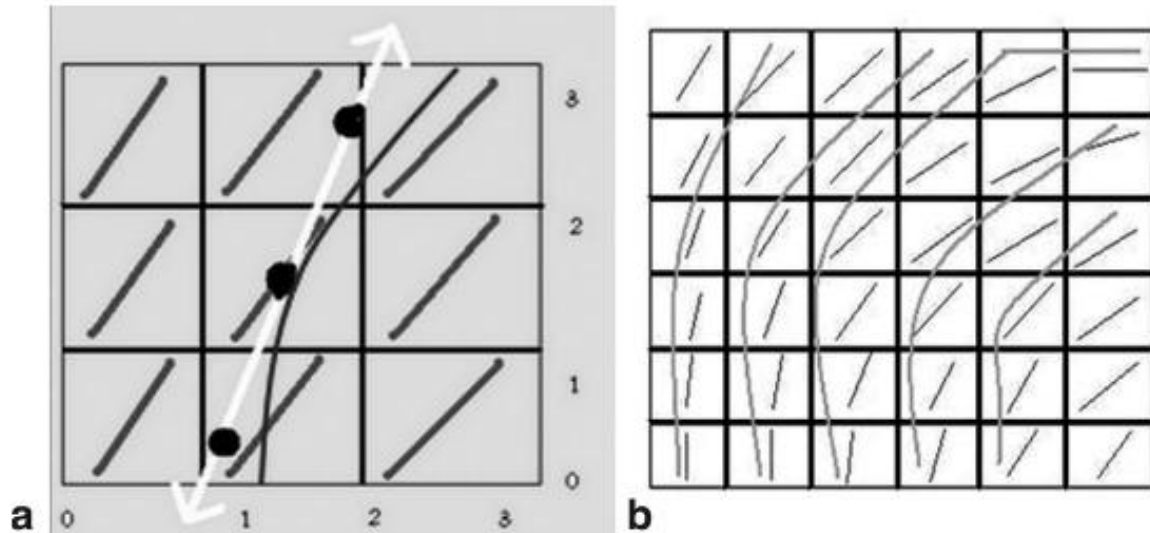


Figure 14: The concept of fibre allocation by continuous tracking (FACT) used for deterministic diffusion tensor tractography. (a) Illustrates a schematic representation of this line propagation technique. The squares represent voxels, and the oblique lines within them, the direction of the largest eigenvector in that voxel. Discrete co-ordinates are converted to a continuous coordinate which yields a “tract” depicted here by the white line. Interpolation is then performed with distance-averaged vector orientation using a predetermined step size to obtain a continuous smooth tract, depicted here by the curved line. (b): FACT performed over several voxels, with predefined track-termination parameters, showing an array of extracted tracts.

1.2.8 DTI- limitations and technical considerations

DTI-MRI images are extremely prone to movement related artifacts caused by head motions and physiological noise such as cardiac pulsations and respiratory movements (Wirestam, Greitz et al. 1996). Also, the DTI sequence itself results in image distortions since it relies on heavy gradient pulses which induce eddy currents in the antenna coils. Moreover, inhomogeneity in magnetic field is a concern in tissue regions of differing magnetic

susceptibility such as in brain areas with soft tissue and air interfaces (Frahm, Merboldt et al. 1988). A number of solutions to these problems have been suggested.

- a) The duration of the experiment should be kept at minimum as prolonged experiments increase the risk of subject's head movements. During scanning session, light physical constraints should be practical and cardiac and respiratory gating may be used for reducing physiological noise. Head-motion and eddy current artifacts can be corrected using several mathematical algorithms. It is also possible to reduce susceptibility artifacts by placing diamagnetic passive shims in the roof of the mouth or more technically by using B₀-field map correction (Anderson and Gore 1994; Jezzard and Balaban 1995).
- b) Limitations also concerned to DTI data analysis. In fibre tractography, the common voxel size is a cube a few cubic millimetres large, which might contain tens of thousands of axonal sections. Tractography is therefore an inaccurate technique in regions with crossing or kissing fibres and for small and winding pathways (Johansen-Berg & Behrens, 2006). The way to solve this problem (Mori & van Zijl, 2002) is to use advanced diffusion imaging techniques such as High Angular Resolution Diffusion Imaging or HARDI (Tuch Reese et al. 2002) and Q-ball imaging (Tuch, Reese et al. 2003). In addition to imaging related artifacts, brain pathological lesions and edema makes tractography even more challenging.

Even though tractography allows for virtual dissection of white matter pathways, it must not be confused with anatomical dissection as significant difference in tract locations are observed between tracts derived from DTI and histology. It should also be noted that tractography is a subjective procedure still missing a gold standard approach, and this process profoundly depends on the user performing the tractography where detailed knowledge of neuroanatomy is a prerequisite, thus making also DFT a user dependent process.

1.3 Voxel Based Morphometry (VBM)

1.3.1 Introduction

VBM is a fully automated technique which involves voxel-wise statistical analyses of MR to explore differences in grey matter concentration between two groups of subjects throughout the brain on magnetic resonance (MR) images with minimal operator dependence (Ashburner and Friston, 2000; Ashburner et al., 2003). In traditional brain morphometric approach, volume of the whole brain or subcortical structures is measured by drawing regions of interest (ROIs) on brain images obtained from MRI and calculating the volume enclosed. However, this method is time consuming and can only provide volume measurements of rather large areas, smaller differences in volume may be unobserved.

The primary goal of VBM is to identify differences in the local composition of brain tissue, while discounting large scale variations in gross anatomy and position. This is achieved by spatially normalising all the structural brain images to the same standard stereotactic space, then segmenting the normalised images into grey and white matter, to take account of interindividual variation in gyral morphology. Normalization method gets rid of most of the large variations in brain anatomy among subjects. Next step involves smoothing the grey and white matter images so that each voxel represents the average of itself and its neighbours and the image volume is compared across brains at every voxel. Final step in VBM employs a statistical analysis to localize significant differences between two or more experimental subject groups. The output of this technique is a statistical parametric map showing regions of grey or white matter signal intensity changes.

Recently, a modified version of VBM so-called optimized VBM (**figure 15**) technique was introduced by Good et al in 2001, which incorporates additional spatial pre processing steps before the statistical analysis. It is an effort to improve image registration and segmentation. In particular, the optimized VBM method also includes automated removal of

non-brain voxels, image registration onto customized stereotaxic templates, and submission of tissue-specific (e.g., grey matter, white matter) normalization parameters. Similar to standard VBM analyses, voxel-wise statistical analyses on these images provide statistical parametric maps of grey matter concentration (GMC) or volume differences between cohorts.

An additional modulation step is also often included in optimized VBM technique, which multiplies grey matter voxel values by the Jacobian determinants, that is, the determinant of the deformation parameters generated from spatial normalization step. This method allows voxel wise comparisons of grey matter volume (GMV) differences between groups.

One important means in which standard and optimized VBMs differ is with respect to the reference neuroanatomical template used for spatial normalization step and segmentation of images. Standard VBM uses the default SPM99 template, the 148 normal MRI data set of Montreal Neurological Institute (MNI148), while optimized VBM uses a study-specific template, obtained by averaging the spatially processed images of all patients and controls. By using VBM, the volume of the whole brain or its subparts can be measured either by drawing regions of interest (ROIs) on images from brain scanning or atlas based method for calculating the volume enclosed. The voxel based morphometric approach for an investigation of regional brain differences across subjects may use the following steps:

- (a) Construction of a study-specific brain image template with a balanced set of left and right handed males and females.
- (b) Construction of white and grey matter templates from brain segmentation.
- (c) Construction of symmetric grey and white matter templates by averaging right and left cerebral hemispheres.
- (d) Segmentation and extraction of brain image, e.g., removal of scalp tissue in the image.
- (e) Spatial normalization onto the symmetric templates.

- (f) Correction for volume change (applying a Jacobian determinant)
- (g) Spatial smoothing.
- (h) Actual statistical analysis by the general linear model, i.e., statistical parametric mapping.

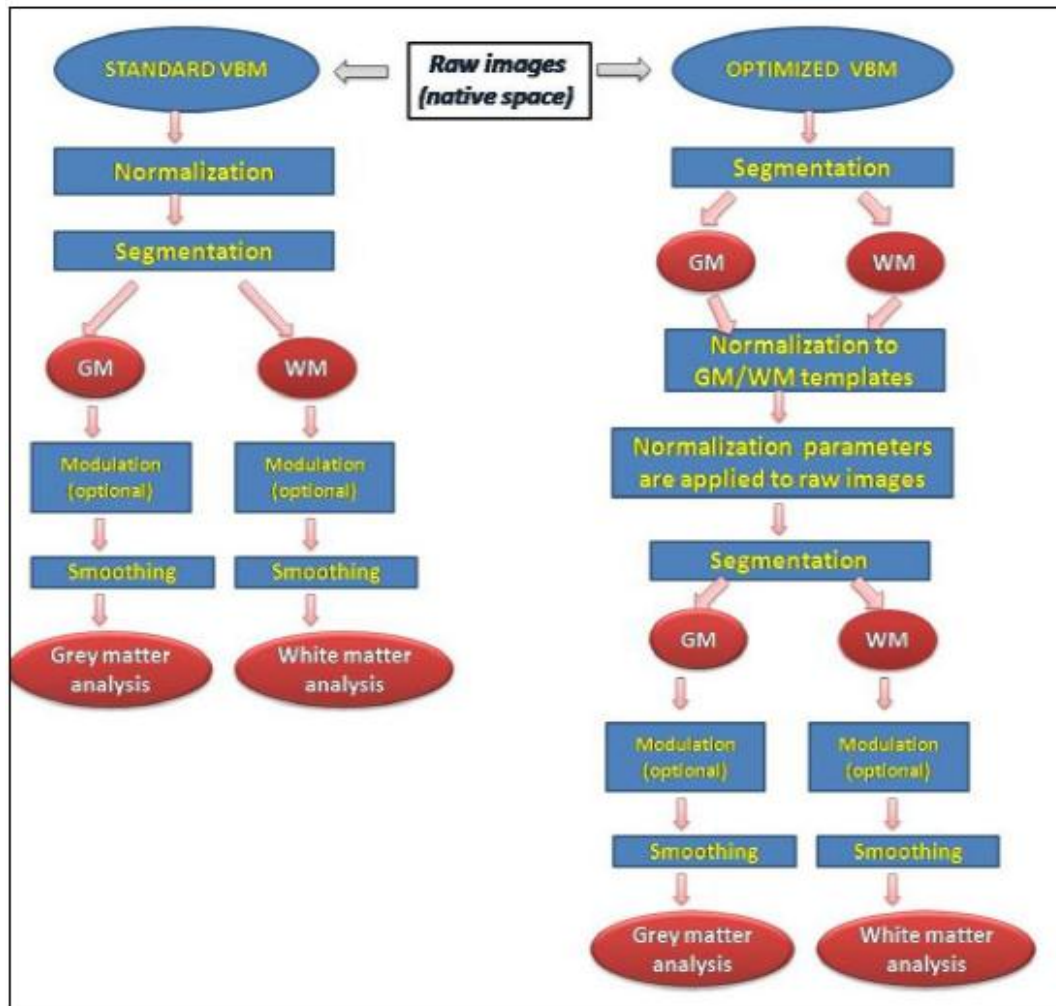


Figure 15: Steps involved in standard and optimized VBM

1.3.2 Steps in VBM analysis

1.3.2.1 Spatial Normalization

Spatial normalization involves registering the subject's MRI images to the same template image. Mainly two steps are involved in this process. The first step (Linear registration) includes estimating the 12 optimum parameters (3 translations and 3 rotations (rigid-body) + 3 shears+ 3 zooms – **figure 16**) affine transformation that maps the individual

MRI images to the standard template. The second step (Nonlinear registration) accounts for global nonlinear shape differences, which are modelled by a linear combination of smooth spatial basis functions. This step involves estimating the coefficients of the basic functions that reduce the residual squared difference between the subject's image and the template, while simultaneously increasing the smoothness of the deformations. The resultant spatially normalised images should have a relatively high-resolution (1mm or 1.5mm isotropic voxels), so that the grey and white matter segmentation is not excessively confounded by partial volume effects, that arise when voxels contain a mixture of different tissue types.

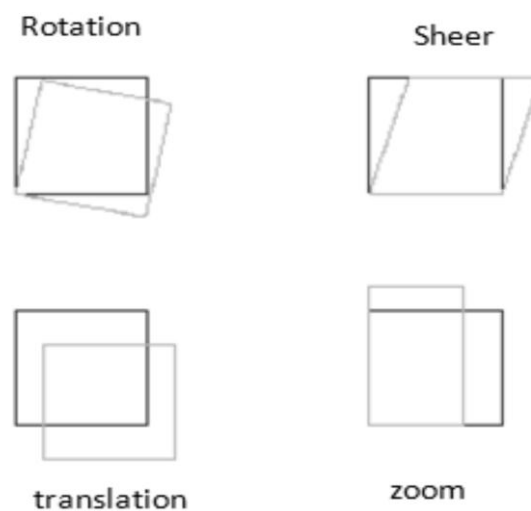


Figure 16: Normalization by 12-parameter affine transformation for linear registration

1.3.2.2 Segmentation

The spatially normalized images are then segmented into grey matter, white matter, cerebrospinal fluid and three non-brain partitions (**figure 17**). This is usually achieved by combining a priori probability maps or “Bayesian priors”, which encode the information of the spatial distribution of different tissues in normal subjects, with a mixture model cluster analysis which identifies voxel intensity distributions of specific tissue classes. The segmentation step also includes an image intensity non-uniformity correction to account for

smooth intensity variations caused by different positions of cranial structures within the MRI coil. In order to obtain optimum results, the segmentation method requires a reasonable contrast between different tissue types.

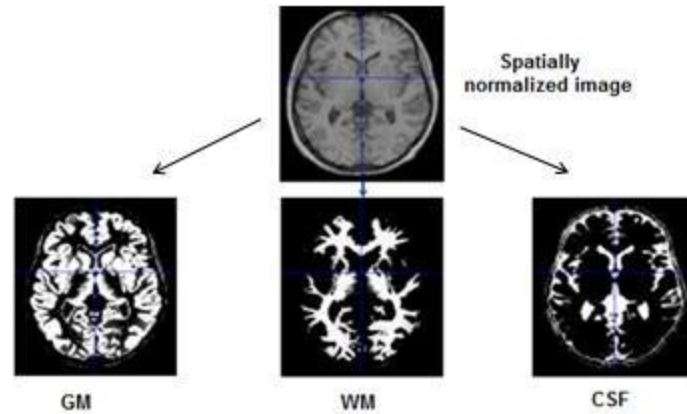


Figure 17: Segmentation of spatially smoothed images to Grey matter, White matter and CSF

1.3.2.3 Smoothing

The segmented grey and white matter images are then smoothed by convolving with an isotropic Gaussian kernel. The size of the smoothing kernel should be comparable to the size of the expected regional differences between the groups of brains, but most studies have employed a 12-mm FWHM kernel. The motivation for smoothing the images before the statistical analysis is three-fold. First, smoothing ensures that each voxel in the images contains the average amount of grey or white matter from around the voxel (where the region around the voxel is defined by the smoothing kernel). Second, the smoothing step has the effect of rendering the data more normally distributed by the central limit theorem, thus increasing the validity of parametric statistical tests. Third, smoothing helps compensate for the inexact nature of the spatial normalisation. Smoothing also has the effect of reducing the effective number of statistical comparisons, thus making the correction for multiple comparisons less severe.

1.3.2.4 Statistical Analysis

The final step of a VBM procedure involves a voxel-wise statistical analysis. This employs the general linear model (GLM), a flexible framework that allows different statistical tests such as group comparisons and correlations with covariates of interest. The standard parametric procedures such as T tests and F tests used are valid providing that the residuals, after model fitting are normally distributed. If the statistical model is appropriate, the residuals are most likely to be normally distributed once the segmented images have been smoothed. The results of these standard parametric procedures are statistical parametric maps. Since a statistical parametric map comprises the results of many voxel wise statistical tests, it is necessary to correct for multiple comparisons when assessing the significance of an effect in any given voxel. A standard Bonferroni correction for multiple independent comparisons would be inappropriate here, given the smoothing and the fact that grey or white matter in contiguous voxels is highly correlated. Thus, corrections for multiple dependent comparisons are made using the Theory of Random Fields. It should be noted that the Random Field correction should be based on the local maxima of the t statistic rather than the extent statistic which relates the cluster size. This is because, for a correction based on the extent statistic to be valid, the smoothness of the residuals needs to be spatially invariant throughout the brain.

1.3.3 VBM limitations and technical considerations

While performing VBM analysis, It should be noted that spatial normalisation does not attempt to match every cortical feature exactly, but merely corrects for global brain shape differences. This is because VBM tries to detect differences in the local concentration or volume of grey and white matter having discounted global shape differences. Indeed, if the spatial normalisation was perfectly exact, all the segmented images would appear identical

and no significant differences would be detected at a local scale. In the case of segmentation process, the central grey matter structures have image intensities that are indistinguishable from that of white matter. So the classification of different tissue types is not accurate in these brain regions.

Another important problem is concerned with partial volume effects. Since the model assumes that all voxels contain only one tissue type, the voxels which contain a mixture of tissue types may not be modelled correctly. In particular, those voxels at the interface between white matter and ventricles. The standard parametric procedures (T tests and F tests) typically used in VBM are valid providing that the residuals, after fitting the model, are normally distributed. This raises the possibility that non-normality in the error terms can make statistical inferences invalid in some VBM studies. The nature of grey and white matter changes identified with VBM is still poorly understood especially in healthy subjects. In studies of Alzheimer's dementia and other degenerative disorders, a neuronal loss is likely to be the primary cause of the grey and white matter changes observed in VBM. However, the interpretation of grey and white matter differences may be problematic when subtle changes in brain structure are observed in association with neurological and psychiatric dysfunction.

CHAPTER 2

LITERATURE REVIEW

2.1 Introduction

2.1.1 Epilepsy and Epilepsy Surgery

Epilepsy is one of the most common neurological conditions characterized by occasional, excessive, disorderly discharge of nervous tissue that result in seizures. A seizure may appear as a brief stare, a change of awareness or as a convulsion. The 19th century neurologist **Hughlings Jackson** defined the epileptic seizure and suggested “a sudden excessive disorderly discharge of cerebral neurons “as the causation of epileptic seizures. There are recurrent and unprovoked seizures in epilepsy. Any seizure disorder that cannot be explained by easily reversed, transient metabolic or toxic conditions is considered as epilepsy in practice (Dodson WE, 2004). Thus, epilepsy is not a single condition, but many diverse syndromes with very various etiologies and pathophysiologies, all sharing the occurrence of abnormal, synchronized electrical activity. Due to this heterogeneity and the large number of syndromes under the broad term of epilepsy, such disorders are further classified according to the type of the seizure and EEG (Forsgren L, 2004; Engel J.2006).

While considering all forms of epilepsy, the occurrence of the disease ranges from 5-17/1,000 people, with 40-150 new cases per 100,000 persons diagnosed annually (Forsgren.L, 2004). Interestingly, 2-4% of all children suffer from febrile seizures between the ages of one and five, but the majority of them do not develop epilepsy. About 90% of the adult epilepsy cases have symptomatic partial or localization related seizures (Hauser, 1992; Camfield & Camfield, 1996). Epilepsy affects both genders nearly equally, in spite of socioeconomic state. The largest annual frequency is seen at the extremes of life, with developmental, congenital and infectious disorders as common beginning in children, and

symptomatic (e.g. secondary to stroke or trauma) epilepsies in the elderly population. Disability due to epilepsy accounts for approximately 1% of the global burden of disease, which position epilepsy just after major affective disorders, dementias and alcohol dependence among primary disorders of the nervous system. Treatment using antiepileptic drugs (AEDs) is the first choice of treatment in both adults and children epilepsy patients. However, this treatment, though symptomatic by preventing seizures from occurring, does not treat the essential cause of the epilepsy.

Approximately two-thirds of patients with epilepsy become seizure-free on established antiepileptic drug treatment (Kwan, P & Brodie, M J, 2000). Patients who respond to drug therapy typically do so using a single anti-epileptic drug. About one-third of epilepsy patients may be referred to as “medically refractory epilepsy”. This group exhibits different etiologies including hippocampal sclerosis, malformations of cortical development inflammatory or infectious conditions, low-grade tumors, arteriovenous malformations, and genetic syndromes. However, in up to 30 % of these patients, a structural reason of the epileptic seizures cannot be found, even if optimal neuroimaging techniques are used. For medically refractory epilepsy, an often used recommendation is to investigate epilepsy surgery as an option in patients with focal epilepsy when AEDs have failed. The common duration of medically refractory epilepsy prior to surgery in adults is of the order of 20 years (Eriksson, S, 1999; Berg, A T, 2004). This may cause unavoidable suffering and high degree of mortality as patients with medically refractory epilepsy has a significantly increased risk of sudden death (Nilsson.L et al, 1999). Hence, patients with epilepsy refractory to medical treatment should be rapidly referred to a dedicated epilepsy centre where different treatment options, including epilepsy surgery, can be done. Epilepsy surgery is defined as a neurosurgical intervention performed to eliminate the epileptogenic tissue (the seizure onset zone) so as to maximize seizure relief, minimize side effects and improve the quality of life.

Considering the severity of the epilepsy in the population operated on, epilepsy surgery can be accepted as a successful therapy (Rosenow and Luders 2001). The main objective of epilepsy surgery is a complete disconnection of epileptogenic zone and this has to be achieved by preserving the eloquent cortex. Eloquent cortex are areas in the brain that sub-serve important and useful functions such as motor, sensory, visual, language and memory functions.

The main eloquent language areas (**figure 18**) are, (a) the posterior superior temporal gyrus pSTG, which is engaged in early cortical stages of speech perception (b) Dorsolateral prefrontal cortex (DLPFC) which is involved in auditory motor integration by mapping acoustic speech sounds to articulator representations (c) Ventrolateral prefrontal cortex (VLPFC), serves as a sound-to meaning interface by mapping sound-based representations of speech to widely distributed conceptual representations.

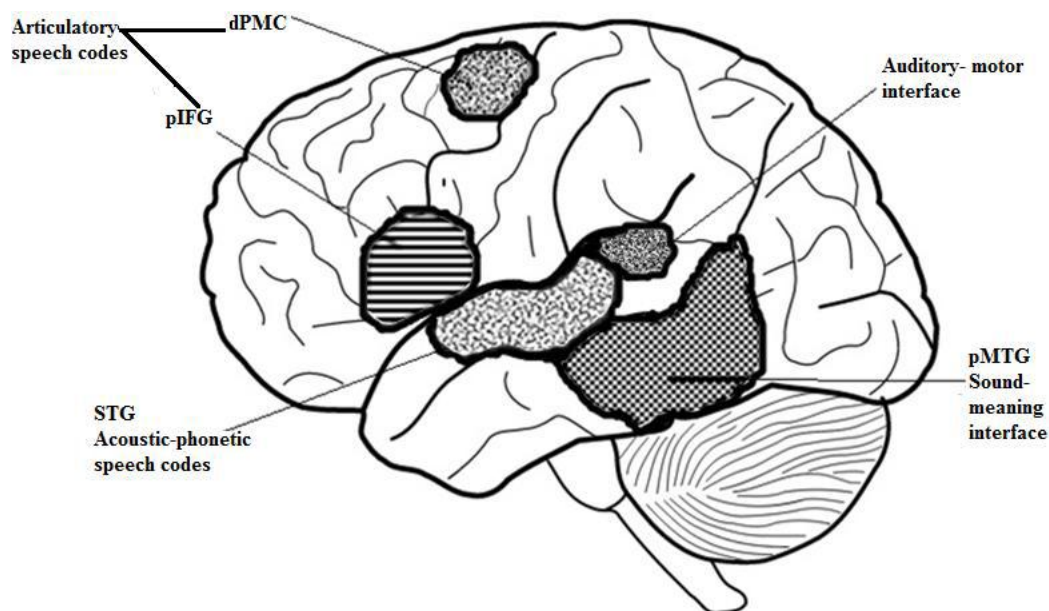


Figure 18: Eloquent cortical language areas. pIFG = posterior inferior frontal gyrus; dPMC = dorsal premotor cortex; STG = superior temporal gyrus; pMTG = posterior middle temporal gyrus.

It must be noticed that the epileptogenic zone is a theoretical concept, even if seizure freedom is accomplished following cortical resection, it is possible that resection of a smaller area may have resulted in the same outcome. Therefore, we can establish that the epileptogenic zone was included in the resection, but do not know its exact extent.

At the end of the nineteenth century John Hughlings Jackson reported that certain brain regions were associated with specific seizure characteristics (Jackson, J H, 1899). Based on Jackson's findings the first successful epilepsy surgery was performed by Victor Horsley in London at the end of the 19th century. The cortical areas to be resected were determined by careful neurological examination and observation of the seizures. With the discovery of electroencephalography (EEG) in 1929 the seizure onset could be localized more accurately. This led to a rebirth of the interest in epilepsy surgery and by 1950 over 70 TLR had been performed by Wilder Penfield at the Montreal Neurological Institute, using only clinical and neurophysiological localisation of the epilepsy (Penfield, H F, 1952). The beginning of video-EEG monitoring and modern neuroimaging, especially high-resolution MRI, has greatly facilitated the localization of epileptogenic lesions (Von Oertzen, J, 2002).

Nowadays, epilepsy surgery is an established treatment for medically refractory epilepsy with proven benefit in terms of seizure outcome and improved quality of life (Wiebe, S et al, 2001). Two main types of procedures can be identified for epilepsy surgery: i) resective procedures, aiming at removing cortical areas responsible for producing the seizure and ii) disconnective procedures, used in the case where the seizure focus cannot be removed, but by disrupting its connections the spread of seizures to adjoining brain regions can be limited or abolished. The resective procedures include Temporal lobe resection, extra temporal resection, lesionectomies including resection of the surrounding epileptogenic zone which can involve any of the frontal, parietal, occipital lobes or the insula and hemispherectomy/hemispherotomy. The main disconnective procedure is callosotomy but

disconnection of hypothalamic hamartoma and subpial transection to control seizure propagation also belong to this group. Vagal nerve stimulation, aiming at reducing the seizure frequency, can be used as a palliative approach when none of the other procedures mentioned are feasible.

2.1.2 Presurgical evaluation in epilepsy

The primary goal of presurgical evaluation is to identify the epileptogenic zone. In the case of localization-related syndrome which does not respond to medication appropriately, the origin of the seizures must be sought in order to estimate the plausibility of its surgical resection and potential cure. By using surface electrodes in a standard EEG it is possible to detect the synchronization of the electrical activity of the pyramidal cells in the brain cortical areas.

Usually, the EEG is performed in the inter-ictal period, when its sensitivity varies from 30 to 80% (Pillai J & Sperling MR, 2006). Long-term (3-15 days) EEG and video monitoring highly increases the power of this diagnostic tool allowing electro-clinical correlations to be made and hence it provides important information on the lateralization of seizure onset (Erlichman M, 1989). Whilst the scalp EEG has good temporal resolution, it has very low spatial resolution, cannot identify small areas of epileptic activity and commonly cannot detect abnormal activity generating from deep gray matter structures. Moreover, a great portion of cortex must be involved in epileptiform activity for it to be measurable with surface EEG (R Cooper et al, 1965). Because of these facts, it is sometimes indispensable to perform invasive intra-cranial EEG, via surgical placement of depth electrodes or sub-dural grids.

Advances in neuroimaging have also considerably changed the clinical approach to the patient with epilepsy. Wide ranges of imaging techniques are available for imaging the epileptogenic zone, including high-resolution T1 MRI, T2 signal quantitation, MR

spectroscopy, diffusion imaging, Positron Emission Tomography (PET), Single- Photon Emission Computed Tomography (SPECT), functional Magnetic Resonance Imaging (fMRI), Diffusion weighted Imaging (DWI) and simultaneous EEG(Electroencephalography)-fMRI. Another goal of pre-surgical evaluation is to determine the lateralization of brain functions and to decrease the damage of brain functions during surgery & intervention to its minimum. To preserve the eloquent brain areas, we have to determine the functionally active areas precisely.

The traditional methods for lateralization of brain functions & mapping of eloquent cortex are, (a) Intracarotid amobarbital (Wada-test) , which was considered as a goldstandard approach for lateralization of language and memory functions but has many limitations such as invasiveness, vascular anomalies and vascular variations interfering the lateralization results and failure to provide intracarotid localization. (b) Intraoperative cortical stimulation in awake patients and (c) Intraoperative recording of sensory evoked potentials. Disadvantage of these methods are their requirement of special devices, the higher costs needed and invasiveness. Since the mesial temporal lobe is the most common epileptogenic region of brain,“Temporal lobe epilepsy” (TLE) is considered as the frequent form of epilepsy. A common cause of medically refractory TLE is Hippocampal Sclerosis (HS) (**figure 19 a**).The condition has a good outcome following a common surgical procedure called Anterior Temporal Lobe Resection (ATLR) (**figure 19 b**).

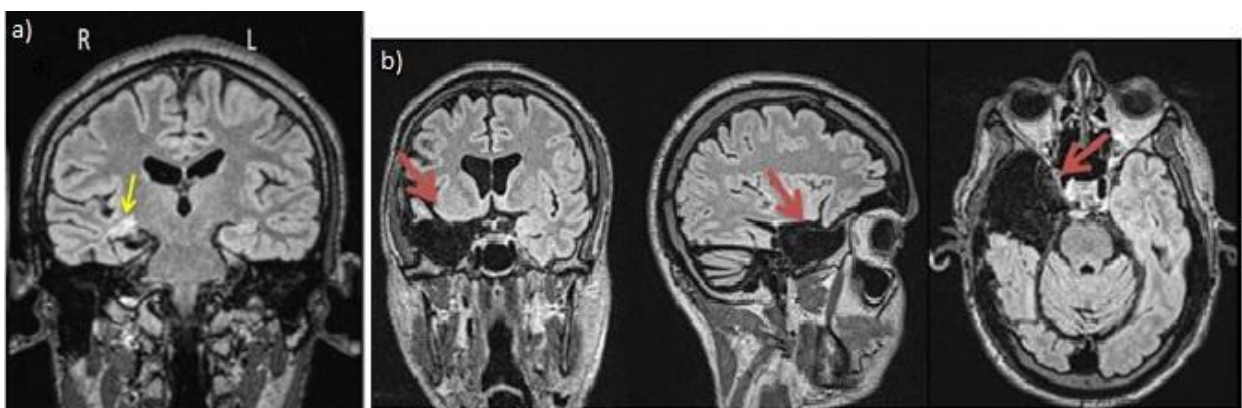


Figure 19: (a) Patient with right hippocampal sclerosis (HS - yellow arrow); (b) Anterior Temporal Lobectomy (ATLR- red arrows)

2.2 Mesial Temporal Sclerosis (MTS)

MTS refers to an explicit lesion of the hippocampus and other mesial temporal structures such as the amygdala, uncus and parahippocampal gyrus, characterized by neuronal loss and gliosis. It is the most widespread temporal lobe lesion resected for intractable seizures (Earle KM et al, 1953; Bruton CJ et al, 1994). Another histopathological feature of MTS is granule cell dispersion, in which the granule cells lose their tightly packed distribution, characterized by thickening and blurring of the dentate nucleus (Houser CR , 1990). TLE can be further classified according to its origin as mesial or neocortical, although the clinical manifestations of both are fairly similar (Burgerman R.S et al, 1995). More than half of the TLE patients experience simple partial seizures, or auras, that are complex in nature and often difficult to describe (Quesney LF et al, 1986).

2.2.1 Anterior Temporal Lobe Resection (ATLR)

ATLR leads to effective treatment of seizures in 60-80% of drug-refractory epilepsy cases (Wiebe et al., 2001; Tassi et al., 2009) but it may be associated with disrupted lateralization and localization of brain language function (Penfield & Jasper, 1954). It carries a 30–50% risk of decline in naming ability when performed on the left temporal lobe. Hence it becomes essential in epilepsy surgery to understand the risks of intervention to the possible neurological deficits. fMRI studies have confirmed a higher occurrence of atypical (right or bilateral) language dominance in preoperative left TLE patients (Adcock et al., 2003; Thivard et al., 2005), suggesting that dominant hemisphere lesions can guide to functional reorganisation of language to contralateral cortical regions. However, ATL may also result in damage to the language related white matter pathways running along the temporal regions. White matter damage is expected when the fibre pathways are close to or even inside the

resection area. The temporal white matter area of MTS patients occasionally shows ectopic gray matter neurons, even though it is not obvious if this is a reliable abnormality specific to MTS (Rojiani AM et al, 1996). Epidemiological studies have suggested that the existence of seizures is a self facilitated phenomenon (Hauser WA & Lee JR, 2002), and several histological abnormalities have been reported to be correlated with disease duration, age at seizure onset or number of generalized seizures (Fuerst D,2001). Volumetric studies (Kalviainen R & Salmenpera T, 2002) have also suggested that in patients with TLE, the volume of the temporal grey matter structures has been found to progressively decline over time.

The relationship between brain morphometry and language function is important for understanding typical and atypical language lateralization and the consequences of brain damage (F. M. Richardson & C.J.Price, 2009). Although it is still indistinct if MTS is the source or the consequence of TLE, it appears certain that it can disseminate an epileptogenic condition. Animal studies (Olney JW et al, 1983) have revealed that repetitive electrical stimulation of the preferred path generates pathological damage comparable to that seen in MTS. An important matter is whether MTS causes TLE or if TLE results in MTS (Mueller et al.,2009).Usually TLE patients had some sort of initial precipitating injury in the first four or five years of their life, but recurrent, unprovoked seizures do not appear until several years later, during which they become visible to be healthy.

Common initial precipitating injuries include febrile seizures, head trauma, birth injury and infection of the central nervous system (Velisek L &Moshe SL, 2003). A majority of patients with refractory TLE can be selected for ATL/lesionectomy based on noninvasive evaluation comprising clinical, interictal scalp EEG, magnetic resonance imaging (MRI) and ictal video-EEG data (Engel. J, 1996). MRI detected mesial temporal sclerosis (MTS) or a neoplasm has been shown to be the best predictor of postoperative seizure outcome in several

studies (Radhakrishnan K et al, 1998). The rate of successful outcome is less in patients with bilateral MTS and in those with normal MRI (Scott C.A et al, 1999). Patients may require invasive monitoring when the results of non invasive monitoring are nonlocalizing or are conflicting.

Invasive monitoring escalates the cost of epilepsy surgery and is associated with morbidity (King D et al, 1997). However in many patients accurate localization becomes difficult and then costly, invasive techniques have to be done.

2.2.2 Techniques used for Temporal Lobe Resection (TLR)

The goal of surgery for medically refractory TLE is to resect the epileptogenic zone, i.e. the hippocampus, parahippocampal gyrus, amygdala and in some cases, parts of the lateral temporal lobe with a minimum of neurological deficit. Three types of resections dominate in reports from epilepsy surgery centres: classical anterior temporal lobe resection (ATL), modified anterior temporal lobe resection (MATL) and amygdalohippocampectomy (transsylvian or transcortical). ATL includes a large resection of the lateral temporal lobe, about 4-6 cms from the temporal pole on the dominant hemisphere and 5-7 cms on the nondominant hemisphere. The resection of the medial temporal structures are not carried far posteriorly thus sparing the posterior hippocampus.

Spencer (Spencer D D et al, 1984) modified the ATL with a smaller lateral resection, 4.5 cms behind the temporal pole in spite of the side and a larger medial extension getting further posterior with the hippocampal resection. The advantage is decreased damage to the lateral temporal lobe structures and more resection of the medial epileptogenic structures. To be even more selective and only remove the medial temporal lobe structures Yasargil and Wieser developed the selective amygdalohippocampectomy (SAHE) performed through a transsylvian approach (Yasargil, M G et al, 1985). In this procedure the lateral temporal cortex is not completely resected, perhaps reducing the risk of cognitive impairment

postoperatively (Wieser, H G et al, 2003). However this technique is more technically challenging and may have an increased risk of vascular injury (McKhann, G M et al, 2006). SAHE may also have a less favourable seizure outcome in children with TLE, and is rarely used in children (Clusmann, H et al, 2004). Most of the techniques described here require the recognition and opening of the temporal horn of the lateral ventricle to resect the medial temporal lobe structures.

2.2.3 Language lateralization in TLE

Language is a form of communication that is unique to humans. It involves interactive system for the manipulation of internally stored words and word meanings. The essence of language is the capacity to retain, retrieve, and combine arbitrary symbols of a native language into an infinite number of potential expressions. Language processing occurs at different levels such as verbal output, reading, writing, hearing as well as visuomotor forms (e.g: sign language). Language is a lateralized brain function, with most activity usually found in left (dominant) hemisphere (Binder, 1997).The “classical model” (**Figure 20**) of language organization consists primarily of two cortical regions of left hemisphere, Broca’s area (Inferior frontal gyrus) -“expressive language area” which is meant for planning and execution of speech and the second one is Wernicke’s area (Superior temporal gyrus) - “temporo parietal receptive language area” which is meant for speech comprehension and identification of linguistic stimuli (M. Smits, 2006). The Arcuate Fasciculus (ArcF), a prominent fiber pathway that originates in the temporal lobe and curves around the Sylvian fissure to project to the frontal lobe (M. Catani et al,2002), was thought to connect these two areas.

Neurobiological substrates of language can be subdivided into four components; Phonology (sounds of words), Orthography (spelling of words), Semantics (knowledge of words), Syntax (grammatical relationship between words) (Hickock, 2009; Price, 2010).

Right handers typically display a strong leftward specialization for speech and language comprehension.

Approximately 97% of right handers have their language lateralized to the left hemisphere, while only 3% demonstrates a right hemisphere language lateralization or bilateral representation (“atypical language”). Thus brain asymmetry, language laterality and handedness are complexly interrelated (Powell et al., 2006; Vernooij et al., 2007).

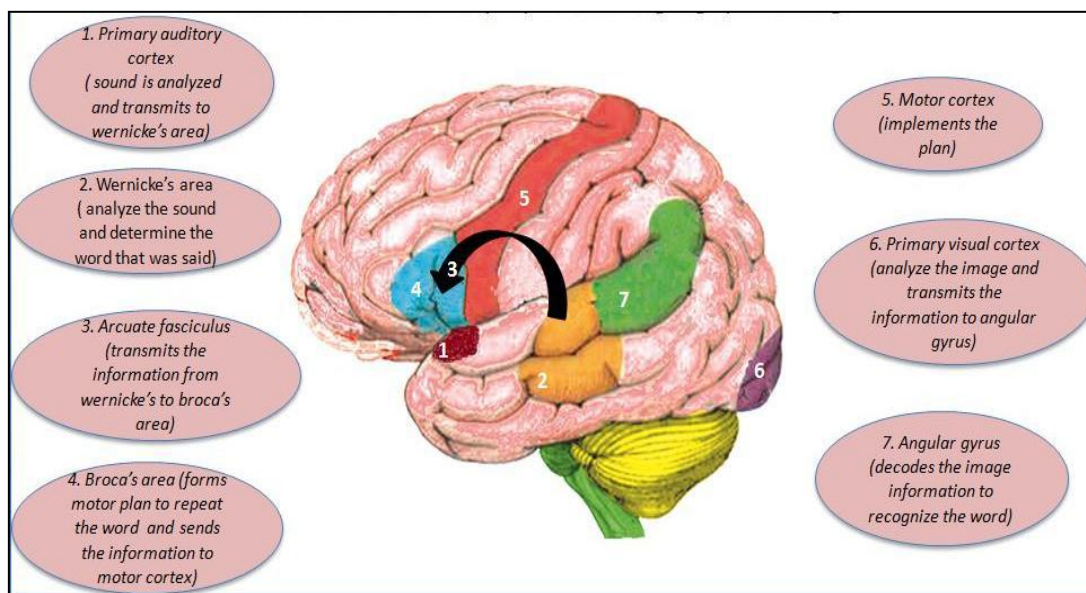


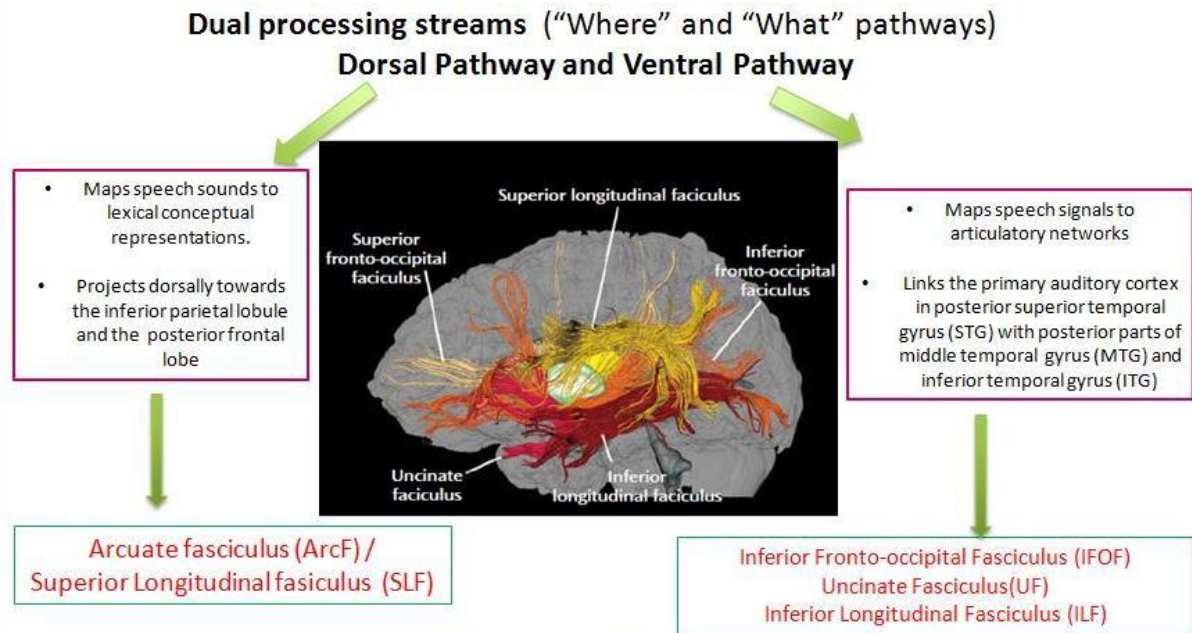
Figure 20: Classical Model (Broca-Wernicke- Lichtheim-Geschwind model) on language processing

Norman Geschwind (1967) further revived the model of language processing called Wernicke's –Geschwind model in which he reported a third region of the brain associated with language, and composed by an anterior segment connecting the Broca's area with the inferior parietal lobe and a posterior segment connecting the inferior parietal lobe to Wernicke's area. This region was named as “Geschwind's territory”. The main white matter connection, Arcuate fasciculus (AF), which is thought to be consistent with its role in language processing (Dronkers & Larsen, 2001) and previous DTI studies demonstrated a higher AF density in the left relative to the right hemisphere atleast in right-handers

(Hagmann et al., 2006; Duffau,2008), although interindividual variability exists in language function.

Differences in handedness between individuals likely used to indicate presence of “atypical language” (right hemisphere or bilateral) organization (Powell et al., 2006; Vernooij et al., 2007).The investigation of neuroanatomical substrates of linguistic processing in atypical language lateralization, particularly in non –right handedness is an interesting area among neurolinguistic researchers (Mechelli et al.,2004, Kovelman et al., 2008). Over the years it has been recognized that, language organization in brain is much more complex than previously thought.

Recently proposed language models based on neurolinguistics and functional imaging studies propose a more dynamic network view in which multiple cortical areas are interconnected by white matter networks in which each holds specific language function. Hickok and Poeppel (2004) proposed a dual-stream model (“where” and “what” pathways) for auditory language process, (**Figure 21**) in which the posterior superior temporal gyrus pSTG is engaged in early cortical stages of speech perception. It diverges into 2 processing streams; (a) The dorsal stream projects dorsally toward the inferior parietal lobule and the posterior frontal lobe (Dorsolateral prefrontal cortex - DLPFC), and is involved in auditory motor integration by mapping acoustic speech sounds to articulator representations. The major white matter components of dorsal stream are, (a)Arcuate fasciculus(ArcF) and (b) Superior Longitudinal fasciculus (SLF). The ventral stream projects ventrolaterally to the middle and inferior temporal cortices and (Ventrolateral prefrontal cortex - VLPFC) serves as a sound-to meaning interface by mapping sound-based representations of speech to widely distributed conceptual representations and the components are , (a) Inferior fronto-occipital fasciculus (IFOF), (b) Uncinate fasciculus(UF) and (c) Inferior longitudinal fasciculus (ILF).



Adapted from Hickok and Poeppel (2004). Nature Reviews Neuroscience

Figure 21: Dual stream model for language processing

Previous studies (Geschwind & Levitsky, 1968) suggested that the information on underlying structural asymmetries and interhemispheric connections could determine functional hemisphere lateralization. Some of the earlier studies combined structural and functional information to test this hypothesis. TLE subjects often have deficits in speech production and comprehension, as shown by behavioural tests of semantic processing such as category matching, naming ability and verbal fluency.

Furthermore, patients with TLE exhibit slowed response times compared to controls on some language tasks such as category decision, rhyming decision, and case decision (Billingsley et al., 2001). These studies evidently demonstrate that TLE affects language function. Atypical language dominance (defined as right handed or bilateral representation of language) is more common in patients with epilepsy than in general population, supporting the hypothesis that insult to the brain in epilepsy induces language re-organization. Focal epilepsy is associated with disrupted localization and lateralization of language functions, and

hence one would expect a higher possibility of abnormal language lateralization. Wada and Rasmussen (1960) determined that over 93% of patients are left language dominant. The left sided language dominance is more intrinsic for right handers but it can also be found in majority of left handers. Some patients also have bilateral representation of language.

Several studies indicate that left temporal lobe pathology is often associated with atypical language lateralization. Patients with fronto-temporal lesions in the dominant hemisphere are particularly prone to suffer from post surgical motor or language deficits. So the preservation of the functional areas and the reduction of morbidity associated with the surgery are crucial.

The functional lateralization of the cerebral cortex was first suggested by Geschwind and Levitsky (1968), who discovered that about 60% of human brains display anatomical differences between the two hemispheres in the posterior temporal lobe (the region which encompasses Wernicke's area). In line with these anatomical observations, language was the first function that was demonstrated to be lateralized in the human cerebral cortex. More recently, various other anatomical and functional differences have been documented between the two cerebral hemispheres. The increased frequency of atypical language lateralization (right sided or bilateral) in patients with focal epilepsy or lesions of the left hemisphere has been known for more than 30 years. Modern neuroimaging studies have shown that a considerable proportion of patients with early acquired or developmental left-sided perisylvian lesions showed evidence of intrahemispheric reorganization of language (i.e, retain typical left-sided lateralization) often near the lesion.

Furthermore epilepsy patients with lesions in the remote language areas more specifically in the mesial temporal cortex, often show atypical, often bilateral language representation. Binder et al performed fMRI on 22 epileptic patients who also underwent a Wada test to determine language lateralization. For fMRI, they used different sets of

language functions (object naming, semantic judgment task etc).A correlation analysis identified voxels significantly associated with task performance. Based on the number of voxels in each hemisphere that exceeded threshold, they calculated a laterality index. The author reported that all patients showed concordant fMRI and Wada results. Eighteen of 22 patients had strong left hemisphere dominance on both tests. The remaining 4 patients showed less strong or atypical language dominance on fMRI. In patients from our series, (Kesavadas et al, 2007) language fMRI results were concordant with Wada results. Eloquent cortex mapping was performed in epilepsy patients with tumor, gliosis, or malformation of cortical development in, or close to the eloquent cortex. Our neurosurgeons have found fMRI for eloquent cortex mapping most useful in patients with gliosis, in whom the distortion in anatomy makes prediction of the eloquent cortex extremely difficult.

2.2.4 Neuroimaging in TLE

Various studies (Fuerst.D et al, 2001; Briellmann R.S et al, 2001) suggest that, over time, temporal lobe seizures may cause progressive changes in structure and function of hippocampus. Magnetic Resonance Imaging (MRI) is the modality of choice for the evaluation of TLE and the main MRI findings are reduced hippocampal and temporal lobe volume, loss of normal architecture of hippocampus, poor grey white distinction of the anterior temporal lobe, increased T2 signal of hippocampus and anterior temporal white matter. Typical MRI protocol for evaluation of TLE subjects begin with a standard non contrast brain imaging which includes both T1- and T2-weighted images, preferably in coronal and axial orientations, as well as a high-resolution three-dimensional volume acquisition. Axial slices, in particular, should be acquired with an angle that makes the slices run parallel to the long axis of the hippocampus. These slices are generally arranged using a para-sagittal slice, where the parahippocampal white matter is plainly visible. Typical care must be taken to avoid a “tilt” in the slices, as asymmetries of the hippocampal size or signal

intensity caused by this could mistakenly be recognized as pathology. Standard slice thicknesses of 4-5 mm are usually employed. Increased hippocampal T2 signal is the most common visually-clear MRI abnormality of MTS (S.F Berkovic et al, 1991) .The increased water content in the tissue secondary to neuronal loss and gliosis considered to be related directly to abnormality in the signal intensity (Briellmann RS et al, 2002). It is further complex to evaluate when thick slices are utilized and artifacts can occur due to partial volume averaging. Therefore, it is suggested to employ CSF-signal-suppressed sequences, such as Fluid-Attenuated Inversion Recovery (FLAIR) (**Figure 22**) to look at the signal intensity change.

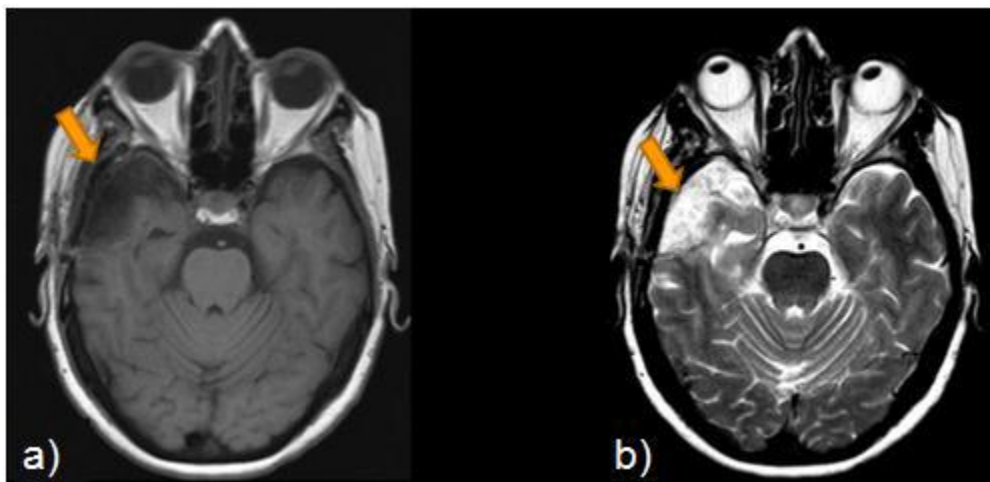


Figure 22: Axial MR image of TLE patient showing a right anterior temporal lobe lesion. (a) Hypointense T1 signal and (b) Hyperintense T2 signal.

By comparing the mesial temporal lobe structures of one hemisphere to the other it is possible to define the evidence of T2 signal abnormalities subjectively. The increased T2 signal of hippocampus in MTS corresponds to decreased signal intensity in T1-weighted images. In general, T2 signal abnormalities are more prominent than T1 signal decrease, although the spatial resolution of T1-weighted images is usually higher, which allows better visualization of mesial temporal lobe structures. Hippocampal atrophy is another common abnormality usually found in MTS, the feature utilized by most neuroradiologists in

particular when randomly-defined, oblique two-dimensional reconstructions can be prepared from a three-dimensional volume. It is not unusual to find hippocampal atrophy in the absence of T2 signal abnormalities in MTS and, because of this reason, obtaining high resolution images is always suggested (Van Paesschen W et al, 1997).

Improvements in image resolution and contrast mechanisms will further lead to images that resemble histopathological sections and will help to improve the diagnosis of MTS. T2 relaxometry based quantitative assessment provides a means to directly quantify the time constant that produces the high signal intensity on conventional T2-weighted images., atleast two different echoes must be acquired in order to quantify the T2 constant of each tissue, and a (typically mono-exponential) decay curve is fitted to these points. The first reported use of T2 relaxometry utilized a modified Carr-Purcell-Meiboom-Gill sequence in epilepsy patients that provided 16 echoes (Bernasconi A et al, 2003).

Several studies have demonstrated that MRS can accurately lateralize TLE in patients with or without mesial temporal sclerosis (Connelly A et al, 1994; Hetherington H et al, 1995). In TLE patients, a gradual decrease of the putative neuronal marker N-acetyl-aspartate (NAA), can be measured with magnetic resonance spectroscopy (MRS) (Bernasconi A et al, 2003), although this reduction appears to be reversible upon seizure freedom. The most regularly reported metabolic abnormalities are reduced NAA/Cr (creatine) ratios and increased choline (Cho)/Cr concentrations. It has been reported that a reduction in the concentration of NAA is indicative of neuronal loss, and that the changes in Cho concentration be a sign of gliosis. It has been also reported that several histological abnormalities of TLE can be correlated with disease duration, age at seizure onset or number of generalized seizures (Mathern GW, 2002).The volume of the hippocampus and extra-hippocampal structures has also been found to gradually decline over time. It has been estimated that studies based on quantitative volume estimation of the mesial temporal

structures provided very good results for over 15 years (Jack CR et al, 1990).It is considered as a simple and reliable method for the detection of hippocampal sclerosis. The volumes of the temporal lobe structures can be defined manually outlining each one on individual slices or automated methods are available for segmentation and quantification of grey matter structures.

Automated tissue segmentation can be achieved by number of ways that are independent of the user. The segmentation of both grey and white matter can be performed throughout the whole brain, which allows for large-scale group analyses using voxel based approach based on statistic parametric mapping software. There are also additional imaging methods that are currently available to help to lateralize temporal lobe epilepsy in patients, when the MRI with routine seizures protocol is normal or reveals bilateral or equivocal abnormalities. They include T2 Relaxometry (T2R), Proton Magnetic Resonance Spectroscopic imaging (1H-MRSI), Diffusion Weighted Imaging (DWI), Diffusion Tensor Imaging (DTI) and Volumetry. Several studies (W.C Weishmann, 2003; J.Duncan ,2009) have shown that these additional techniques can give better information of lateralization in patients with TLE. However they consume more scanning time and hence the patient could be charged more for scanning.

Functional MRI (fMRI) can be employed to identify eloquent cortical areas and their relationship to the epileptogenic lesion (Kesavadas et al., 2007). However, structural MRI and fMRI do not provide any information concerning the relationship of the epileptogenic lesion and eloquent cortical areas to adjacent white matter tracts (Radhkrishnan .A et al, 2011).

2.2.5 Advanced Neuroimaging techniques for presurgical evaluation in TLE

2.2.5.1 fMRI

BOLD fMRI (Ogawa et al, 1990) is clinically widely accepted tool mainly for mapping presurgically functional areas in neurosurgical patients especially epilepsy patients with resectable lesions. The complete non invasiveness, the absolute safety, the extensive availability of MRI in comparison with other neuroimaging modalities, the good sensitivity, the ease of imaging and its widespread use in cognitive neuroscience have lead to the increased clinical use of fMRI in presurgical planning. fMRI allows non-invasive mapping of eloquent areas to be performed prior to surgery. Functional brain mapping of motor, sensory and language functions is considered to be appropriate for pre-surgical mapping (Bookheimer, 2007; Stippich, 2007; Kesavadas et al., 2007).

By combining fMRI results with a high resolution anatomical reference image, the relationship between lesion margins and functional areas can be established. This information can be utilized for pre-operative risk assessment, allowing the neurosurgeon to make an informed decision about treatment options. If functionally intact tissue is too close to the desired resection margin, the fMRI results indicate that intra-operative mapping is mandatory. As the distance between resection margin and functional activity increases, the risk for postoperative neurologic deficits decreases (Hagberg et al., 2004). Some groups have demonstrated that there is a safe distance between resection margin and eloquent cortex, where surgery can be considered safe (Hagberg et al., 2004). However, defining such a safe distance between neuronal activity and margin of resection is challenging for several reasons. For instance, the distance will be influenced by numerous parameters including the applied imaging sequence, data analysis options (smoothing) and the statistical threshold used to interpret activations etc. In the case of TLE patients, it is important to understand language lateralization as a part of presurgical planning. By doing fMRI in epilepsy cases, it is possible to establish the relationship between the margin of the brain lesion and the adjacent language feasible cortical brain area

The main goals of presurgical fMRI are: (a) Assessing the risk of neurological (language) deficit that follows ATL procedure, (b) Selecting TLE patients for invasive intraoperative mapping, (c) Guiding of surgical procedure itself. fMRI is useful in determining language lateralization and suggesting the risk of postoperative decline and nowadays it is widely considered to be a valid noninvasive alternative approach to intracarotid amobarbital test. While there is good agreement between invasive Wada testing and fMRI findings, fMRI is more sensitive to involvement of non dominant hemisphere. MRI studies confirm and broaden Wada test results, revealing that LTLE patients typically have less left-lateralized language compared to healthy controls in both frontal and temporal areas (Adcock et al, 2003). With reference to RTLE patients, some studies have suggested normal left lateralization (Adcock et al. 2003; Thivard et al., 2005), while others reported decreased lateralization, coupled with further recruitment of right frontal and right temporal areas (Powell et al., 2007), depending on the fMRI experimental task employed.

Language functions are usually affected in TLE cases particularly during seizures. In LTLE, ictal and postictal language impairments (peri-ictal aphasia) occur in 75-82% of LTLE patients (Gabr et al., 1989) and are associated with left language dominance on the Wada test. LTLE patients without peri-ictal aphasia are therefore more likely to have atypical (i.e. bilateral or right) language dominance. In spite of the established clinical relevance of language fMRI in presurgical evaluation in TLE, only a few studies have investigated its role in predicting postsurgical deficits. In preoperative LTLE patients, fMRI left-lateralization during semantic decision and fluency (Bonelli et al., 2012) tasks was predictive of naming decline after ATL. However, in these studies, language was only assessed in the first 6 months after surgery, while functional reorganization may continue over a longer time.

Language can be mapped using speech comprehension and expression tasks. For generating activation in comprehensive and expressive language areas, task involving

Broca's area (Inferior frontal gyrus), middle and superior temporal gyri are used. Usually patients are instructed to perform covert language production tasks, as words spoken aloud would induce gross head movement artefacts. In the case of tasks that are too difficult to perform by cognitively slowed down patients, listening to spoken language or reading written language may be used as an alternative. Sometimes the function may be relocated to other brain areas in response to pathology. Such anatomical relocation which is designated as cortical reorganization or plasticity is usually found in epilepsy patients if early brain lesions are present as in the case of vascular malformations or focal cortical dysplasia.

2.2.5.2 Diffusion Tensor Imaging (DTI) and Tractography

DTI has the potential to demonstrate the structural reorganization of connectivity networks involved in memory and language that reflects changes in cerebral function. DTI studies revealed that there will be an increased diffusivity and a reduced fractional anisotropy has been shown in sclerotic hippocampi (Yoo SY, 2002). Increased ADC and decreased FA also found in Malformations of Cortical development (MCD) and also in normal appearing surrounding brain tissue (Eriksson S H, 2001). Overall, the occurrence of dynamic diffusion changes was documented in the majority of epilepsy cases, but the correlation between the supposed epileptogenic zone and the diffusion changes remained quite variable.

The DTI measures can be used to explore language lateralization in healthy controls and in patients with epilepsy (Powell et al., 2006; Vernooij et al., 2007). The Arcuate fasciculus (ArcF) was shown to be prominent white matter tract found in the language dominant hemisphere, and the left-right asymmetry of this pathway was reduced if pathology was present in the dominant hemisphere. In patients with TLE, diffusion abnormalities in the Arcuate and Uncinate fascicule (UF) and left inferior fronto occipital fascicule (IFOF) were connected with naming impairments. In agreement with this finding, patients with right-sided TLE had mostly ipsilateral diffusion abnormalities and individuals with left-sided TLE had

widespread and bilateral diffusion abnormalities. However, in one study (Rodrigo, S. et al, 2008), symmetry of language activation pattern and diffusion parameters in the ArcF were correlated in cases of right-sided TLE patients, but such correlations were not found in cases of left-sided TLE. Diffusion abnormalities in left-sided ArcF and UF correlated with duration of epilepsy in patients with left-sided TLE (Govindan, R. M et al, 2008).

Voxel-based statistical analyses of DTI in 15 healthy volunteers demonstrated an asymmetry of the Arcuate fasciculus (ArcF) with higher fractional anisotropy in the left hemisphere (Buchel et al., 2004). Leftward structural asymmetries have also been reported in the subinsular region in right handed healthy volunteers (Cao et al., 2003), and a cohort of 27 right handed healthy volunteers showed a higher relative fibre density in the left ArcF compared to the right in virtually all participants. This strong degree of asymmetry was specific to the ArcF, and was not found in the motor pathways. These findings reveal that in a control population regional brain function indeed corresponds to higher connectivity in those areas. Patients with left hemisphere focal epilepsy have a higher proportion of atypical language lateralization (Adcock et al., 2003; Thivard et al., 2005). Such changes may be disease correlated, with epileptogenicity leading to disruption of the language network on the affected side.

Right hemisphere lateralisation of language in a percentage exceeding the incidence in controls may represent an expression of plasticity. Such changes in function are likely reflected by changes in structure and connectivity. The first report on evaluating language lateralisation and DTI asymmetry in epilepsy included nine focal epilepsy patients, eight had left hemispheric focal epilepsy (5 temporal, 3 frontal). In two patients with atypical language lateralization as per fMRI result, these findings were supported by atypical anisotropy value lateralisation to the right hemisphere using a ROI approach (Briellmann et al., 2003). Generally activation maps generated by fMRI language paradigms (verb generation and

reading comprehension tasks) were used to define starting regions for a probabilistic tractography.

The white matter density, tract volume and FA connecting the anterior and posterior language areas delineated by the fMRI activations are the commonly used DTI measures used to assess structural connectivity. In a combined fMRI-DTI study (Powell et al, 2007) , it has been shown that controls and patients with right TLE had a more left hemisphere lateralization in both fMRI activation pattern and structural connectivity and Patients with left TLE had more symmetrical language activation pattern, which was paralleled by increased right hemispheric structural connectivity. Besides, individuals with highly lateralized functional activation had more-lateralized white matter connectivity than patients with low functional activation lateralization. These findings provide evidence of a close structure function relationship with confirmation for the language dominant hemisphere showing better connectivity and. evidence of language reorganisation to the right in left TLE, paralleled by language plasticity in connectivity. The lateralization of connectivity indices for expressive language areas predicted language deficits after speech-dominant ATR (Powell, H. W. et al, 2008). A diffusion study (Yogarajah, M. et al, 2010) conducted based on pre and post anterior temporal lobe resection showed a postoperative increase in FA in the ipsilateral external capsule in patients with left-sided TLE. This area corresponded to the ventromedial language network. Individuals with the significant increase in FA had the smallest postoperative word-finding difficulties, signifying that expansion of the parallel language network can occur in the months following surgery.

2.2.5.3 Structural neuroimaging based VBM analysis

Structural neuroimaging studies typically involve the regional comparison of brain structure across two groups of subjects (e.g., controls vs patients) or the correlation of brain anatomical structure with language abilities. Both approaches assist to localise brain regions

that sustain language function. Ultimately, a more precise understanding of the brain areas that support various language skills (e.g., verbal fluency, reading, and comprehension etc) could confirm useful in predicting deficits on the basis of pathogenic lesions. The most promising technique used in structural MRI studies of language in the damaged and undamaged brain VBM (Ashburner & Friston 2000).

Voxel-based statistical analysis is usually performed on T1- weighted magnetic resonance (MR) images and has revealed details of anatomical differences in vivo. VBM is a non-invasive magnetic resonance method used to detect tissue abnormalities between groups of subjects. VBM creates SPMs of group-wise regional gray matter differences between TLE patients and healthy control population. VBM conducts a mass-univariate voxel-by-voxel analysis of the whole brain, and in this sense is an impartial and objective technique for analysing structural brain images that does not rely on a priori regions of interest or the manual parcellation of cortical regions.

Another advantage of VBM is that it is able to provide an accurate localisation of any detected differences (as opposed to characterising these in terms of broadly-defined regions), making it possible to connect findings more closely to functional neuroimaging data. Moreover VBM is a fully automated computerized quantitative MR image analysis technique that does not rely on investigator expertise in neuroanatomy and is not restricted to the study of single brain region at a time, unlike manual region-of-interest (ROI) volumetric analysis (F.M Richardson & C.J. Price, 2009). While using VBM, the concentration of grey or white matter in a given cortical brain region may be measured as volume or density.

VBM studies (Keller et al., 2002) on refractory TLE have found gray matter volume (GMV) alterations not only in mesial temporal lobe structures (e.g., hippocampus, amygdale and so on), but also in other brain regions which includes the frontal lobe and sub cortical areas. A recent study suggested that greatest GMV reduction was usually found in the

ipsilateral mesiotemporal lobe structures in both LTLE and RTLE patients. (J.P Li et al, 2011). To take account of interindividual variation in gyral morphology, during the VBM analysis, the gray matter is segmented and smoothed. Good et al in 2001 proposed an advanced technique called optimized VBM which incorporates additional spatial processing steps before statistical analysis so as to improve image registration and segmentation. Also earlier studies (Sandok et al., 2000, Dreifuss et al., 2001) in TLE cases have reported greater volume reduction of the cerebral grey matter structures of temporal lobe region. In the current study, we addressed the question whether in TLE patients; the language dominance is associated with changes in grey matter (GM) structure volume measured using voxel-based morphometry.

Morphological structural asymmetries favouring the left hemisphere in the planum temporale (PT) and Heschl's gyrus (HG) have both been supposed to related to the typical left-hemisphere dominance for language related functions (R.D pierre et al,2006). Geschwind and Levitsky reported that the PT, a region found on the superior temporal plane and part of the classical Wernicke's area, was larger in size on the left hemisphere relative to the right. This finding was interpreted as providing the first clear neuroanatomical evidence for the left hemisphere's specialization for speech. Another structural asymmetry of interest relevant for speech is found in HG, which contains primary auditory cortex (PAC). Penhune et al (R.D Pierre et al, 2006) found that the left HG was associated with a larger white matter volume than was the right HG. Functional neuroimaging studies also demonstrated that the insular cortex plays a major role in auditory processes, such as allocating auditory attention and tuning in to novel auditory stimuli, temporal processing, phonological processing and visual–auditory integration

CHAPTER 3

DESIGN OF THE STUDY

3.1 Materials and Methods

3.1.1 Subject details

The study designed as a case-control study which includes 60 normal healthy volunteers (42 males, 18 females; age range: 15-40 years; 54 = Right handed, 6 = Left handed) with no history of any brain disorder and 57 Intractable TLE patients (38 males and 19 females; age range: 20-48 years; 25 = Right TLE, 32= Left TLE). **Table 1** illustrates patient demographics. All the refractory TLE cases were recruited from R.Madhavan Nayar Center for Comprehensive Epilepsy Care (RMNC), with the help of an epileptologist.

Patients	Gender	Handedness	Seizure duration	MRI findings
RTLE (25)	Males (18)	RH= 22 LH= 3	Mean (6-18 years)	Mesial Temporal Sclerosis (13)
	Females (7)			Granuloma (4) Cavernoma (2) Gliosis (3)
				Dysplastic tumours (3)
LTLE (32)	Males (21)	RH = 28	Mean (10-21 years)	Mesial Temporal Sclerosis (11)
	Females (11)	LH =4		Granuloma (7) Temporal gliosis (8) Dysplastic tumours (6)

Table 1: Patient demographics

3.1.2 Inclusion criteria

3.1.2.1 Patients

Temporal Lobe Epilepsy patients subjected to presurgical evaluation based on neuropsychological evaluation, EEG and video-EEG findings.

3.1.2.2 Healthy controls

- (a) Normal Healthy age matched male or female volunteers willing to cooperate for the study.
- (b) Subjects must understand the nature of the study.

3.1.3 Exclusion criteria

3.1.3.1 Patients

- (a) Subjects unsuitable to receive MR examination or claustrophobic subjects.
- (b) Subjects with intracranial metallic bodies from prior neurosurgical procedure

3.1.3.2 Healthy controls

- a) History of substance abuse
- b) Abnormal MRI or history of known structural brain abnormality other than as signs of the condition studied in the present protocol.
- c) Claustrophobic subjects

3.1.4 Ethics Approval

The Institutional Ethics committee of Sree Chitra Tirunal Institute for Medical Science and Technology (SCTIMST) approved the study. A written informed consent and a questionnaire regarding previous medical history were obtained from all participants before the experiment.

3.1.5 Data Acquisition

The MR Imaging was performed using 1.5 Tesla Magnetic Resonance scanner (Avanto SQ engine, Siemens, Erlangen, Germany) with Echo Planar Imaging (EPI) capabilities. I properly trained each participant before the experiment and a brief information

regarding education, occupation, language ability (monolinguals or multilinguals) and handedness were obtained prior to the MRI experiment.

During the whole study, proper head coils and soft pads were used to immobilize the subjects head. Before the fMRI session, a high resolution 3D T1 weighted images of entire head were obtained with a 3-D spoiled gradient-recalled acquisition in the steady state sequence (3-D FLASH (Fast Low Angle Shot); TR/TE 11/4.94 ms, flip angle 15°, FOV 256 mm, slice thickness 1 mm, matrix 256×256) and a 3-D FLAIR (Fluid Attenuated Inversion Recovery) sequences with TR/TE/TI 5,000/405/1,800 ms, FOV 256 mm, slice thickness 1 mm, matrix 256×256) , which was used for final co-registration of the fMRI images to the anatomical images. For fMRI data acquisition , we used a gradient-echo echo planar sequence based on BOLD effects (TR/TE 3,580/50 ms, flip angle 90°, FOV 250 mm, matrix 64×64,slice thickness 3mm) which was applied after the gradient field mapping to acquire T2* weighted functional images.

For the acquisition of DTI data, we used a spin-echo echo-planar DTI sequence with diffusion gradients along 30 non-collinear directions with the following imaging parameters: TR 3500 ms, TE 105 ms, matrix 192 × 192, field of view 230 mm², 2mm slice thickness with 1.5 mm gap averaged twice and with a b factor of 0 and 1000 s/mm². A high resolution T1 weighted 3D MPRAGE (Magnetization Prepared Rapid Gradient Echo), TR 5,600 ms and, TE 504, with excellent grey matter- white matter contrast was used for VBM based volumetric analysis.

3.1.6 fMRI Language paradigms

To invoke the functionally active areas for language processing, I designed 4 different blocked/boxcar model language paradigms, which consisted of sequence of blocks each of

which constitutes an active or baseline conditions and typically lasts 30 seconds. Within each block, a series of trial events of each condition were presented and the signal acquired during one block (active) was then compared with the signal acquired during other block(baseline). The different language paradigms are (1) Visual verb Generation (VG), (b) Syntactic task (ST), (c) Semantic task (SeT) and (d) Word pair task (WP). All Stimuli were presented visually in subject's native language using MR compatible mirror projected through a common desktop personal computer. A response box also provided for monitoring the subject's response to particular stimuli (**figure 23**). Each fMRI session were presented as an off-on fashion and consisted of 100 dynamics with 5 activation (active phase) and 5 baseline (rest phase) conditions (**figure 24**). The total time for each fMRI session is 6.02 minutes. The rest condition was same for all paradigms, during which different simple patterns were shown to the subjects and they were asked to concentrate on this patterns in a relaxed state. The clinical implementation and optimization of the procedure was done with the help of an experienced radiologist and MRI technician.

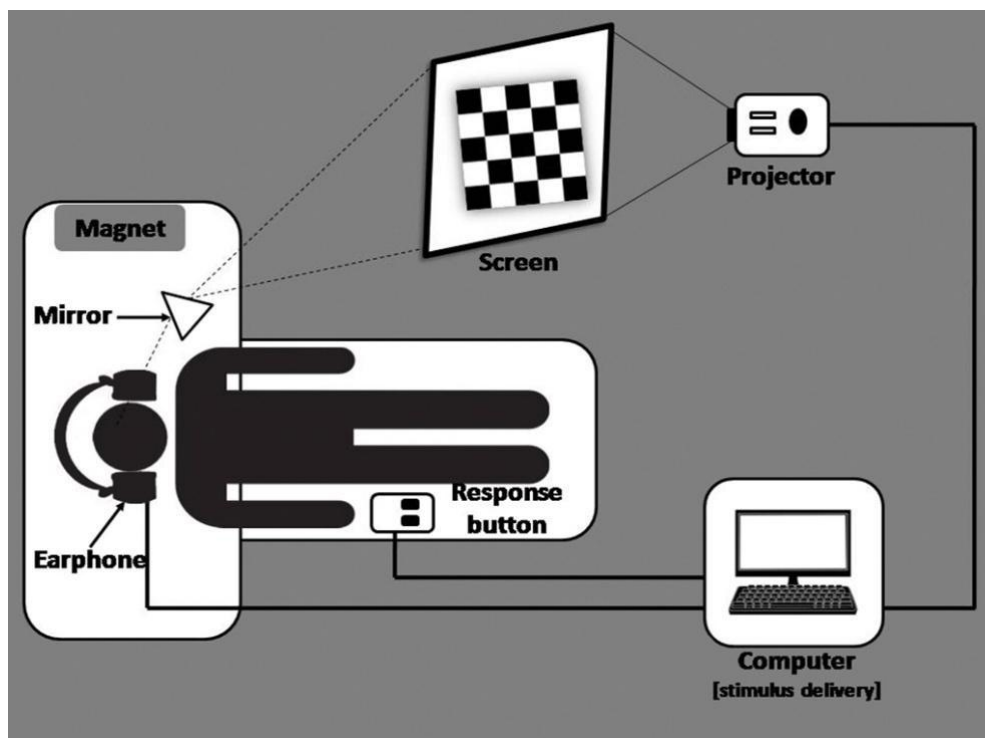


Figure 23: Schematic representation of fMRI setup. The subject receive the stimuli either through projection screen (visual) or head phone (auditory) and responds to stimulus by pressing the response button.

3.1.6.1 Visual Verb Generation task

During this session, the subject was instructed to silently generate verbs that are semantically related (i.e., “what to do with”) to a presented noun (i.e., chair, pencil etc). It is the most commonly used fMRI language paradigm and probably the most reliable test in the clinical field. It is generally used to localize expressive and receptive language functions in inferior frontal gyrus and superior temporal gyrus respectively.

3.1.6.2 Syntactic task

This task includes visual presentation of grammatically correct (Ramu wrote a story) or incorrect sentences (e.g: I go market yesterday) to the subject. In this case, linguistically complex sentences are presented rather than single words. The subjects were instructed to press right response button upon seeing a correct sentence and left response button upon seeing a grammatically incorrect sentence.

3.1.6.3 Semantic task

During this session, semantically related and factually correct (e.g.: Peacock is our national bird) or semantically unrelated and factually incorrect (e.g: Sachin Tendulkar is a great singer) sentences were visually presented to the subjects and they were instructed to press right response button upon seeing a semantically related sentence and left response button upon seeing a semantically unrelated sentence.

3.1.6.4 Word pair task

During this session, pair of matched (e.g: Table, chair) or mismatched words (e.g: Pen, key) were visually presented to the subjects. They were instructed to press right response

button upon seeing a matched word pair and left response button upon seeing a mismatched word pair. This task is comparatively simple and easy to perform than syntax and semantic task.

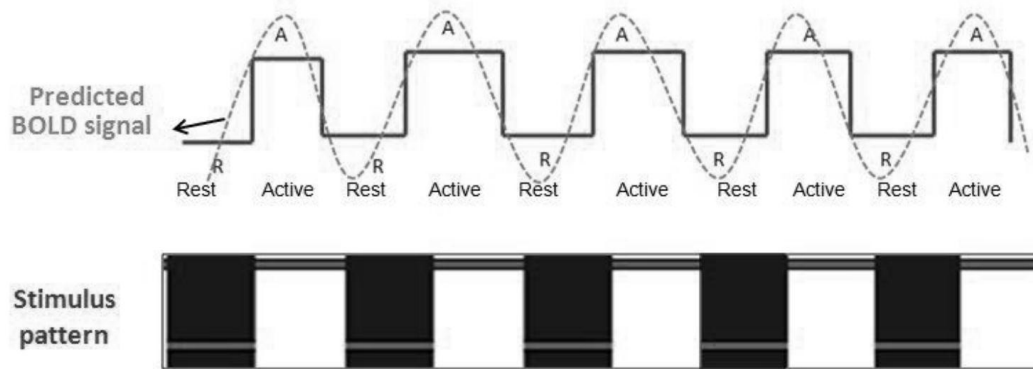


Figure 24: Blocked Design paradigm for stimulus presentation and predicted BOLD signal pattern

3.1.7 Data Analysis

Analysis of imaging data was performed by two independent operators. The operator who performed the DTI & VBM processing was blinded to the results of fMRI processing.

3.1.7.1 fMRI Data Analysis

fMRI data analysis was done using Statistical Parametric Mapping (SPM5, Wellcome Trust Department of Cognitive Neurology, London, UK, www.fil.ion.ucl.ac.uk/spm) software implemented in MATLAB (Matlab 7.1, MathWorks, Natick, MA) environment. The fMRI data from each subject were slice acquisition-corrected, removed motion artifacts, and coregistered to the coplanar anatomical image and represented in a stereotaxic template, a standard brain-space coordinate system for anatomical reference. The first ten measurements (baseline) were not considered for analysis to compensate for T1 saturation effects. The T1 weighted image (FLAIR 3D) was normalized to the standard MNI (Montreal Neurologic Institute) template with the transformation matrix applied to the co-registered functional

images. The normalized functional images are then spatially smoothed with a 8- mm FWHM (Full-Width at Half-Maximum) Gaussian kernel and interpolated to 3-mm isotropic voxel. Single subject analysis was done by modeling the active and control conditions with a boxcar function convolved with the hemodynamic response function using the general linear model and applying a 128-second high pass filter. This procedure generates statistical parametric maps (SPMs) of t statistics reflecting differences between active and baseline states at each voxel location for each subject. For the description of differences between activation and control conditions in single-subject data, a probability threshold of $p < 0.05$ (FDR corrected) was chosen. Schematic representation of fMRI data analysis by SPM is shown in **figure 25**.

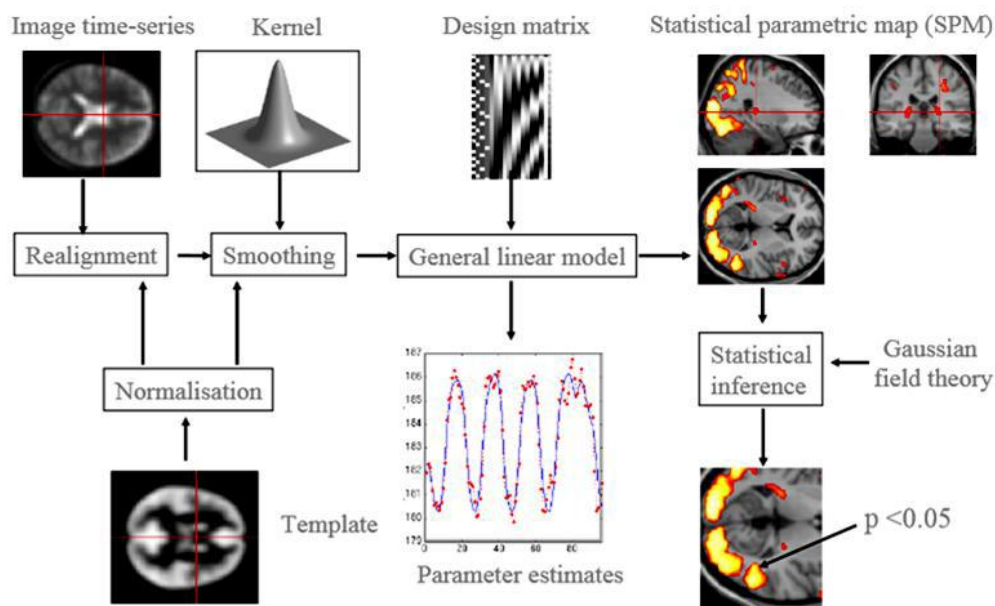


Figure 25: Work flow of Statistical Parametric Mapping software

A Region of Interest (ROI) analysis was done by using MarsBar (<http://marsbar.sourceforge.net/>), for predicting the language related activated clusters within the anatomical landmark. For the quantification of hemispheric dominance, fMRI language laterality (LI) index was calculated by counting the total number of activated

clusters in each of the defined ROIs on left and right hemisphere for each subject separately by using the equation , $LI = L-R / L+R$; where L= number of activated voxels on the left hemisphere and R = number of activated voxels on the right hemisphere .The positive (+) value denotes left hemisphere language lateralization, negative (-) value denotes right hemisphere language lateralization and zero (0) represents bilateral activation of language function. Each step involved in fMRI data analysis is explained below.

3.1.7.1.1 Pre-processing of fMRI data-preparing data for analysis

The essential pre-processing steps are, Realignment, Co-registration, Normalization and Smoothing.

3.1.7.1.1.1 Realignment

During the scanning session, subjects may move inside the scanner. Even small head movements can cause movement artifacts, which may add up to the residual variance and reduce sensitivity. Data may be lost if sudden movements occur during a single volume and it may be correlated with the task performed .So movement related variance components in fMRI present one of the most serious confounds of analysis . A rigid body registration with 6 parameters, 3 translations (X, Y, Z) and 3 rotations (pitch, roll and yaw) was used for realignment in SPM (**figure 26**). It minimizes the squared sum of differences between each successive scan and references scan (usually the first or the average of all scans in the time series) and resample the data.

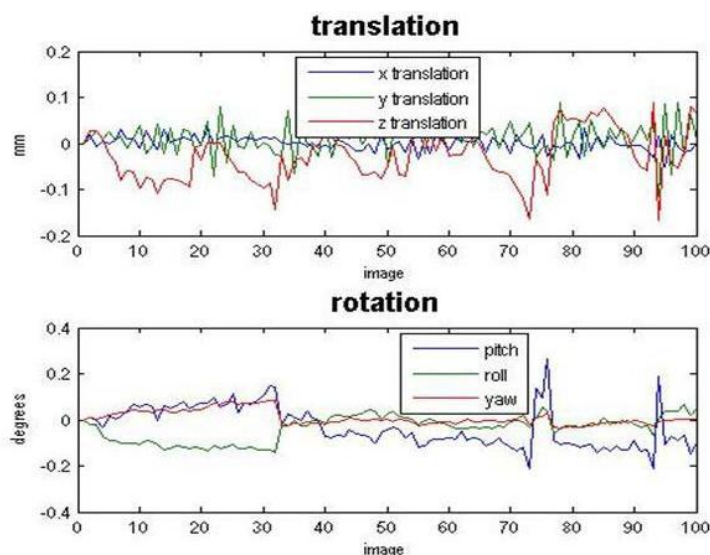


Figure 26: Realignment of fMRI datasets

3.1.7.1.1.2 Co-registration – within subject registration

By means of co registration between two modalities (a structural image (example: T2 weighted) to a functional image series, EPI), it is possible to overlay functional activations onto an individual's own anatomy and also enables overlay of group-level functional activations onto an average structural scan. Co registration gives a better spatial image for further use in normalisation step, as warps derived from the higher resolution structural image can be applied to the functional image. This is again a rigid body transformation but the registration cannot be simply performed by minimizing the residual sum of squares due to the different imaging modalities. The 12 parameters affine transformation (3 translations, 3 rotations (rigid-body), 3 shears and 3 zooms) step register the structural image and the first image of the functional image series to template images. These transformations are constrained in such a way that only the parameters that describe the rigid body transformation is allowed to differ. Next the images are segmented using tissue probability maps of grey matter, white matter and cerebrospinal fluid. At last, the image partitions were simultaneously co registered to produce the final solution.

3.1.7.1.1.3 Normalization – between subject registration

In order to average the signal across different subjects, it is important to warp brain images into roughly the same stereotactic space. The advantage of spatially normalized images is that areas of functional brain activation can be reported within this standard space (Talairach and Tournoux (1988), in SPM'94 – SPM '99) according to their spatial coordinates (**figure 27**). The SPM2 uses MNI (Montreal Neurological Institute) template, an average of 152 brain images and hence more representative of the population as compared to the Talairach and Tournoux atlas. The present study used SPM5 software, which make use of ICBM (<http://www.loni.ucla.edu/Atlases>) template. The Normalization step not only considers the 6 rigid-body transformations but also considers 3 shears and 3 zooms to match the individual subject's images to the template. A nonlinear transformation also done for accurate normalization which corrects gross differences in head shapes that cannot be accounted for by the affine transformation. The normalisation step need not be done while doing a single patient fMRI analysis in clinical setting. The technique is used more often while analysing group data in a research setting.

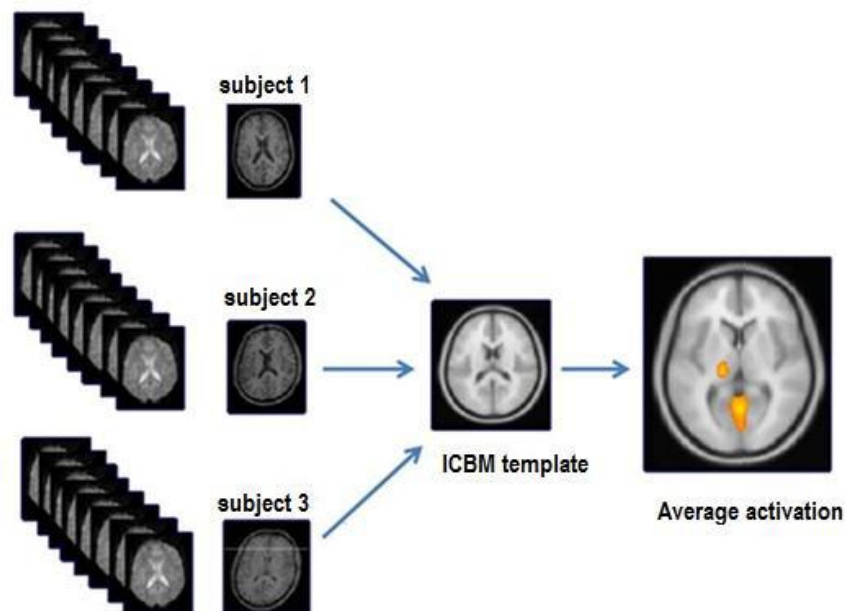


Figure 27: Group level activations overlaid on a standard template image

3.1.7.1.1.4 Smoothing

Functional images need to be smoothed prior to the statistical analysis, especially in group level analysis, so that corresponding sites of activation from the different brains are superimposed. Smoothing is generally done by convoluting the data with a Gaussian kernel and it potentially increases signal to noise ratio according to the matched filter theorem. Since, hemodynamic response functions (HRFs) are modelled to have the shape of a Gaussian filter, we used a Gaussian kernel of size at least twice the voxel size (FWHM (Full Width Half Maximum) of about 6 or 8 mm) for smoothing the functional images (**figure 28**). During smoothing, the intensity value within each voxel is replaced with a weighted average that incorporates the intensity values of the adjacent voxels. It also compensates for inter-subject variability between individuals after normalization. Smoothing allows the application of Gaussian random field theory to make inferences at the statistical analysis stage.

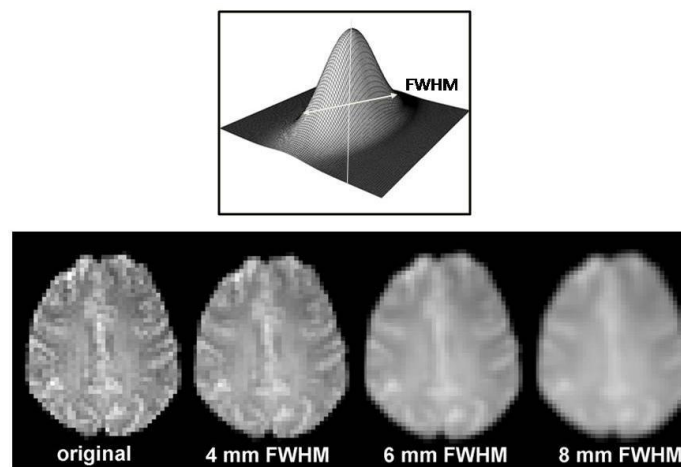


Figure 28: Smoothing by convoluting with Gaussian kernel of varying size of FWHM

3.1.7.1.1.5 Statistical Analysis – using General Linear Model (GLM)

The GLM was used to specify the different conditions/ blocks in the form of a design matrix, which defines the experimental task and the nature of hypothesis to be tested (**Figure 29**). It provided a framework that allows us to make refined statistical inferences taking into account, (1) the (pre-processed) 3D MRI images, (2) BOLD time series, (3) user defined

experimental conditions , (4) Hemodynamic response function (HRF) and (4) technical / noise corrections. The basic idea behind GLM is that the observed data (y) is equal to a weighted combination of several model factors (x), plus an additive error term (ϵ). It is a model (i.e.an equation: $Y = X \cdot \beta + \epsilon$), where , Y is the BOLD signal at various time points at a single voxel (Observed data) , X represents several components which explain the observed data, i.e. the BOLD time series for a particular voxel (Design matrix) , β define the contribution of each component of the design matrix to the value of Y (Parameter estimates) and e is the difference between the observed data, Y, and that predicted by the model, $X\beta$ (Error). The design matrix has one row for each scan and one column for each effect one has built into the experiment or explanatory variables that may confound the results. Each column of the design matrix corresponds to experimental conditions of interest (the hypothesis under test) and a set of columns that model effects of no interest (**figure 30**). In this stage, the groups designated for the images are specified. This stage represents modelling the data to observe neurophysiologic responses, confounds and error.

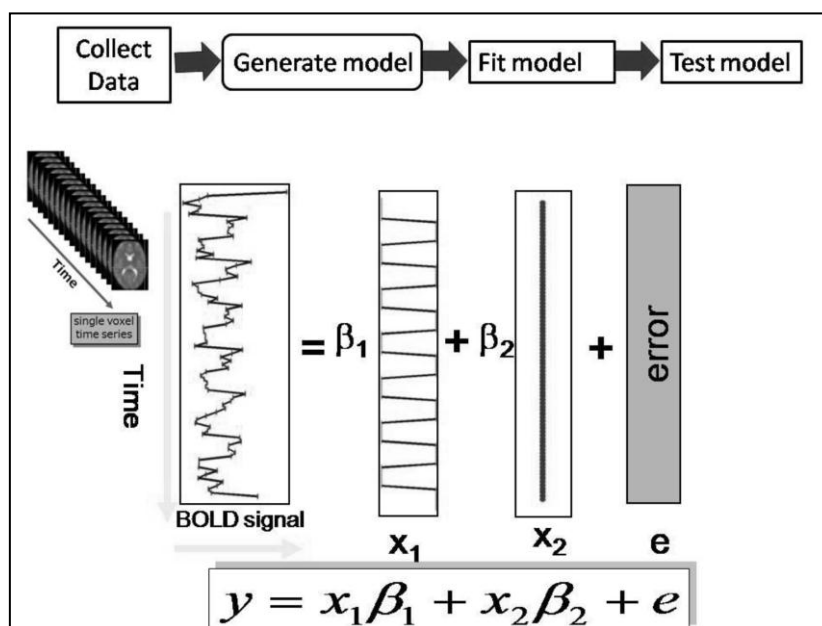


Figure 29: General Linear Modelling

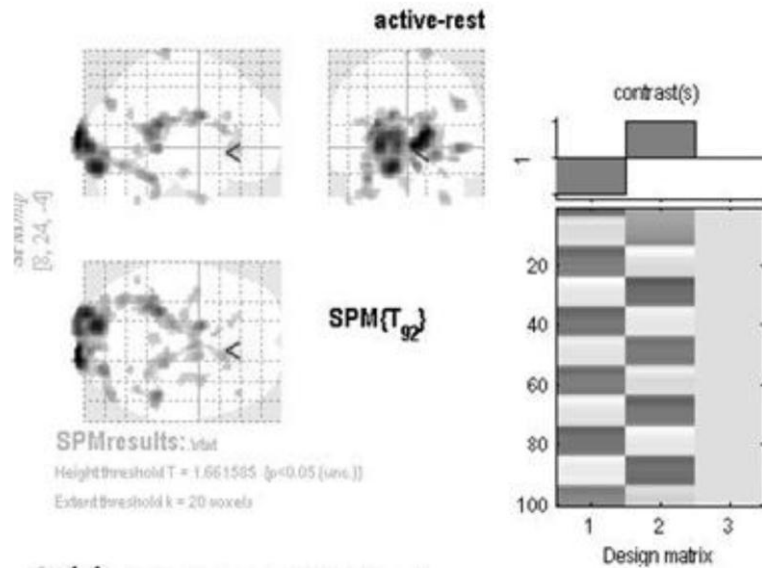


Figure 30: Glass brain view for group level analysis and corresponding design matrix with t contrast specifying active versus rest condition

3.1.7.1.1.6 Inference and Interpretation of results

The neuronal activities in response to different experimental tasks were obtained by specifying linear contrast (T contrast). Cognitive subtraction logic was applied to predict brain activity scales in a linear fashion. The conditions of interest (active condition) are given a positive value, such as 1, and conditions (baseline condition) that are to be subtracted from these conditions of interest take on a negative value, such as -1. The end result was a statistical parametric t map. The functional activations (blobs) obtained can be further overlaid or rendered onto the high-resolution structural image of the subject in order to accurately locate the neural activity (**figure 31**). Since Statistical parametric mapping follows a univariate approach, each voxel should be separately analyzed. So for a statistical threshold of $p < 0.05$, 5% of the voxels would show activation by chance alone (false activation – type I error), which means a multiple comparison correction was required.

Bonferroni correction is the traditional way of doing this, However, due to involvement of huge number of voxels, a direct implementation would severely reduce the estimated number of degrees of freedom. Hence, to the extent that the image data approximate a random Gaussian field correction for multiple comparison need to be only made for number of voxels that can be resolved independently (resells or resolution elements). The multiple comparisons correction is controlled for family-wise error (FWE) rate. This assumption of random Gaussian field is assured by applying a Gaussian smoothing filter in the pre-processing stages.

A serious limitation of correcting for multiple comparisons is that the number of false negatives (type II error) is greatly increased. Further approach is to define the false discovery rate (FDR) that controls for 5% at ($p < 0.05$) of observed activations can be false positives. The FWE method controls for a 5% chance of a single false positive. To correct for multiple comparison, some alternative approaches was used in the study (i) employed a strict uncorrected threshold (e.g. $p < 0.05$), (ii) used an inference over the cluster size (iii) done small volume corrections in regions where a prior hypothesis exists (iv) a region of interest (ROI) analysis in which the average signal for all voxels in an anatomical or functional ROI was used, thereby decreased the number of multiple comparisons voxel space to the number of ROIs.

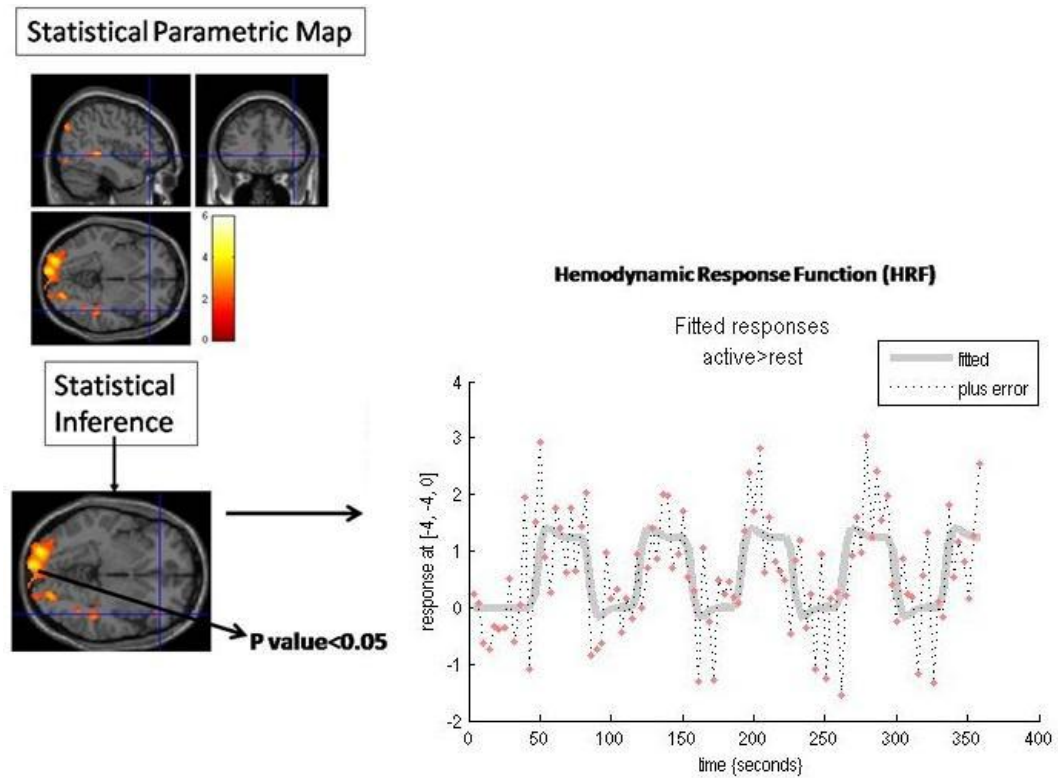


Figure 31: Final interpretation of statistical parametric map

3.1.7.2 Diffusion fiber Tractography for white matter tract reconstruction

Diffusion fibre Tractography (DFT) was done by using DTI studio software (developed and distributed by H.Jiang & S.Mori, John Hopkins University and Kennedy Krieger Institute, <http://Ibam.med.jhmi.edu>). For 3D reconstruction of white matter tracts, we followed Deterministic approach based on Fibre-Assignment by- Continuous-Tracking (FACT) algorithm.

A multiple ROI (Region of Interest) approach was followed to reconstruct language related white matter pathways based on manually defined ROIs on the axial, coronal or sagittal color FA map of each subject. When multiple ROIs were used for tract reconstruction, AND, OR, and NOT Boolean operators are used depended on the characteristic trajectory of each fibre tract .The OR is the first operator to be used, which selects all fibres that comes through a marked region. After “OR”, a combination of AND and NOT was used to manually fine tune and trim the selection based on visual inspection.

The AND operator discards fibres that do not go through the marked region, and NOT operator rejects all fibres that pass through the marked region (**figure 32**). It is therefore relatively straightforward to segment and virtually reconstruct prominent white matter structures. The ROIs were placed with the help of experienced neuroradiologists. The path is propagated from each seed point and from here it propagates, parallel to the principal eigenvector until the boundary of the voxel is encountered, at which point, the algorithm traverses the next voxel in a direction parallel to the eigenvector at the centre of the new voxel (Mori et al, 2002; Wakana et al 2004). An FA threshold of 0.2 and a turning angle of 30° were selected to terminate the tract propagation (**figure 33**). For each white matter pathway, following quantitative parameters were calculated, (a) Fractional Anisotropy (FA), (b) Mean Diffusivity (MD), (c) Fibre Tract volume (FTV) and (d) Relative fibre density (RFD).

To determine the hemisphere dominance based on structural asymmetry values, a fibre Asymmetry Index (AI) was calculated by using the formula,

$$AI = (RFD \text{ in left} - RFD \text{ in right}) / (RFD \text{ in left} + RFD \text{ in right})$$

If AI > 0.20, it indicates leftward structural asymmetry and if AI < -0.20 = indicates Rightward structural asymmetry and value close to “0” represents bilateral fibre tract asymmetry index.

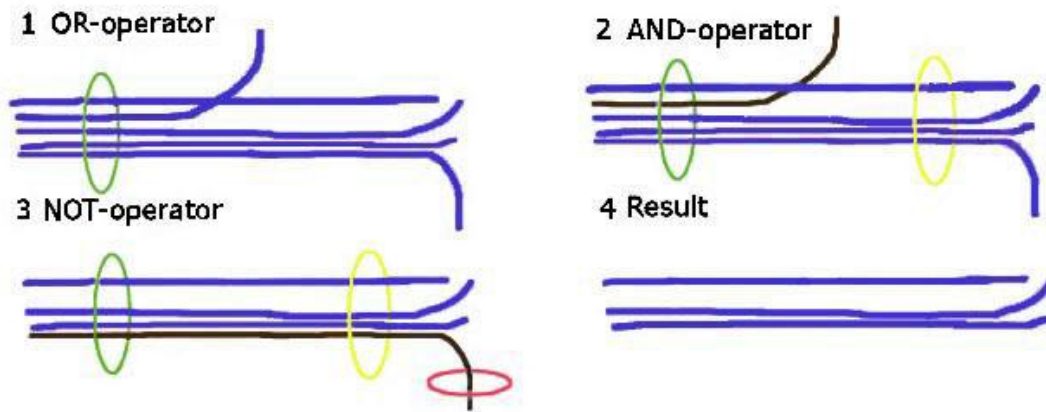


Figure 32: Procedure for selecting the desired white matter tract using Boolean operators. The colors of the ring depict different operator. OR= green; AND = yellow; NOT = red.

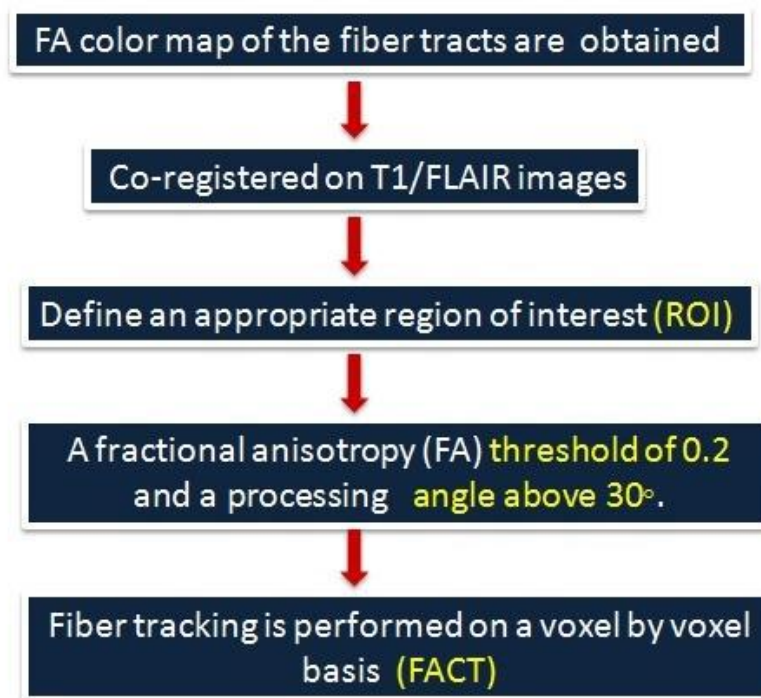


Figure 33: Work flow of Deterministic fibre tractography

Tractography of language networks have done under two broad categories;

Dorsal pathways and Ventral pathways

3.1.7.2 .1 Dorsal Language pathways

3.1.7.2.1.1 Superior Longitudinal Fasciculus (SLF) / Arcuate Fasciculus (ArcF):

White matter tract located in the lateral part of cerebral hemisphere above the insula , connecting Inferior frontal area and Superior temporal area as a “C” shaped trajectory (**figure 34a**) .It consists of 2 pathways, (a) Long direct pathway connecting Broca’s with Wernicke’s area, i.e, ArcF and (b) Indirect pathway consisting of 2 segments , anterior segment linking Broca’s territory with the inferior parietal lobule and posterior segment linking the inferior parietal lobule with Wernicke’s territory. For the reconstruction of SLF, a coronal section of color DTI map was selected. First ROI was drawn in a region, in which the fornix can be identified as a single intense structure and for the second ROI, an axial slice was selected at the level of anterior commissure and the projections located laterally to sagittal stratum. From color FA maps, green fibers lateral to the vertical corona radiata were identified as arcuate fasciculus. For tracking ArcF, an ROI was drawn on inferior frontal gyrus and another on a region, which includes posterior part of superior temporal gyrus on a sagittal slice of the DTI color map (**figure 34b**).

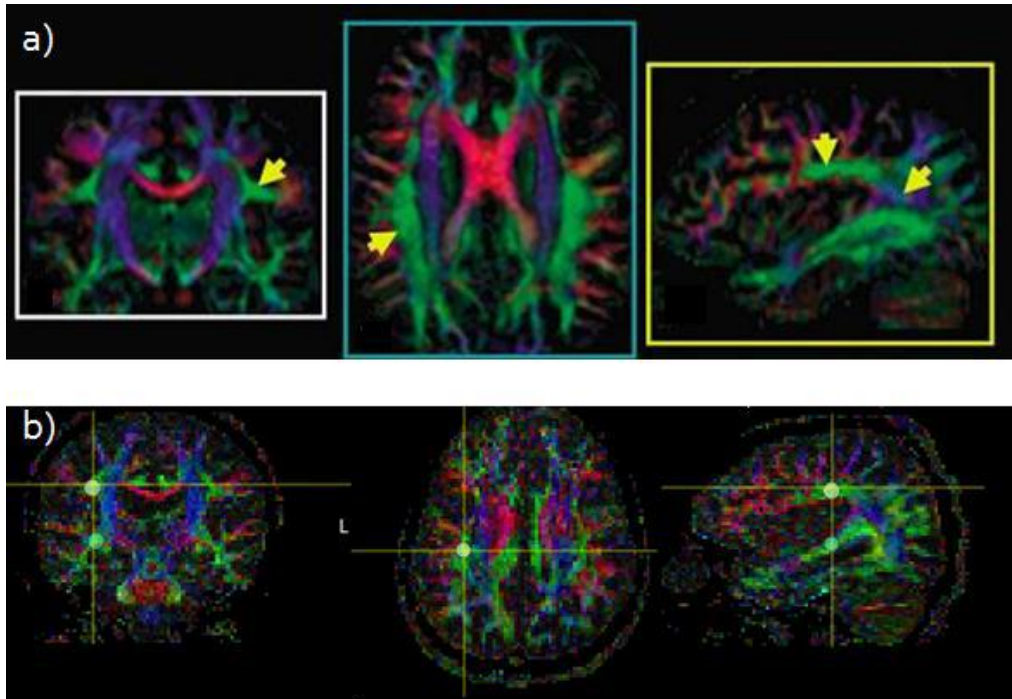


Figure 34: (a) The trajectory of Superior Longitudinal Fasciculus and its identification in color FA maps. Green fibers lateral to the vertical corona radiata belong to the arcuate fasciculus (yellow arrows indicate the anterior and posterior extent of the arcuate fibers).(b). ROIs drawn on respective trajectories of SLF/ArcF.

3.1.7.2.2 Ventral Language Pathways

3.1.7.2.2.1 Uncinate Fasciculus (UF)

The uncinete fasciculus is a ventral associative bundle that connects the anterior temporal lobe with the medial and lateral orbitofrontal cortex (**figure 35a**).In the temporal pole, the UF is lateral to the amygdala and hippocampus and then curves upward, passing behind and above the trunk of the middle cerebral artery into the lower segment of the extreme capsule, lateral to the claustrum and medial to the insular cortex. From there, it continues into the posterior orbital gyrus. Tractography of UF was done by selecting the most posterior coronal slice in which the temporal lobe is separated from the frontal lobe.

First ROI drawn on the inferior temporal lobe and the second ROI includes posterior frontal lobe (**figure 35b**). A NOT operator was used to remove association and projection tracts running close to UF.

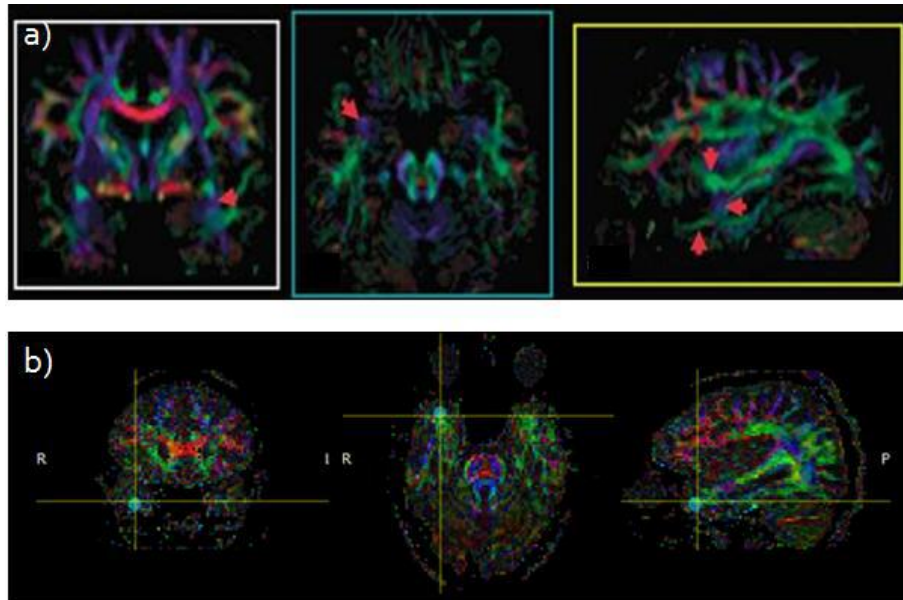


Figure 35: (a) The trajectory of the uncinus fasciculus (red arrows) and its identification in color maps at various slice levels and orientations. (b) ROIs drawn on respective trajectories of UF.

3.1.7.2.2.2 Inferior Longitudinal fasciculus (ILF):

The ILF is a ventral associative “U” shaped fiber with long and short segments connecting the occipital and temporal lobes. The occipital branches of the ILF arise from the dorsolateral surface of the occipital region, ventromedially from the posterior fusiform and lingual gyrus and dorsomedially from the cuneus. The fibers run parallel to splenial and optic radiation pathways and gather as a single bundle at the level of lateral ventricle (**figure 36a**). To reconstruct the ILF, a coronal slice is selected that identifies the posterior edge of cingulum, which includes the first ROI in the medial occipital white matter. Next, the most posterior coronal slice, which includes the entire temporal lobe, is selected and the second ROI is drawn in the green bundle on the far lateral aspect of the sagittal stratum. Alternately,

both ROIs can be drawn on an axial slice of the color DTI map that shows the ILF (**figure 36b**).

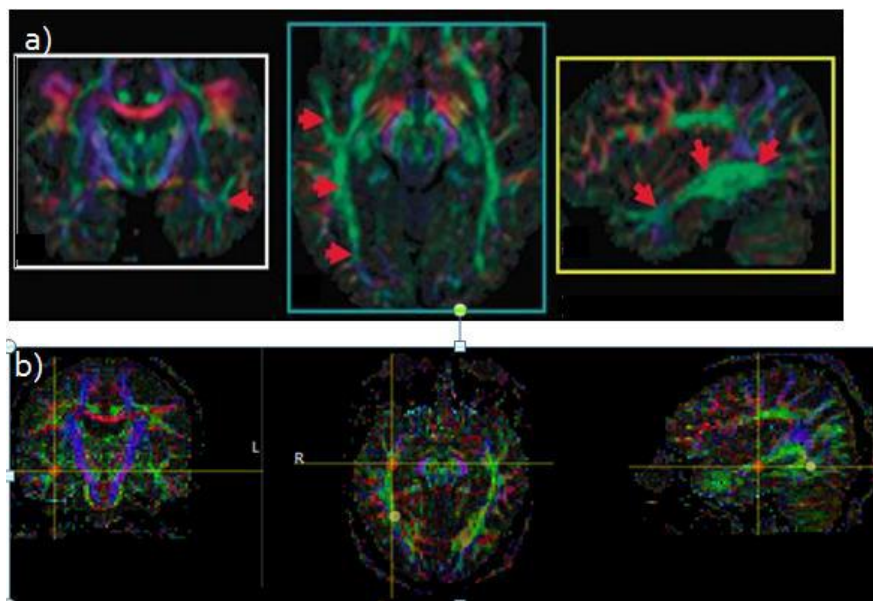


Figure 36: (a) The trajectory of the Inferior Longitudinal fasciculus (red arrows) and its identification in color maps at various slice levels and orientations. (b) ROIs drawn on respective trajectories of ILF.

3.1.7.2.2.3 Inferior fronto Occipito Fasciculus (IFOF):

This is a ventral associative bundle that connects the ventral occipital lobe and the orbitofrontal cortex. In the temporal stem and extreme capsule, the IFOF runs posterior to the uncus. These ventral pathways are linked to the perisylvian network at least in two different regions, posteriorly connected the Wernicke's area and lateral temporo-occipital cortex through short U-shaped fibres and anteriorly through intralobar fibres connecting lateral orbitofrontal cortex to Broca's area (**figure 37a**).

IFOF tracts were identified by placing the first ROI on a coronal slice, at the midpoint between the posterior edge of cingulum and posterior edge of parieto-occipito sulcus. For the second ROI, a coronal slice was selected at the anterior edge of the genu of corpus callosum (**figure 37b**).

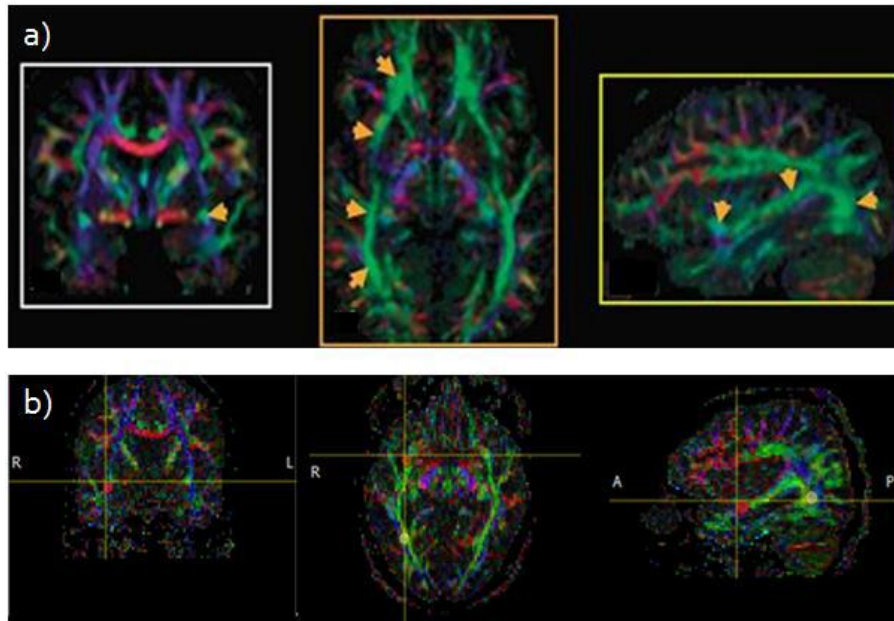


Figure 37: (a) The trajectory of the Inferior fronto-occipito fasciculus (yellow arrows) and its identification in color maps at various slice levels and orientations. (b) ROIs drawn on respective trajectories of IFOF

3.1.7.3 VBM based volumetric analysis

The volumetry of PT, HG and Insula were done by voxel based morphometric approach using SPM. Volumes of selected regions of interest were measured using an approach based on Automated Anatomical Labeling (AAL- Anatomical Automatic Labeling; <http://www.cyceron.fr/web/aal>), which is a digital atlas of the human brain. The technique used a high resolution T1 image (MPRAGE) of the subject with excellent GM-WM contrast, which was further normalized to the customized template through affine and nonlinear transformations. The normalized images were then segmented into GM, WM, and CSF using the customized prior probability maps. Further undergone modulation step, in which voxel values of the GM images were multiplied by the measure of relative volumes of warped and unwarped structures derived from the nonlinear step of spatial normalization. The modulated gray matter images were then smoothed with an 12 mm isotropic Gaussian kernel. Individual grey matter structures were segmented out (**figure 38**) based on AAL atlas with the help of

matlab based segmentation algorithm. Final output represented as a three-dimensional matrix, which includes the spatial x, y, and z coordinates of voxels in the standard space, and each value of the 3D matrix is proportional to the gray matter structure volume within each voxel (**figure 39**). The total volume of the individual gray matter structures (measured in cm³) were computed by multiplying voxel value by voxel volume and summing the result throughout all voxels.

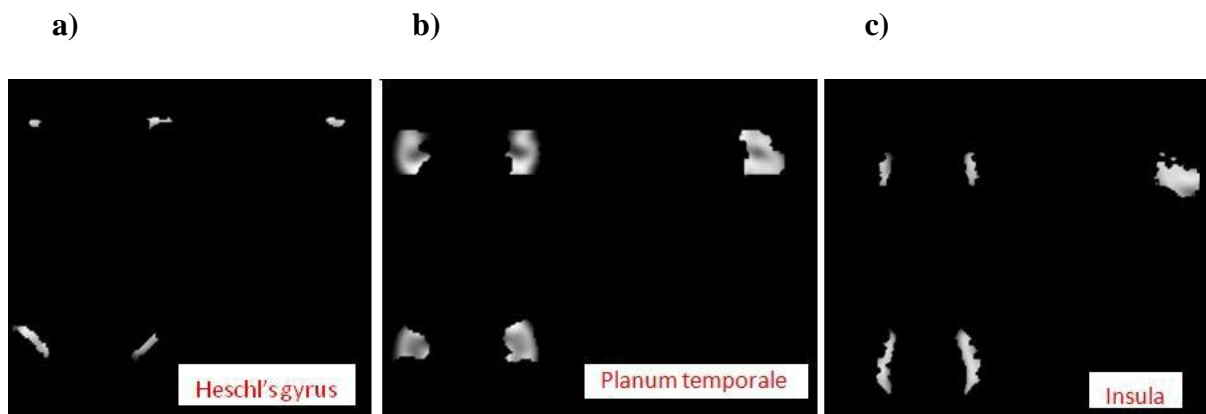


Figure 38: Segmentation of grey matter structures

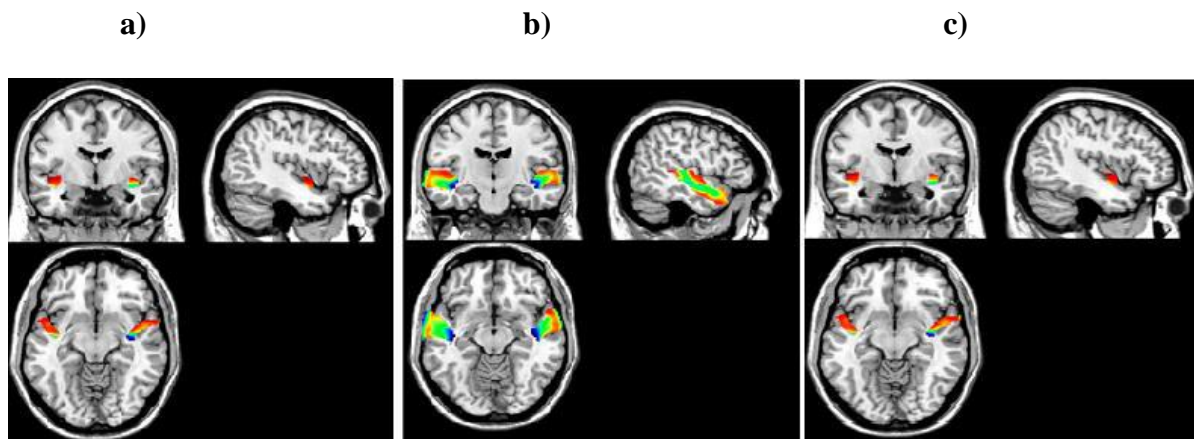


Figure 39: 3D overlay of grey matter structures. a) HG; b) PT and c) Insula

3.5 Statistical Analysis

All statistical analysis was performed using SPSS (Statistical Package for Social Science) software Version 17.0. To assess the reproducibility of fMRI and DTI measurements, an inter-rater agreement between the two independent operators was calculated using kappa statistics. Independent sample t tests were used to compare fMRI

laterality scores, FA and MD values for patient and control subjects. Post hoc test was used for correction of multiple comparison errors. An ANOVA test with specific post hoc test was performed for VBM based volumetric measurements in both controls and patients to determine the degree of language lateralization. In order to test relation between relative fibre asymmetry index and fMRI lateralization Index, a linear Regression analysis was carried out and the correlations between the three imaging modalities were calculated by using Pearson correlation coefficient. Statistical significance was considered at the $p < 0.05$ level.

Chapter 4

RESULTS

s4.1 Major findings of fMRI experiment

fMRI scanning was successfully done in all subjects. The results of group level analysis by SPM revealed significant BOLD fMRI activations in both control and TLE subjects. Detailed results explained in the following section.

4.1.1 Control subjects;

- a) In general, VG and SeT language tasks produced optimum BOLD fMRI activation results in healthy controls than Syn and WP tasks.
- b) Obviously the VG task produced significant BOLD fMRI activation results ($p < 0.001$) in language expression and language comprehension areas, the classic Broca's area and often in Wernicke's area in the dominant hemisphere.
- c) During SeT task, a similar network of VG activation was found, but more predominantly in brain areas which are involved in reading comprehension (Wernicke's area) and less activation was found in speech production area.
- d) Significant ($p = 0.001$) patterns of HRF were found for VG and SeT language task than Syn and WP ($p = 0.101$).

Detailed BOLD results of control subjects were shown in **Table 2**.

4.1.2 TLE subjects;

- a) In left handed TLE subjects, the verbal fluency tasks were associated with strong activations in the right anterior language network (inferior frontal gyrus, insula) and also produced significant activations in the right and left superior temporal language area, inferior parietal lobule and supplementary motor area.

- b) Right handed TLE patients showed predominant activations within the left inferior frontal, middle frontal and temporal regions and less activations was found in right posterior language areas.
- c) The semantic association task showed strong activations in both anterior and posterior language areas in TLE subjects.
- d) The syntactic task produced activations in frontal language areas and no significant activation was found in speech comprehensive areas in either RTLE or LTLE.
- e) The word pair task failed to produce any significant activation in LTLE subjects, however comparatively less activation in left speech production areas were found in RTLE subjects.

4.1.3 Hemodynamic response functions in controls and TLE.

- a) The HRF response patterns for VG and SeT paradigms was found to be fitted well with the experimental boxcar / blocked design model compared to Syn and WP tasks in both subject groups. It was predicted by comparing the group level HRF plots for different experimental paradigms (**figure 40, 42**).
- b) Significant differences ($p= 0.001$) in fMRI BOLD HRF responses was found between the TLE group and the control subjects, especially in inferior frontal gyrus (Broca's area), inferior parietal language (Geschwind's area) and superior temporal gyrus (Wernicke's area).
- c) In TLE subjects, relatively good HRF BOLD activation patterns were found during VG and SeT tasks than Syn and WP tasks
- d) While considering the percentage BOLD signal intensity change, the LTLE patients were found to have significantly reduced signal intensity in the right temporo -parietal language areas during VG ($t=-3.551$, $p=0.002$) and SeT tasks ($t=-2.035$, $p=0.052$) compared with healthy controls.

- e) The pattern of BOLD activation in LTLE subjects was less left lateralized (independent sample t test; $t = -2.36$, $p = 0.021$) relative to controls.
- f) RTLE patients showed a trend for reduced left temporal activations during VG ($t = -1.897$, $p = 0.069$) but not during SeT task ($t = -0.717$, $p = 0.48$). BOLD signal intensity in the inferior frontal area was found to be not reduced on either task ($t = 1.752$, $p = 0.094$ for VG and $t = 0.429$, $p = 0.675$ for SeT) relative to controls.

From the HRF responses, the mean percentage BOLD signal intensity changes in regional left temporal and frontal areas was tested for both VG and Set tasks in three subject groups.

- a) LTLE subjects were found to have significantly reduced BOLD signal intensity during VG task ($t = -2.568$, $p = 0.002$) and SeT task ($t = -2.351$, $p = 0.032$).
- b) No difference was found between the TLE groups in mean left frontal area signal during either above mentioned tasks. However, RTLE patients showed a trend for reduced left temporal lobe activation during VG task frontal lobe activations in these subjects was not reduced relative to controls.
- c) In general, significant differences ($p = 0.023$) were observed between LTLE and RTLE patients in percent signal intensity change for VG and SeT tasks but no significant differences ($p = 0.310$) were observed for Syn and WP tasks for both groups.
- d) No significant differences was observed between RTLE and LTLE patients in the left temporal or frontal lobe mean or maximum signal intensity change for either task.

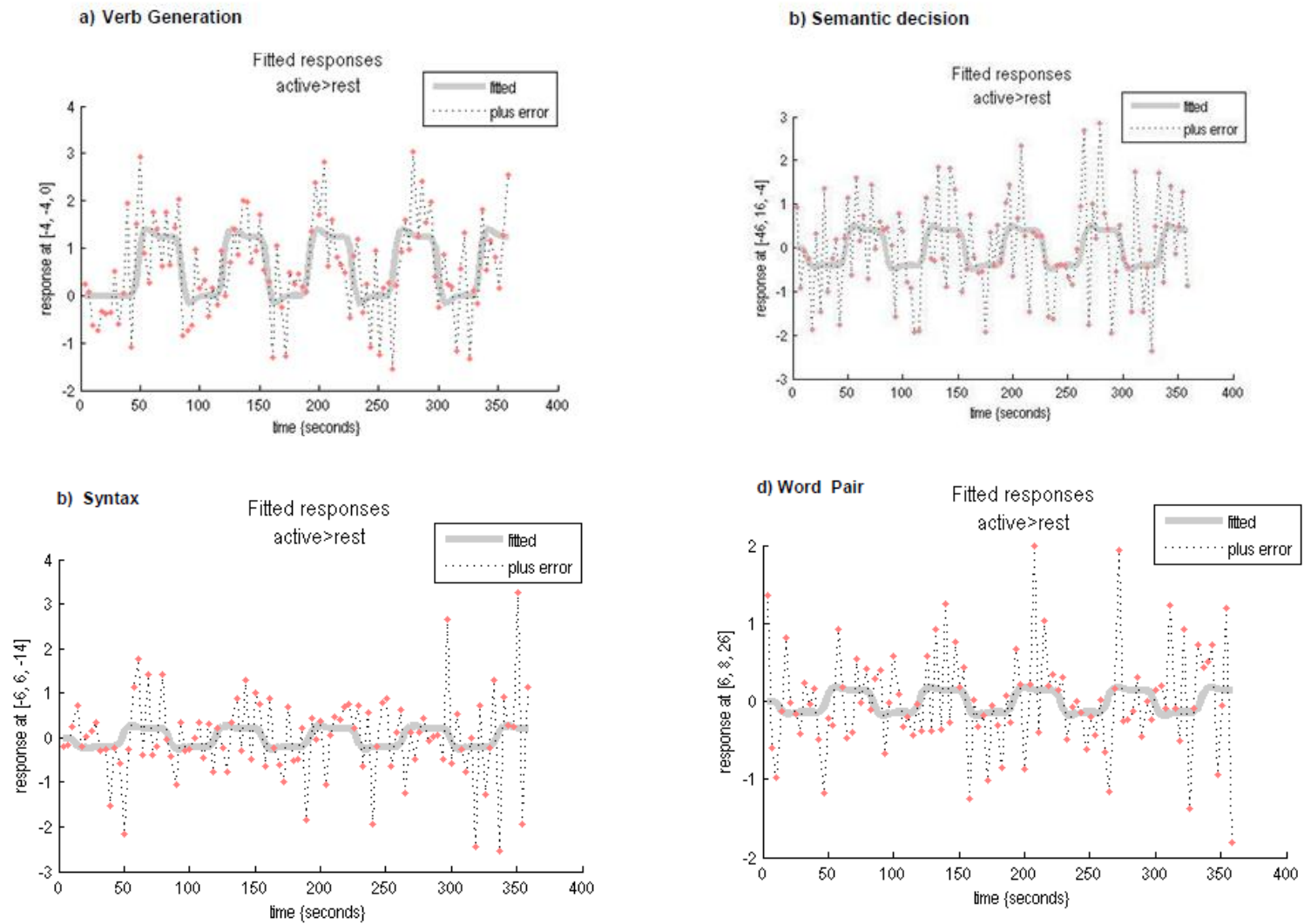


Figure 40: Plots showing hemodynamic response functions for different language tasks in control subjects.

Paradigm	Areas of activation	MNI coordinates	Cluster size (mm ³)	Z score	P value
Visual verb generation	Inferior frontal gyrus,	-46 32 10	899	4.32	0.002
	Middle frontal gyrus	-44 -56 12	741	3.58	0.031
	Supplementary motor area	-4 4 50	542	2.14	0.001
	Superior temporal gyrus	62 -28 4	956	5.13	0.025
Syntax	Inferior frontal gyrus	-45 30 8	245	3.21	0.114
	Middle frontal gyrus	46 53 -8	316	2.22	0.012
	Inferior parietal area	58 -49 1	211	2.36	0.005
Semantics	Inferior temporal gyrus	52 -18 3	789	5.47	0.023
	Superior temporal gyrus	-58 14 -10	845	2.65	0.025
	Inferior parietal area	-35 47 -6	889	2.32	0.058
	Middle frontal gyrus	-44 30 22	652	4.99	0.044
Word Pair	Inferior frontal gyrus	-35 12 9	233	3.69	0.126
	Middle frontal gyrus	-44 10 17	412	2.22	0.033
	Supramarginal gyrus	-52 -41 44	326	2.28	0.061

Table 2: BOLD fMRI activation results in healthy controls

4.1.4 Variability in language localization by measuring laterality Indices

For all subjects, language-related activations in the frontal and temporo-parietal areas were localized well within the anatomically predefined regions of interest. These activated clusters were further used for calculation of the functional laterality index (LI). Significant differences ($p=0.004$) were found in LI values between the TLE and control group

The major findings explained in the following section,

- a) No significant difference was observed on LI measurements between LTLE patients and healthy controls either during verbal fluency task ($t=0.584$, $p=0.566$) or semantic decision task ($t=-0.096$, $p=0.925$), however a tendency was seen for reduced left lateralised activation widely in LTLE.
- b) The overall functional LI showed left-sided functional hemispheric language lateralization ($LI \geq 0.10$) in 50 right-handed and 3 left handed control subjects.
- c) A bilateral pattern of language lateralization was found in 4 right handed controls and 3 left handed subjects.

- d) Out of 25 RTLE patients, left lateralized language dominance was found in 18 right handed RTLE subjects and out of remaining 5 right handed subjects, 2 showed symmetrical language activation pattern ($-0.10 < LI < 0.10$).
- e) Out of 32 LTLE subjects, and 25 right handed LTLE had left sided functional hemispheric language lateralization and 3 had bilateral pattern of language lateralization. 4 left handed LTLE subjects had right hemisphere language dominance ($LI < 0.01$).

Distribution of language laterality index in RTLE and LTLE subjects were demonstrated in **figure 41**.

Figure 43 and Table 3 illustrates the BOLD fMRI activation results and corresponding measurements obtained for TLE subjects. Determination of hemisphere dominance from voxel count based laterality indices are strictly depended on arbitrarily chosen statistical thresholds.

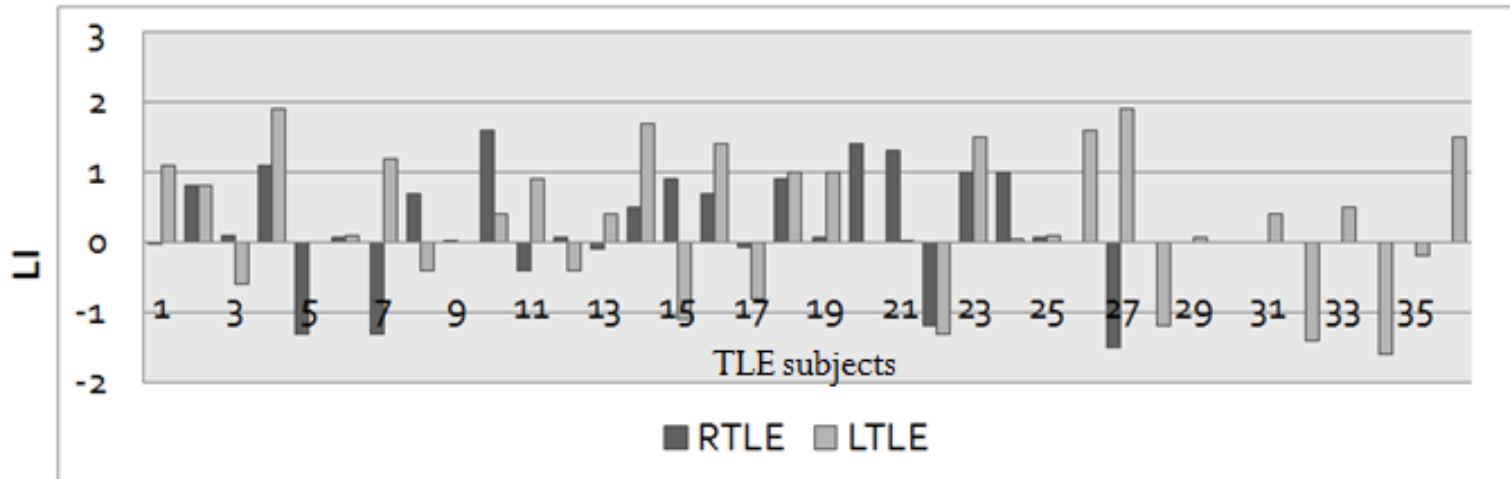


Figure 41: Bar diagram showing LI of right and left TLE patients. A positive number indicates left lateralization, a negative number indicates right lateralization and the number close to zero indicates bilateral pattern of activation.

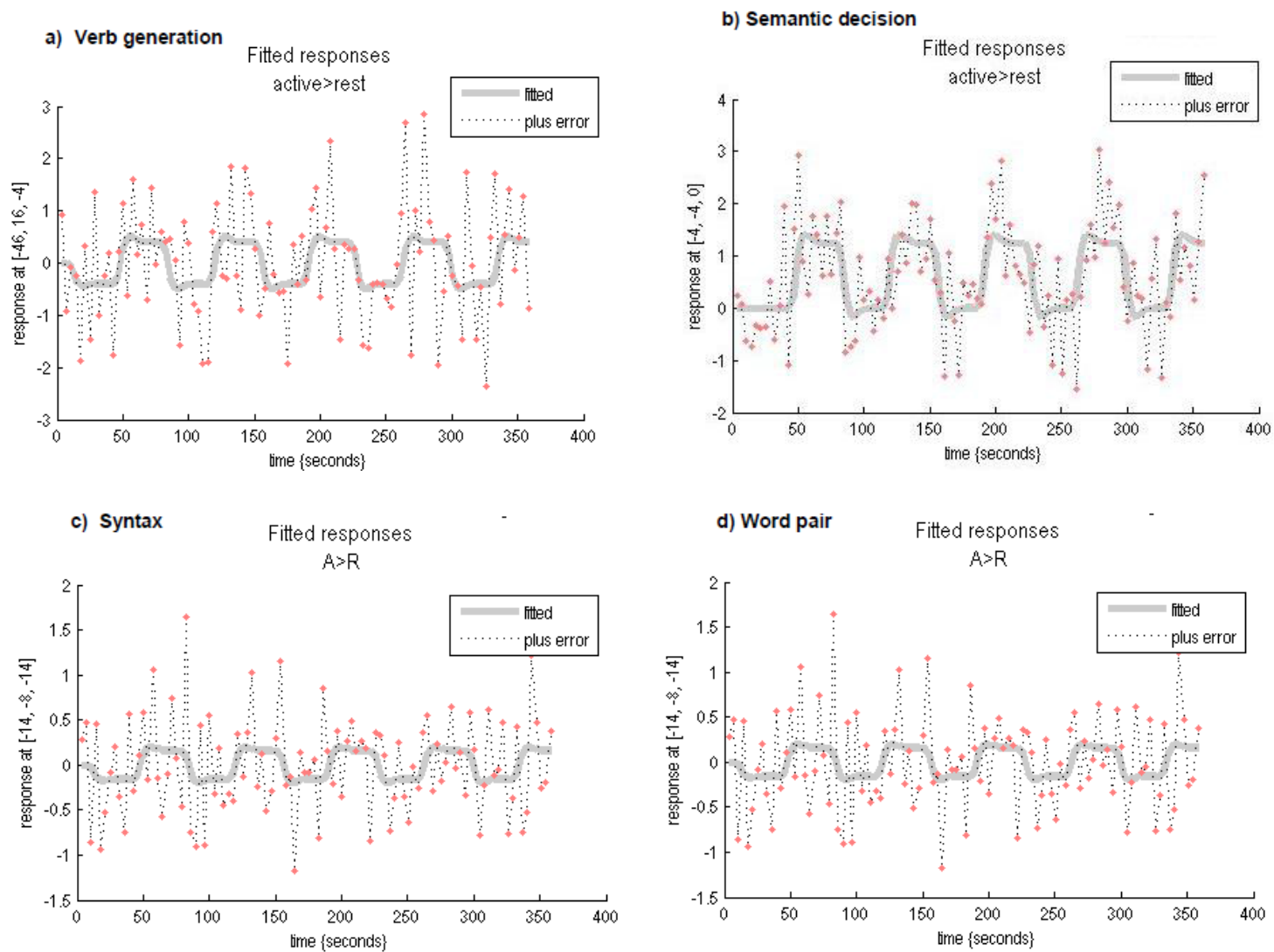


Figure 42: Plots showing hemodynamic response functions for different language tasks in TLE subjects.

Activated brain areas according to fMRI task	RTLE MNI co-ordinates	Z score	P value	LTLE MNI Co-ordinates	Z score	P value
VG – LH						
Inferior frontal gyrus	-46 32 10	4.32	0.002	-45 32 11	6.32	0.054
Middle frontal gyrus	-44 -56 12	3.58	0.031	-44 -56 12	5.45	0.004
Supplementary motor area	-4 4 50	2.14	0.001	-5 6 48	4.25	0.028
Superior temporal gyrus	62 -28 4	5.13	0.025	59 -24 8	5.69	0.041
VG-RH						
Superior temporal gyrus	60 -21 6	4.98	0.023	59 -18 7	5.32	0.027
Inferior parietal area	58 -52 18	2.56	0.035	56 -54 20	4.25	0.035
Insular region	42 22 -10	2.14	0.024	44 25 -15	2.65	0.036
Syn- LH						
Middle frontal gyrus	-44 -56 12	5.32	0.021	-45 -55 13	4.99	0.054
Supramarginalgyrus	-56 44 12	3.44	0.022	55 -45 -17	3.58	0.047
Syn-RH						
Inferior frontal gyrus	-45 30 8	5.65	0.041	-48 35 10	5.26	0.006
Middle frontal gyus	46 53 -8	3.21	0.006	45 56 -10	4.55	0.074
Inferior parietal area	58 -49 1	2.89	0.001	57 -48 2	3.65	0.058
SeT – LH						
Inferior temporal gyrus	52 -18 3	5.47	0.023	54 -20 7	4.33	0.050
Superior temporal gyrus	-58 14 -10	2.65	0.025	-58 14 -10	2.65	0.014
Inferior parietal area	-35 47 -6	2.32	0.058	-37 45 -9	4.89	0.081
Middle fontal gyrus	-44 30 22	4.99	0.044	-46 28 35	5.69	0.005
SeT-RH						
Superior temporal gyrus	-52 -26 6	6.35	0.032	-54 -23 9	4.89	0.032

Middle temporal gyrus	-50 -22 10	5.33	0.044	-44 -28 18	5.47	0.005
Inferior frontal gyrus	-36 12 10	6.19	0.065	-40 18 -27	3.68	0.080
WP-LH						
Supramarginalgyrus	-56 -40 12	3.21	0.031	57 -47 -26	4.36	0.030
Superior temporal gyrus	-51 -25 8	2.95	0.045	-55 -36 7	3.65	0.005
Supplementary motor area	4 12 50	2.33	0.036	7 25 -14	2.11	0.024
WP-RH						
Inferior frontal gyrus	-35 12 9	6.58	0.022	-38 15 27	3.32	0.050
Middle frontal gyrus	-44 10 17	5.32	0.056	-48 28 -36	2.89	0.006
Supramarginalgyrus	-52 -41 44	2.14	0.004	-58 -35 24	4.21	0.024
WP- LH						
Inferior frontal gyrus	40 -18 -32	3.69	0.026	47 -20 -38	3.68	0.063
Inferior parital area	-38 20 16	2.22	0.033	-41 25 18	2.69	0.040
Insular region	42 22 -10	2.28	0.041	44 26 -18	2.14	0.036

Table 3: BOLD fMRI activation results in RTLE and LTLE patients.

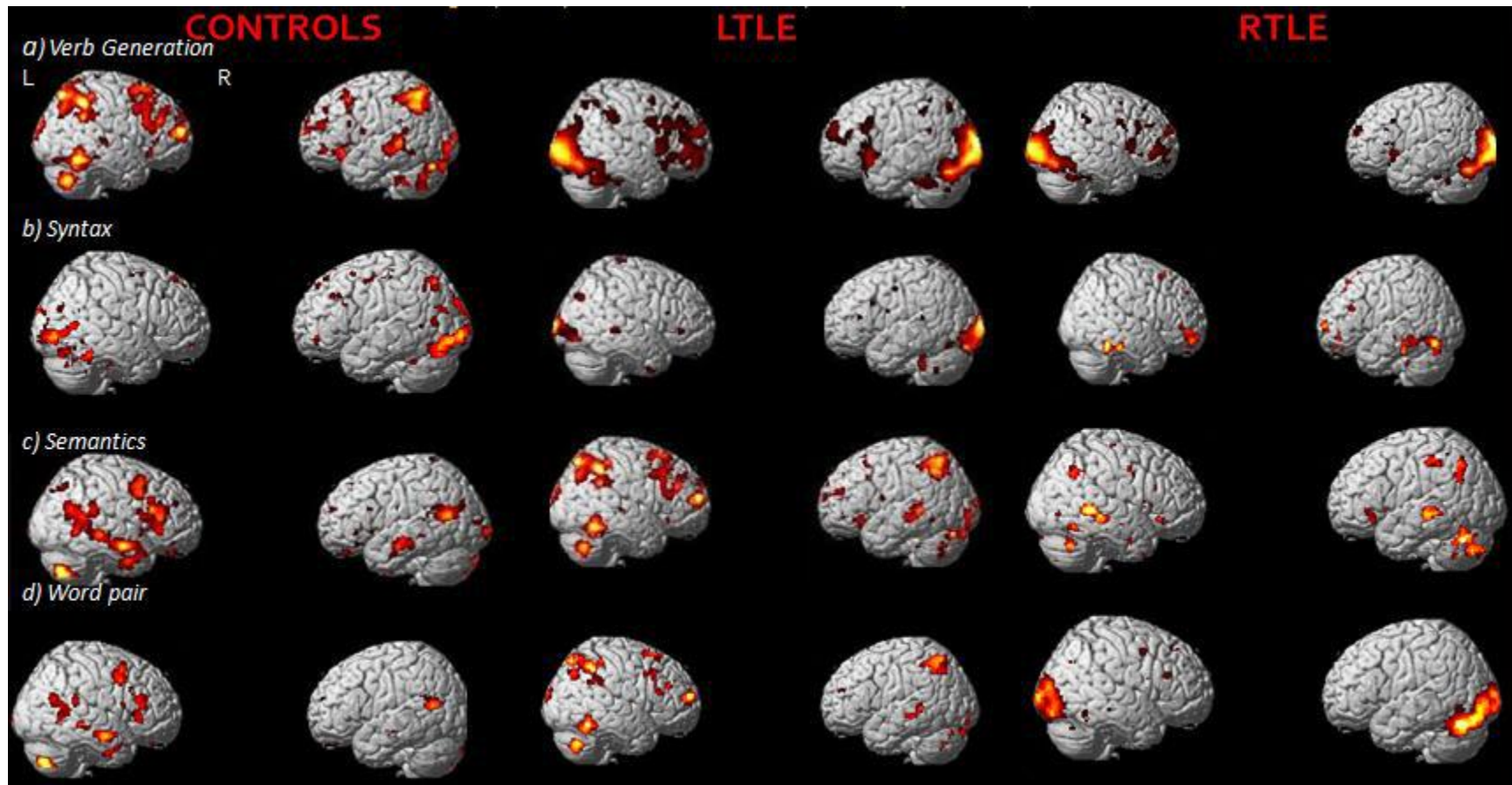


Figure 43: Group level average activation SPM t maps (3D rendered) generated for control and TLE subjects. Increased activation was observed in frontal and temporal language areas in controls for VG and SeT tasks and reduced activation was observed in Syn and WP tasks. LTLE showed increased activation in left frontal and temporal regions for VG and SeT tasks compared to other two tasks. RTLE patients showed a trend for reduced left temporal activations during VG, WP and Syn tasks but not during SeT task.

White matter tracts	FA			MD (mm ² /s)			RFD			Tract volume (mm ³)		
	RH	LH	BL	RH	LH	BL	RH	LH	BL	RH	LH	BL
ArcF												
R	0.522	0.536	0.456	959	987	965	0.43	0.55	0.41	2416.33	3012.56	2956.36
L	0.624	0.571	0.425	1005	899	951	0.52	0.49	0.43	3365.41	2965.22	2924.12
<i>P</i> value	0.021	0.002	0.103	0.036	0.011	0.213	0.005	0.041	0.13	0.032	0.027	0.124
UF												
R	0.525	0.426	0.372	914	874	899	0.48	0.45	0.51	2323.21	2654.25	3012.02
L	0.532	0.412	0.368	928	897	878	0.56	0.47	0.49	2358.47	2541.29	3022.65
<i>P</i> value	0.022	0.131	0.127	0.011	0.028	0.109	0.038	0.124	0.101	0.039	0.014	0.211
ILF												
R	0.424	0.528	0.412	974	1021	974	0.42	0.49	0.42	3582.12	3654.98	2361.02
L	0.521	0.498	0.423	1124	986	962	0.45	0.46	0.43	3741.56	3412.32	2355.24
<i>P</i> value	0.014	0.012	0.112	0.069	0.054	0.314	0.041	0.017	0.218	0.003	0.018	0.146
IFOF												
R	0.541	0.557	0.544	821	901	854	0.51	0.49	0.55	2801.29	2789.54	3120.14
L	0.547	0.552	0.538	801	899	861	0.57	0.54	0.56	2811.32	2658.66	3122.52
<i>P</i> value	0.033	0.103	0.144	0.028	0.137	0.221	0.033	0.087	0.119	0.116	0.054	0.202

Table 4: Tract based statistics results of language white matter tracts = Right Hemisphere; L=Left Hemisphere; BL= Bilateral; FA (Fractional Anisotropy); MD (Mean Diffusivity); RFD (Relative Fibre Density).* = mean values.

4.2 Reconstruction of white matter language pathways using Deterministic Tractography

The standard deterministic fibre tracking approach using FACT algorithm was used to explore the major white matter pathways (ArcF, UF, ILF and IFOF) involved in human language function. In order to determine the variability in structural integrity of each white matter pathway, “tract based statistics” [Relative Fibre Density (RFD) Fractional Anisotropy (FA), Mean Diffusivity (MD), and Tract Volume (TV)] was calculated for both control and TLE group. Tractography of dorsal and ventral language tracts in control subjects were depicted in **figure 44**.

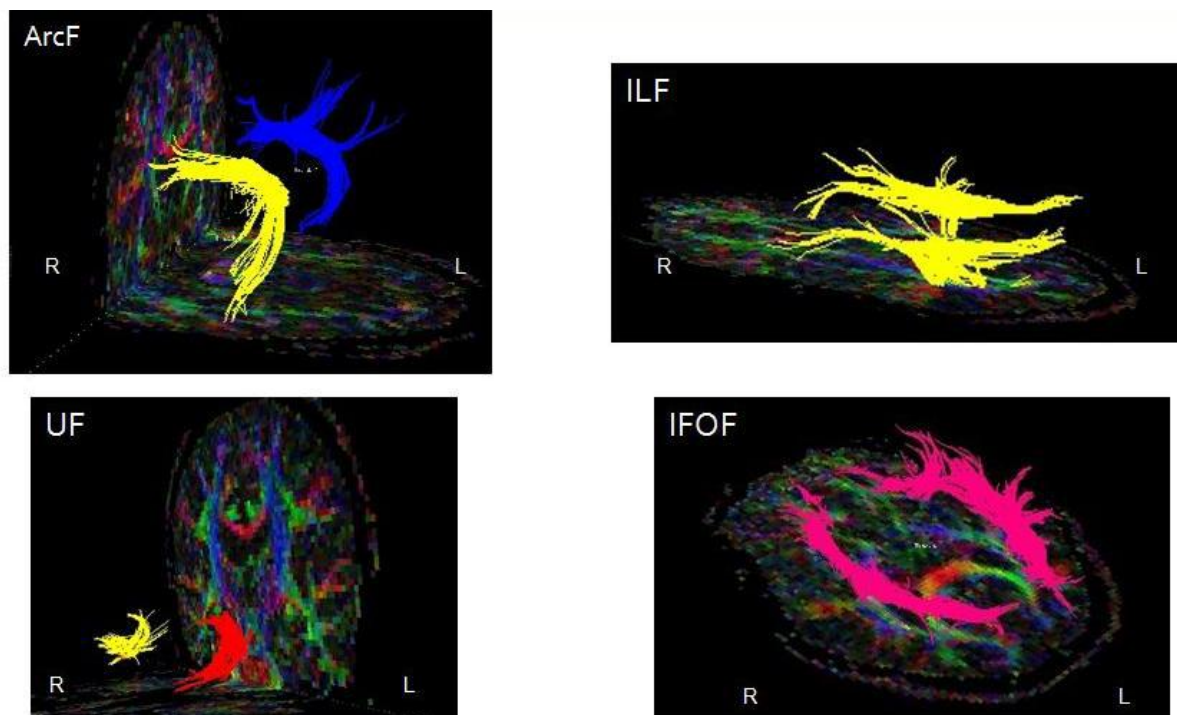


Figure 44: Tractography of dorsal (ArcF) and ventral (UF, ILF and IFOF) pathways in control subjects

4.2.1 Tract specific measurements in controls and TLE subjects

- a) The right handed control subjects, with predominant left sided fMRI activation, an asymmetry of left ArcF and ILF was observed with high FA and low MD values.

- b) The RFD, mean FA and tract volume of left ArcF, ILF and UF was also found to be higher than right sided tracts.
- c) There were no significant differences ($p=0.001$) in FA, MD or RFD values between right and left ArcF, UF and IFOF tracts in control subjects with bilateral fMRI activation.
- d) An asymmetry was observed in FA and RFD of right ArcF and ILF with increased tract volume in left handed subjects compared to left ArcF, and ILF.
- e) Tract volume of UF and IFOF were symmetric bilaterally. No significant differences were observed in any of the DTI parameters for IFOF and UF tracts in these subjects.
- f) The RFD of white matter structural connections also varied depends on disease pathology and handedness. In MTS cases, the study revealed more bilateral involvement of ArcF and unilateral involvement of ILF with significantly increased MD and decreased FA in both right and left TLE patients.
- g) More specifically, in the left TLE group, FA values in the entire left and right AF tract were comparable to controls; however MD values and RFD were elevated bilaterally.
- h) The right TLE group demonstrated higher MD values and lower FA values in right and left ArcF and right ILF. The FA and RFD of UF and IFOF were comparable to controls in RTLE.
- i) The LTLE patients have abnormal diffusion measures in UF and IFOF bilaterally. For patients with right TLE and left TLE, significant bilateral FA reduction was shown in two white matter tracts (ILF & ArcF) and ipsilateral FA reduction was shown in one tract (UF).
- j) In MTS cases, paired t tests revealed three tracts (ArcF, ILF and UF) with greater FA reduction on the left side without significant asymmetry. Mean MD values in the left TLE group was found to be higher in left ArcF and ILF, but not in the right TLE as

compared to controls. However, mean tract volume of left and right UF and IFOF was symmetrical in both TLE group.

- k) In right TLE cases, significantly higher MD values and lower FA values in the both left and right ArcF compared to controls were observed. **Figure 45** illustrates tractography of language pathways in TLE subjects and details of tract based statistics in both subject groups were shown in **Table 4**.

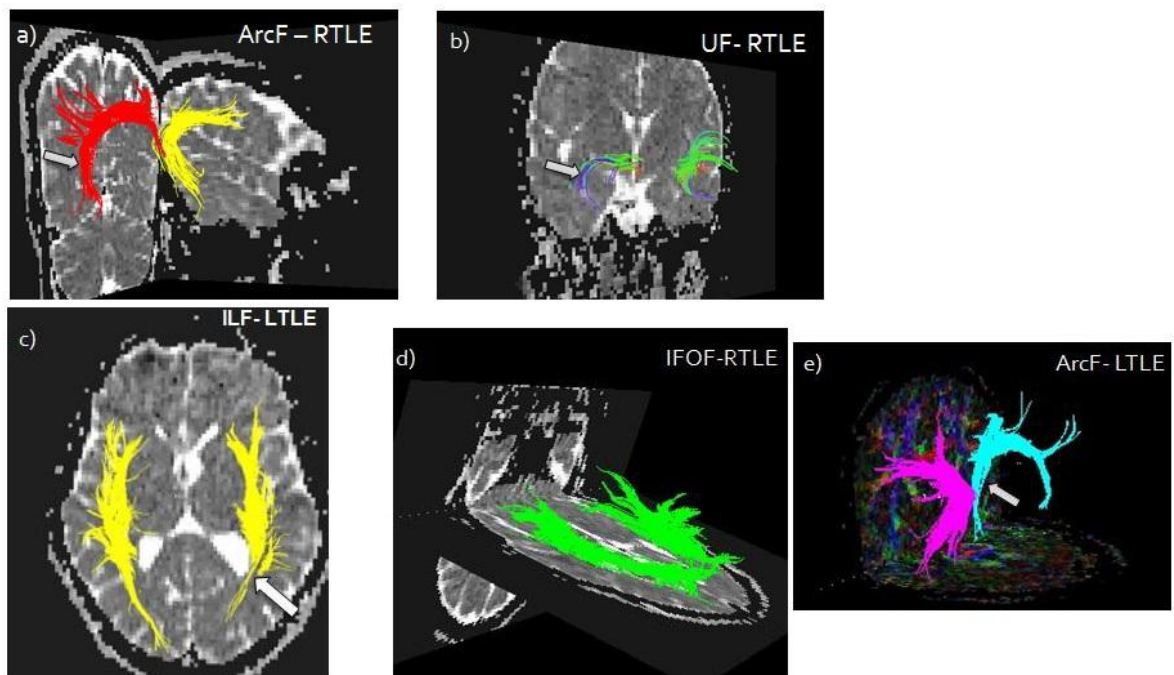


Figure 45: Fibre tractography in TLE patients demonstrates (a) reduced fibre density in right ArcF and (b) right UF in RTLE (c) LTLE subject showing decreased number of left ILF fibres than right (c) and ArcF (e) RTLE subject with unaffected IFOF(d) LTLE subject showing reduced ArcF fibre density

4.2.2 fMRI- DTI correlation for language lateralization

In order to investigate the structure –function relationship in TLE group, the study tested the correlations between the lateralization scores of fMRI activation measures (fMRI laterality indices) and asymmetry scores of DTI derived parameters (fibre asymmetry indices) obtained for both right and left TLE patients. The linear regression analysis demonstrated a good correlation in TLE group between language fMRI laterality index and fibre tract

laterality index, more specifically for Arcuate fasciculus (right ArcF: $r^2 = 0.2120$, $P = 0.004$; left ArcF: $r^2 = 0.280$, $p = 0.020$) and Inferior longitudinal fasciculus (right ILF: $r^2 = 0.2330$, $P = 0.007$; left ILF: $r^2 = 0.214$, $p = 0.003$) (**figure 46**). The findings suggest that in both RTLE and LTLE cases, the more lateralized pattern of fMRI activations found to be strictly correlated with increased ArcF and ILF connectivity. A negative correlation was found between uncinete fasciculus asymmetry index and fMRI lateralization indices in both TLE groups (RTLE UF: $r^2 = -0.012$, $p = 0.216$; LTLE UF: $r^2 = 0.023$, $p = 0.211$). There was no correlation between Inferior fronto occipito fasciculus asymmetry and fMRI measurements in LTLE patients ($r^2 = 0.285$, $p = 0.245$) and negative correlation was found between fMRI laterality index and fibre laterality indices in RTLE patients ($r^2 = -0.021$, $p = 0.226$) (**figure 47**).

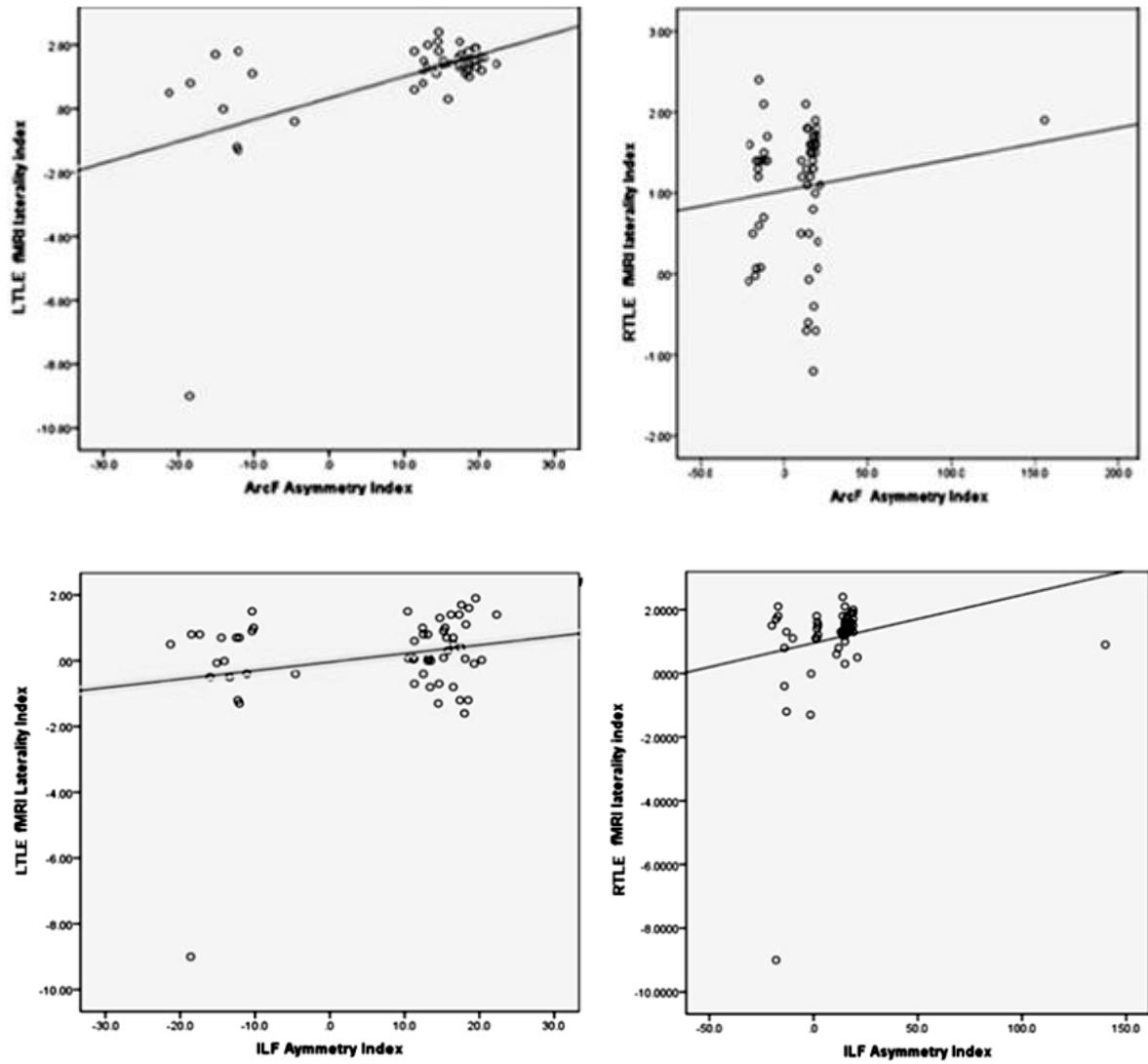


Figure 46: Positive correlation between fibre tract (ArcF & ILF) asymmetry index and fMRI laterality in TLE subjects

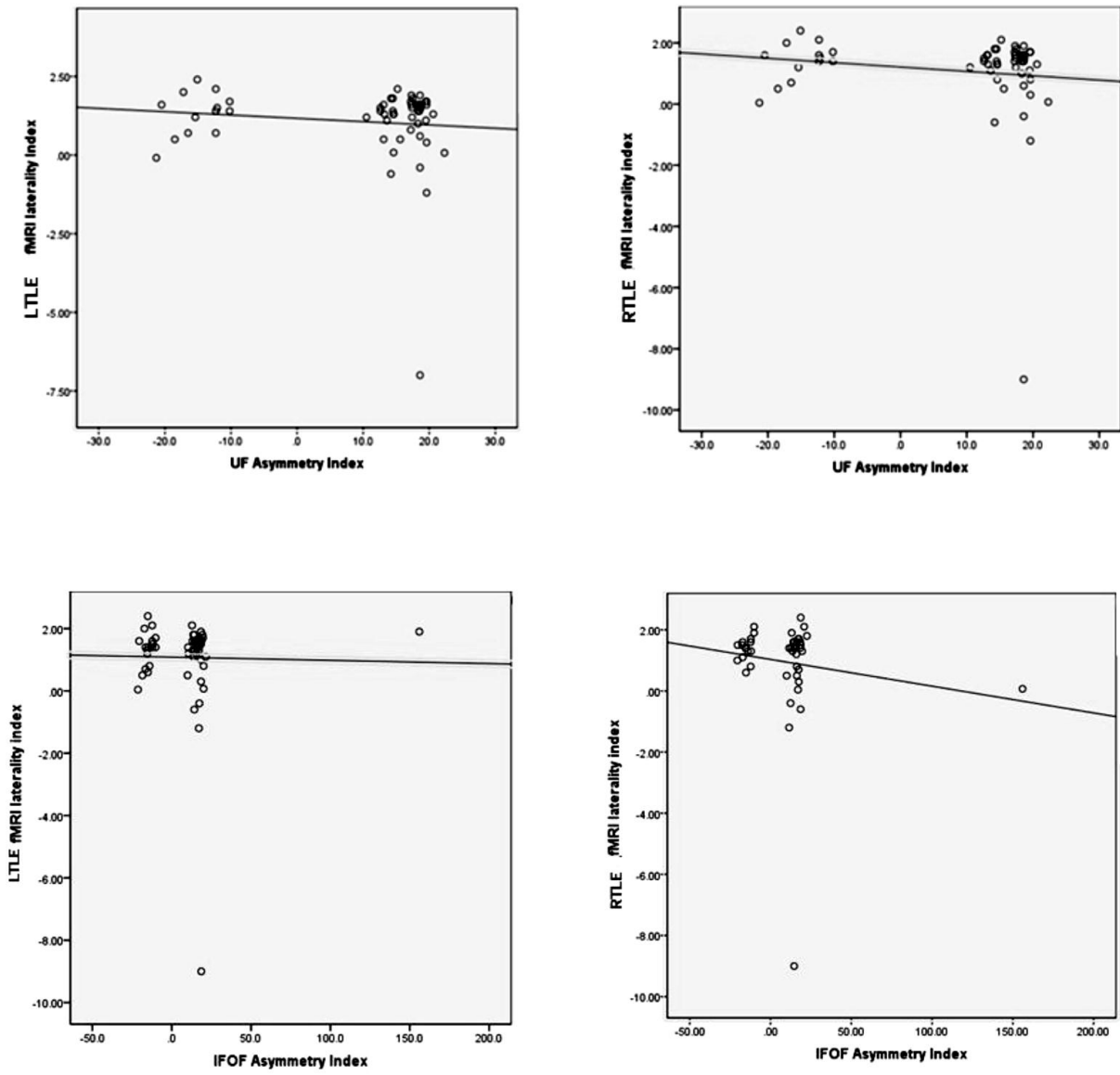


Figure 47: Negative correlation between UF and IFOF asymmetry index and fMRI laterality in TLE subjects.

4.3 VBM based volumetric measurements in controls and TLE

In normal healthy controls, an increased PT and HG volume was found in the language dominant hemisphere. **Figure 48** illustrates segmentation and volumetric analysis of PT, HG and insula by means of VBM. No significant differences ($p=0.210$) was observed for insular volume in left handed control subjects, however slightly increased volume was observed in right insula relative to left in right handed control subjects (**figure 49**).

Significant grey matter reductions of temporo-parietal grey matter structures (PT, HG and insula) were found in TLE subjects compared to normal controls during standard VBM approach (**figure 50**). Independent sample t tests revealed significantly ($p<0.01$) reduced left HG volume and left PT volume in 75% of LTLE group than the control and a significant reduction ($p=0.031$) in left insular volume were observed in about 20% of these patients compared to controls. The RTLE group showed a reduced right HG and PT volume compared to controls and LTLE. However, right insula was not different among LTLE groups, only significant volume differences ($p=0.021$) was observed in right insula for about 8% of RTLE group compared to controls. Post hoc tests revealed that total (left and right) HG and PT volumes was significantly ($P<.05$) lesser in LTLE patients compared with RTLE patients and healthy control subjects.

4.3.1 Correlation between grey matter volumetry and white matter structural integrity

The study tested the correlation between volumetric measurements obtained in TLE patients and associated structural integrity (FA) of white matter tracts using linear regression analysis. There exist a strong one to one correlation between atrophied ArcF (**figure 51**) and ILF (**figure 52**) in LTLE patients with reduced volumetric measurements of left PT ($r^2 = 0.2110$, $P<0.005$), HG ($r^2= 0.2130$, $P<0.022$) and insula ($r^2 = 0.214$, $P<0.241$) relative to healthy controls.

In RTLE a good correlation was found between FA of atrophied ArcF and ILF and reduced grey matter [HG ($r^2 = 0.2231$, $P < 0.002$) and PT ($r^2 = 0.231$, $P < 0.020$)] volume. No significant correlation ($r^2 = 0.465$, $P = 0.741$) was found between insular volume and atrophied white matter tracts. Study also revealed that IFOF and UF asymmetry was not correlated with volumetric measurements of any of grey matter structures (**figure 53**).

Detailed agreement between fMRI-DTI-VBM measurements were shown in **Table 5**.

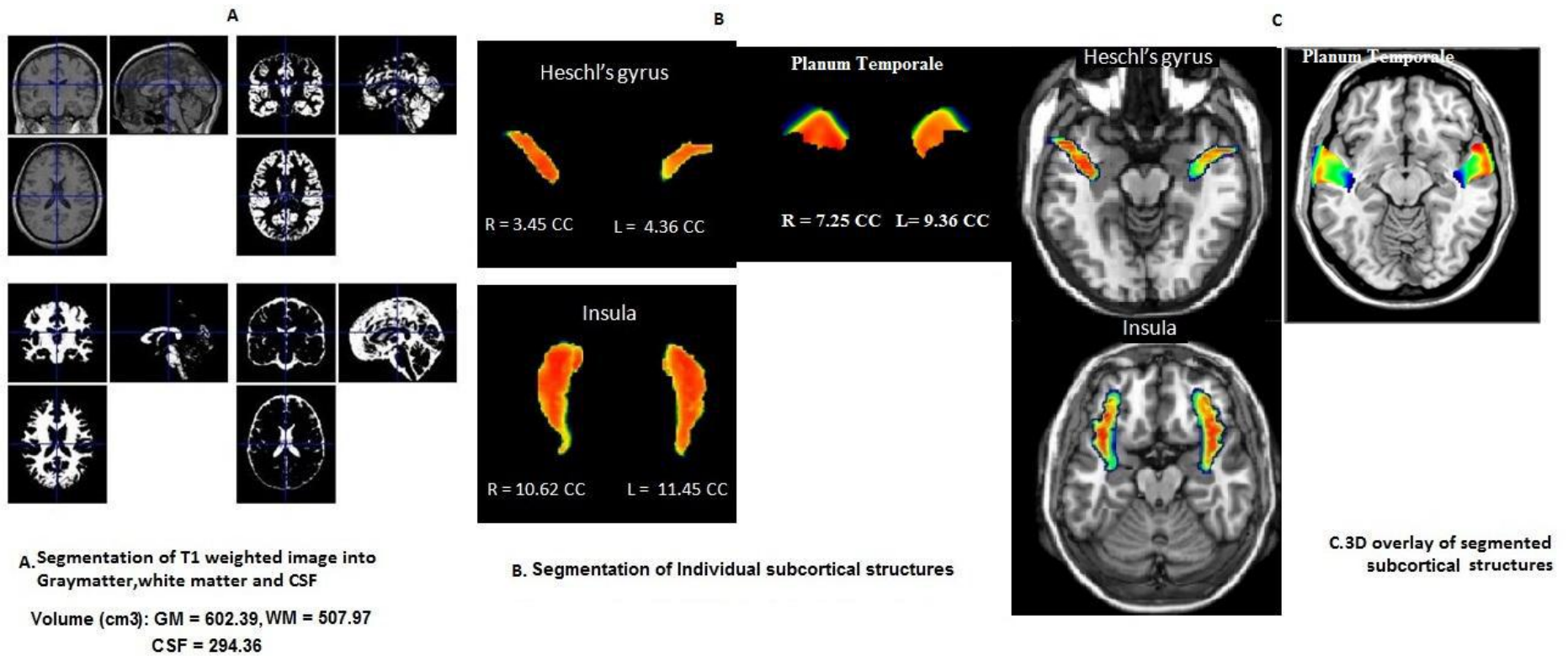


Figure 48: Segmentation and volume calculation of subcortical grey matter structures using Voxel Based Morphometric technique.

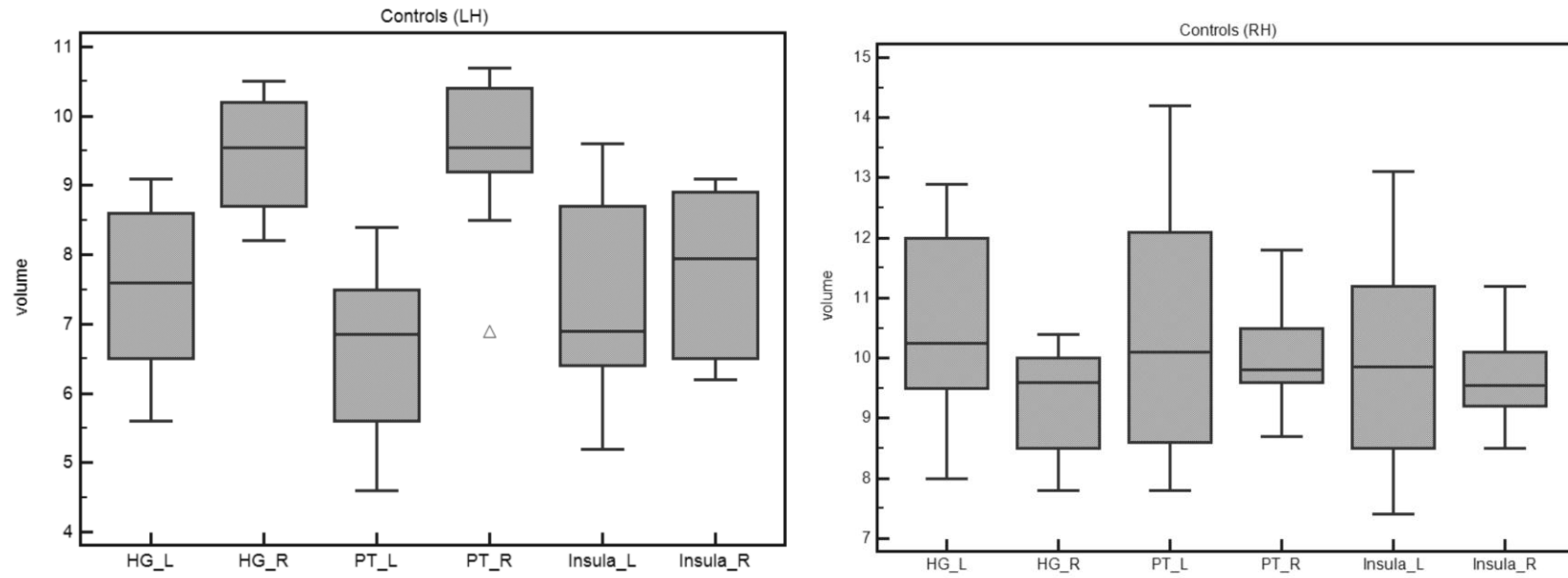


Figure 49: Box plot showing HG, PT and insular volume differences in control subjects

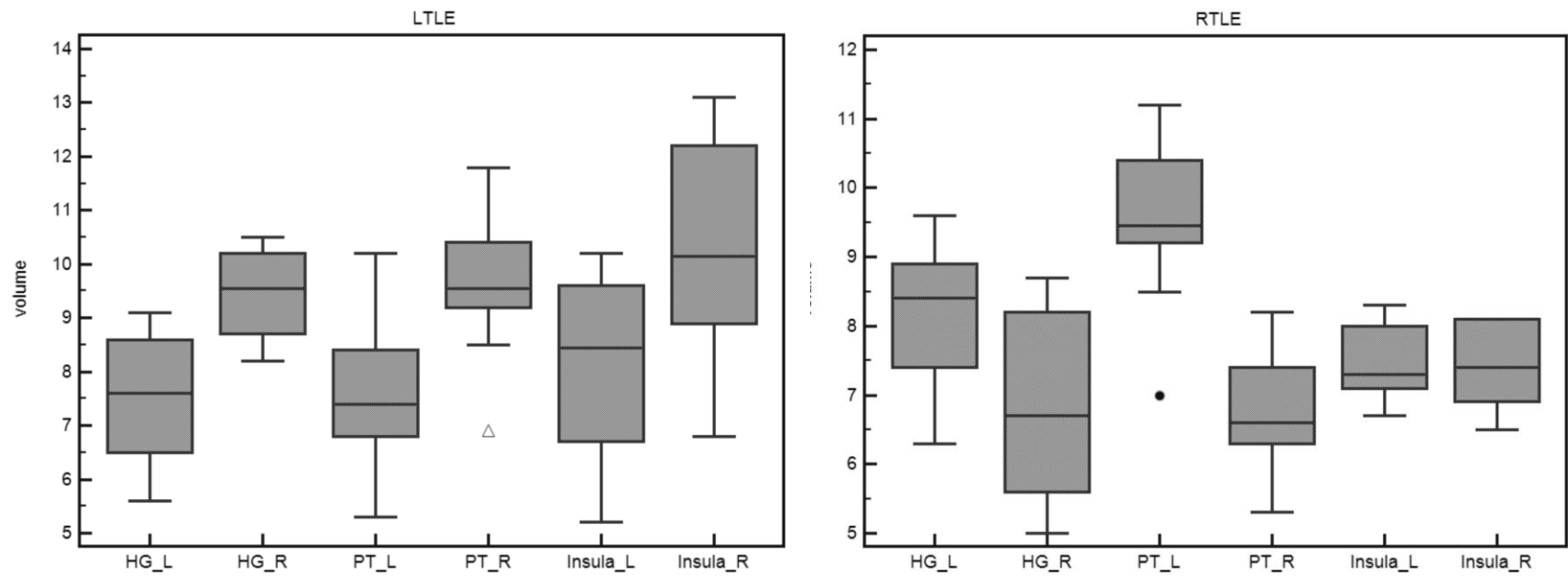


Figure 50: Box plot showing HG, PT and insular volume differences in TLE subjects

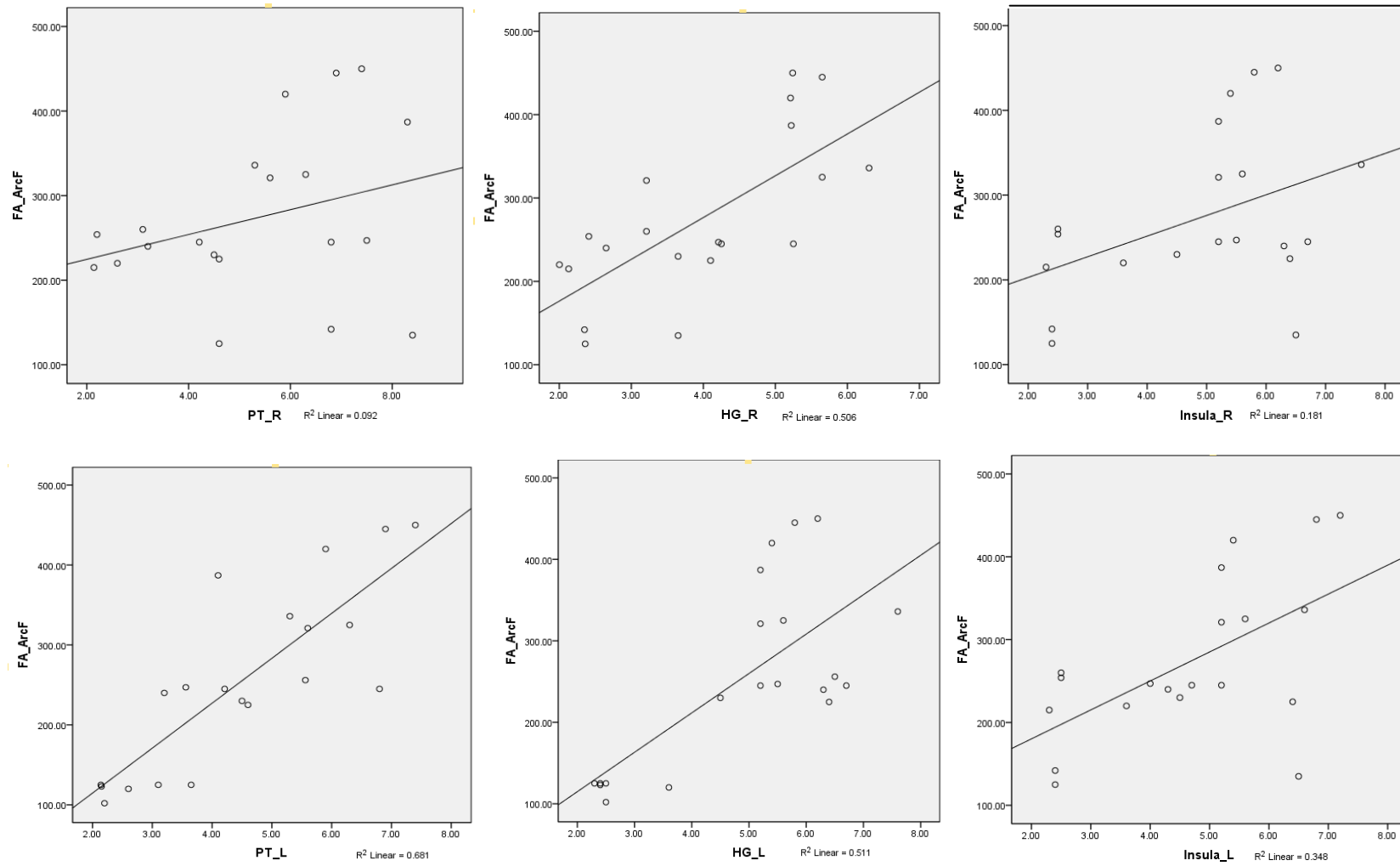


Figure 51: Correlation between ArcF FA and grey matter volume in LTLE

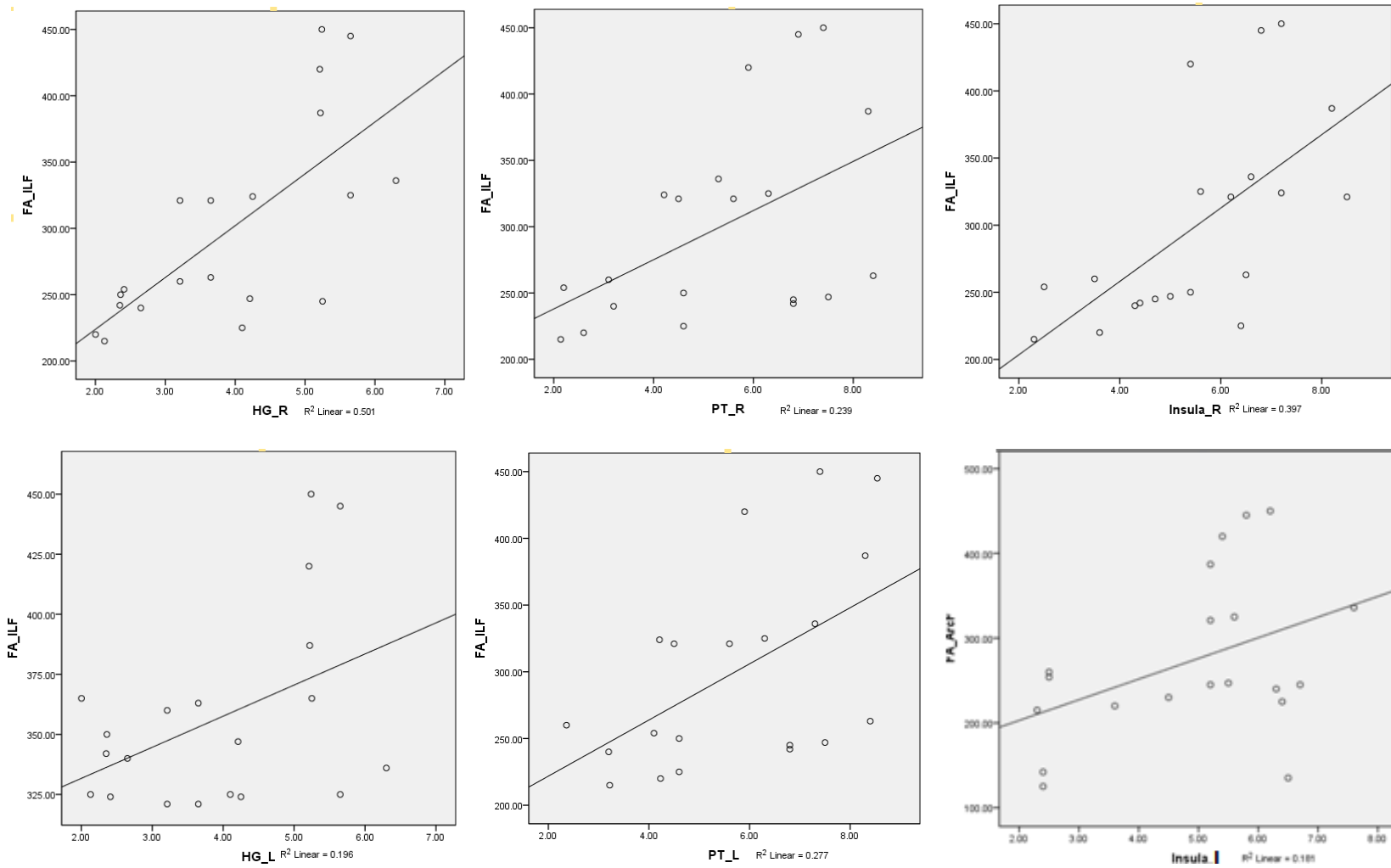


Figure 52: Correlation between ILF FA and grey matter volume in LTLE

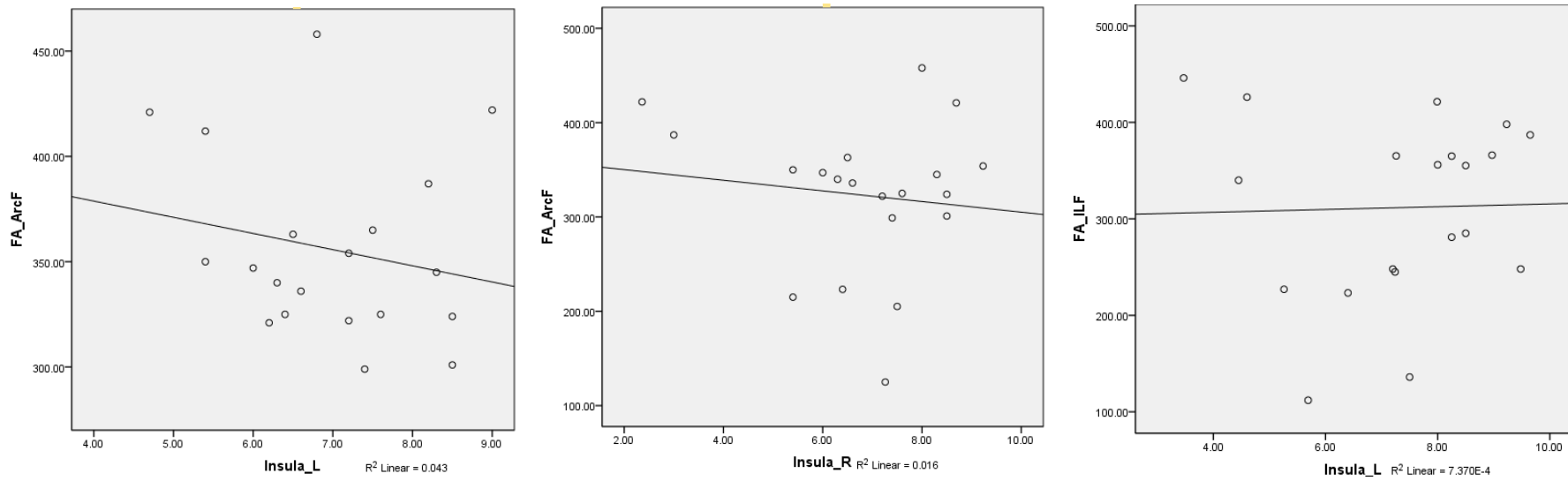


Figure 53: Negative correlation between FA (ArcF,ILF) and insula volume in RTLE

Subjects	fMRI results		DTI					Volumetry	
	Language dominance	Areas of activation	FA	RFD	MD	HG	PT	Insula	fMRI-DTI-VBM correlation
Controls (60)									Excellent (45)
									Good (11)
									Bad (4)
RH (54)	Left (42)	LIFG,LSTG, LSMG	LArcF↑ LILF↑	↑ ↑	↓ ↓	↑	↑	↓	
LH (6)	Right(4)	RILG,RIPL,RMTG,RSTG	RArcF↑	↑	↓	↑	↑	↓	
			RILF↑	↑	↓				
			RUF↑	↓	↑				
RTLE(25)	Bilateral(14)	RIFG,LIFG,RSTG,LSTG	RArcF ↑,LArcF↑	↑,↑	↓,↓	↑	↑	↑	Excellent (9)
			RILF↑	↑	↑				Good(13)
RH(22)	Left (18)	LIFG,LSTG,LMTG,LMTG	LArcF↑	↑	↓	↑	↑	↓	
			LILF↑	↑	↓	↑	↑	↑	
			LUF↑	↓	↑	↑	↓	↓	
LH(3)	Right(2)	RIFG,RMFG,RSTG,RMT	RArcF↑	↑	↓	↑	↑	↓	Bad (3)

LTLE(32)		G	RILF↑	↑					
	Bilateral (5)	LIFG,RIFG,RSTG,LSTG	RArcF↑,LIFG↑	↑	↓	↑	↓	↓	
									Excellent (14)
									Good (13)
									Bad(5)
RH (21)	Left (16)	LIFG,MFG, LSTG	LArcF↑,LUF↑,LI LF↑	↑,↓,↑	↓,↑,↑	↑	↑	↓	
LH(11)	Right (9)	RIFG,RSMG,RSTG	RArcF↑,RUF↑	↑,↑	↑,↓	↑	↓	↓	
	Bilateral (7)	RIFG,LIFG,	RArcF↑	↑	↓	↑	↑		

Table 5: Correlation between fMRI, DTI and VBM parameters in control and TLE subjects. RH= Right Handed; LH=Left Handed; RIFG=Right inferior frontal gyrus, LIFG=Left inferior frontal gyrus, RMFG=Right middle frontal gyrus; LMFG = Left middle frontal gyrus; RSTG= Right superior temporal gyrus; LSTG= Left superior temporal gyrus; RSMA=Right supplementary motor area.

Chapter 5

DISCUSSION

The study utilized functional and structural neuroimaging techniques to examine the functional hemispheric language lateralization as well as the structural asymmetry of language white matter tracts in healthy controls and TLE patients. The major strength of this study is that it combined the two sophisticated non-invasive neuroimaging modalities such as fMRI, DTI and correlated the values obtained from these techniques with grey matter structural asymmetries of language function generated by using automated VBM technique.

A good agreement was found between these three methods, suggesting that the tractography and morphometry techniques could be used in a similar way to the fMRI for lateralization of language functions in human brain.

5.1 Functional hemispheric language lateralization in TLE by fMRI

In both controls and TLE subjects, the study investigated the relative effectiveness of four different commonly used clinical language fMRI paradigms in lateralizing language function in various brain regions containing language-eloquent cortex. The results of this study demonstrate that VG and SeT paradigms are the best among this group of paradigms for the lateralization of expressive and receptive language areas. Language fMRI paradigms described in this dissertation are typically dependent on frontal and temporal lobe language functions and these paradigms were custom designed and composed of a visual stimuli interpretation and motor task (pressing “response button”). Both components are nonexecutive and functionally unrelated. To ensure subject compliance, pre scanning training was given. In addition the paradigm was not randomized in order to ensure that the epilepsy patients were not fatigued during the performance of task.

The success rate indicated that sufficient subject compliance was achieved. During data analysis, significant between group difference in neural activity, and correlation between neural activity and stimuli was found. This study may represent an important contribution toward the standardization of paradigms for presurgical language mapping, which will be necessary for the promotion of the more widespread clinical utilization of BOLD fMRI beyond established academic centers.

The main language components involved in our VG task are both speech production and speech comprehension since the word is seen and verb needs to be produced and during the semantic task, the verb needs to be related to the noun. In TLE patients, a similar pattern of BOLD response activation was found that but less extensive networks compared to controls. Although some of LTLE patients (12%) in our sample retained left hemisphere dominance for language, it is possible that chronic epileptic activity in the left temporal lobe would lead to intra hemispheric reorganization in language function. In particular, this is expected to be reflected as variability in language activation away from the left temporal area, towards the left frontal area.

The research assessed whether there are any relative hemispheric differences lateralization of language functions in TLE patients with respect to controls. Although reorganization of language functions from left hemisphere to the right hemisphere has been reported frequently in LTLE patients during verbal fluency and semantic decision tasks, there was little evidence for altered language patterns in our TLE group. Only a tendency was seen for less left lateralized global activation in LTLE patients on the verbal fluency task. In our patient group, only epilepsy duration and handedness, not age at onset of seizures was found to relate to temporal lobe laterality during language tasks in LTLE patients, such that prolonged epilepsy duration was associated with less lateralized temporal lobe activation.

In addition mean signal intensity changes measures on verb generation and semantic decision tasks were correlated with the laterality scores in LTLE patients and not in RTLE. In line with the observed results, the performance of verb generation task and semantic decision tasks predominantly engaged in the language networks of dominant hemisphere in normal controls, primarily in the left IFG and STG. These findings confirm the good lateralizing capability of mentioned tasks for lateralizing expressive and receptive language in this particular cohort of patients.

In a similar study conducted by Binder et al., they found 100 % concordance in 22 cases for a semantic decision task and Carpentier et al., 2001 reported concordance between the fMRI LI scores and the Wada test in 8 of 10 patients using both auditory and visual stimulus presentation during language tasks. Both of these study used semantic decision paradigms similar to our group. Also Szaflarski et al.,2002 reported a high correlation ($r < 0.75$, $p < 0.001$) between the fMRI and the signal intensity changes for a semantic decision task using a global language region of interest including functional Broca's and Wernicke's areas. In spite of these findings, a variable agreement (from 63 %) was found in a study by Baciu et al., 2003; they used four different semantic tasks (category judgment, word stem completion, and semantic and phonological association).

We also tested the possibility of reorganization of language lateralization based on the laterality scores but the LI results revealed the absence of differences in laterality and the local changes might occur due to left temporal lobe pathology. An alternative explanation for clear absence of inter or intra hemispheric reorganization in LTLE patients relative to controls relates to high degree of variability in laterality scores in patients relative to controls.

The functional laterality index in our study was strictly based on positive fMRI activation in the anatomically predefined regions including both frontal and temporo parietal language areas. Thus it was biased towards positive activation only (language task vs visual

patterns) and did not take into account negative activation (visual patterns vs language task). However, several studies (Woermann et al., 2003, Benke et al., 2006) have shown that assessing functional laterality based on positive BOLD response provide accurate measurement of language lateralization as compared with wada test.

A conventional approach of ROI definition and examination was adopted in this study, in which anatomical ROIs defined in the standard MNI space were carefully chosen to label and encompass both the frontal and temporal language regions, taking into account the anatomical variability of language representation in these areas. This variability is particularly true for the parieto-temporal language area, the ROI of which consequently included areas in the temporal area that are also involved in the auditory language processing. These potentially false-positive regions are known to be left-hemispheric lateralized irrespective of language-related hemispheric lateralization (Hutsler and Galuske, 2003).

Using fMRI with VG and Set tasks, a differential involvement of right IFG and STG was noted between LTLE patients and healthy controls. For example, the right IFG is thought to be primarily concerned with semantic processing such as constructing context. The left IFG, although also important for semantic tasks, is additionally concerned with individual word processing not found in the right IFG. The right and left STG mainly involved in phonemic encoding of the heard word and production of a phonemic string. These findings recommend firstly that verbal fluency following left hemisphere damage does not rely on right hemisphere regions usually engaged by task, but involves recruitment of more posterior right IFG area. Secondly, the activation of right IFG in LTLE patients involved the anatomical regions distinct from those recruited in the left IFG. This shows that the right IFG regions involved in language processing following left temporal lobe pathology are not anatomical homologous of ILF language areas. Right IFG activation in healthy controls, likewise, was not anatomically homologous to left IFG activation.

The results of the present study provide evidence of major involvement of right IFG in the reorganization of language functions following left hemisphere injury. Similarly, a study by Thivard and colleagues (L.Thivard et al, 2005) found that LTLE patients with atypical language LIs had higher scores on neuropsychological measures than patients with normal LIs, suggesting that right hemisphere in these patients makes a positive contribution to language recovery following chronic left temporal lobe seizures. Another study by Thiel and co workers (A.Thiel et al, 2001) observed language related activation in right fronto lateral regions in their tumour patients , but found no difference in performance measures on the task between patients with dominant and patients with non–dominant hemispheric activations, which they interpreted to suggest that right frontal activation performs a compensatory role. Although most of the right frontal activations of our LTLE patients primarily involved in BA44 and BA45, some subjects showed frontal activations including anterior insula.

Group level statistical analysis results generated using SPM were examined for average activation differences between the three groups (explained in results section, **figure 43**).It was noted that highly variable individual factors such as seizure related processes may induce relative variations in the language function distribution at the individual level, which will not have appeared in the group level activation spm t maps, which detect only regions robustly activated across subjects. Brazdil et al, 2003 suggested a similar approach of complex highly individual mode of language organization and a significant variation in individuals in the anatomical targets of variability language functions.

The findings reported here support a broad spectrum of research studies suggesting that language is predominantly left lateralized. This is consistent with considerable previous observations (Loring et al., 1990) suggested that language function restricted to the right hemisphere is found in less than about 2% of the normal subjects. However, a small number

of left handed TLE groups (4) in our study shows bilateral or even right hemispheric dominant language representations. The lower degree of left hemisphere dominance in patients with left-TLE is reliable with the notion that there may be an adaptive compensation to the right hemisphere of relative language dominance with chronic disease affecting the left temporal lobe area. There are also two important factors in interpreting the function brain activations in our patients groups. The first is that it is hard to identify disease related changes in brain activation patterns in the presence of performance differences between the subject groups. Subjects performed each experimental language tasks silently during the scanning session and no measures were obtained at that phase. The behavioural parameters obtained prior to scanning session can only therefore offer an estimate of the numbers of words generated during the scanning sessions. The second and the most important factor is that in spite of suffering medically resistant seizures, most of the patients included in our studies were taking a variety antiepileptic drug. Dupont et al 2002, raised an important cofound of AED action to description for group differences when using healthy volunteers as a control group as certain AEDs affect not only cognitive performance but may also induce changes in observed HRF BOLD effects (H.Jokeit et al, 2001).

In this study the extent of fMRI activation the mesial temporal lobes induced by a task based on the retrieval of individual visuospatial knowledge was correlated with the serum carbamazepine level in 21 patients with refractory temporal lobe epilepsy .The finding suggested that carbamazepine level can significantly influence the amount of fMRI activation. The exact interaction between certain AEDs and the BOLD fMRI activation effects remains still unclear. However it is probable that their effects may have affected sensitivity to functional activation. It is possible that with larger patient population, it may be likely to verify factors important for language modifications, such as seizure duration or extent of left hemisphere structural damage. Our results are therefore, are consistent with the

emerging notion that the right IFG contributes to language processing following left hemisphere injury. Moreover the study established that functional reorganization of language network is highly dependent on the nature of the lesion and its chronicity, as well individual factors. The pattern of language activation in our patients suggested that compensatory functional mechanism of language to the right hemisphere might occur only in chronic disease states in which restoration of the normal left hemisphere network is not possible .Despite absence of evidence for this in our study, language related activation changes seen in the adult brain may also differ from those arising from injury early in development.

Overall, our results provide further confidence that fMRI measures of language lateralization may provide a practical and reliable alternative to invasive monitoring for presurgical language lateralization in patients with TLE. The present paradigms can be administered as part of a set of tasks, demonstrating that multiple functional activations can be mapped in a single fMRI session. The technique also offers distinct advantages. (a) Coregistered with high-resolution structural brain images, the activation maps provide neuroanatomically specific information regarding the localization of functional areas that can guide surgery directly. (b) They also provide quantitative information that eventually may provide a better estimate of relative risk of surgical procedures. (c) Further understanding of local connectivities may allow more refined measures based on relative lateralization in specific regions.

5.2 Functional hemispheric language lateralization in TLE by DTI and fibre tractography

The goal of the DTI study presented here was to track and visualize white matter pathways subserving experimentally dissociable aspects of language processing. The results of language lateralization that obtained from fMRI put together with findings obtained from

the tracking experiment to model a neurocognitively motivated framework of language interaction in phonological and semantic language processes.

First, we established that from a cognitive point of view, phonological language processing can be regarded as a generative system with that is to some degree independent from syntax and semantic processing. Then, the findings from the deterministic tracking experiment, showed a dual pathway system for fronto-parietal interaction (ArcF) and frontotemporal interaction (ILF) of phonological and semantic language processing This approach will be discussed within the framework of already existing neuroanatomical and neurocognitive models on language processing focusing on phonological issues, specifically Hickok and Poeppel (2004, 2007).But exemptions are found for orbito frontal fibers (UF) and occipito – temporal projection fibres (IFOF)

In the brain of control subjects, the mean FA and RFD of the language tracts, especially for dorsal network, were found to be dependent on tract size and tract volume Apart from MD, slightly more variations in the FA values were detected for major dorsal (ArcF) and ventral (ILF) pathway, suggesting that in control subjects, a strong degree of asymmetry was explicitly found for ArcF and ILF language pathways We noticed quantitative differences between right and left hemispheres , with overall tract volumes being significantly higher on the left than the right hemisphere Examination of these white matter tract volume as a function of commonality showed that the degree of lateralization was higher for left ArcF and ILF than UF and IFOF Moreover the mean FA of the estimated tracts was also significantly higher on the left than right. This data reflects that in this population, regional brain function indeed corresponds to higher structural connectivity. Our findings in control population supports the results of a study by parker et al, 2005, which has used tractography to investigate the lateralization of language pathways demonstrating stronger connection in the left hemisphere.

The study also measured RFD to compare the language tracts between the two hemispheres within the same individual. It is important to note that the calculated RFD is not an effort to count white matter fibers. It is only a ratio of reconstructed fibre pathways based on mathematically derived tensor directions. The RFD therefore simply reflects a theoretical representation of the structural density of anatomical connections. The RFD measurement may, however, be influenced by methodological problems that are inherent to fibre tractography. Regardless of these known limitations of DT tractography, we are able to noninvasively study the white matter pathways in the human brain in vivo only with this technique, rendering it a unique and invaluable tool in the field of neuroimaging research. The results of diffusion measurements showed that TLE group have considerable diffusion abnormalities in DTI parameters when compared to the control group (refer **Table 4**).

Tractography of language pathways demonstrated abnormalities in brain's connectivity network that are specific to TLE and MTS. We observed widespread abnormalities of white matter tracts within and beyond the temporal lobe were demonstrated in TLE with MTS patients, while non MTS TLE (dysplastic tumour cases) patients demonstrated fewer white matter abnormalities. These results suggest the disruption of brain networks in TLE patients with and without MTS, although the affected network was more extensive in MTS. Interestingly, in our group of subjects, TLE patients with right MTS showed more extensive bilateral changes than in TLE patients with left MTS, regardless of similar ages of onsets or seizure durations.

The RFD of white matter structural connections also varied depends on seizure type and handedness. This study showed more bilateral involvement of ArcF and unilateral involvement of ILF with significantly increased MD and decreased FA in both right and left TLE patients. Specifically, in the left TLE group, MD values in the entire left and right AF tract were comparable to controls; however FA values and RFD were elevated bilaterally.

The right TLE group demonstrated higher MD values and lower FA values in right and left ArcF and right ILF. The FA, MD and RFD of UF and IFOF were comparable to controls. From these observations, we confirmed that an increased MD and reduced FA of dorsal and ventral streams were found in MTS patients, in the zones of seizure foci. It also provided the evidence that the abnormal DTI parameters may be related to axonal pathway damage that are involved in ictal spread.

Alternatively, neuronal damage from seizures may lead to secondary white matter loss in connected cortical areas. It is possible, though those changes may not be obvious because of the small sample size. Both TLE groups were comparable in age at seizure onset and epilepsy duration. Indeed, both groups showed evidence of comparable patterns of DTI abnormalities in both ArcFs. However, as the number of seizure or seizure types was not prospectively investigated, it cannot be determined whether there is a correlation between degree of DTI abnormalities and severity of disease. Good correlations were found between DTI measures of major tracts (ArcF and ILF) and fMRI laterality scores suggesting that damage to these tracts strongly related to language dysfunction in TLE subjects. One similar study by S. Rodrigo et al., 2008 suggested that Right TLE patients with more left lateralized functional activations showed a leftward-lateralized ArcF than IFOF. The current study predicts that in LTLE patients, the atrophied left ArcF and ILF diffusivity related to reduced phonological and semantic language processing. In RTLE patients, no such correlations could not be demonstrated, which may be due to the limited sample size of RTLE subjects.

In the dominant hemisphere, a strong structure – function relationship was found between fMRI and DTI measures in majority of TLE subjects. Patients with more lateralized functional activation had also more highly lateralized DTI values. In LTLE, more symmetrical language activations were seen on fMRI, along with reduced left hemisphere and increased right hemisphere structural connections. This asymmetry was most remarkable

feature in the connectivity pattern from inferior frontal regions with more widespread connections to temporal lobe areas on the dominant hemisphere. Similarly when fibre tracking was initiated in the left temporal lobes, greater connectivity to inferior frontal regions was seen on the dominant hemisphere. The study also demonstrated that a significant correlation was between the structural lateralization of the white matter language tracts and left right differences in functional BOLD activation in both frontal and temporal lobes, with subjects with more lateralized language function, having predominantly more lateralized connectivity pattern. Our DTI findings demonstrated good agreement with similar studies conducted by H W R Powell et al, 2006 and Brandstack et al, 2013, in which they demonstrated an asymmetry in language connectivity patterns with greater connections between frontal and temporal on dominant hemisphere reflecting the lateralization of language functions.

In this study, linear regression analysis identified the areas where the mean FA of the language tracts correlated with voxel wise fMRI activity. Correlation in the left frontal and inferior parietal language area demonstrated during verb generation task and in the temporal area during semantic decision task. These areas of activations are found to be more widespread supporting the evidence of highly distributed networks involved in language function. Because language processing requires involvement of a distributed neural system in the dominant hemisphere the present finding of structural connectivity in the language areas of the dominant hemisphere provides a possible structural substrate for the functional asymmetry.

Agreement between lateralization from the fibre tractography results and the fMRI results was sought as a validation for the clinical utility of fMRI in TLE subjects. Here we found good agreement between the two methods, suggesting again that the DTI method could be used in a similar way to the fMRI for lateralization of brain functions especially in

children who fails to perform complex language tasks. The lack of perfect agreement is perhaps not surprising, may be due to the variability in our patient population .We also found that fMRI is more sensitive to activity in the less dominant hemisphere. More generally, the technique emphasises that language functions are complexly distributed, often through both hemispheres.

5.3 Functional hemispheric language lateralization in TLE by VBM

The goal behind using VBM analysis in the present study was to (a) confirm the volumetric data of grey matter structures, (b) explore other possible structural asymmetries in the brain that could relate to language lateralization. Our results about volume of PT and HG indicate that the relatively larger volume on the left sided compared to right amongst controls. In an MRI based study Pierre et al, 2006 found that the left HG was associated with larger white matter volume than the right HG. It was hypothesized that this grey matter asymmetry was related to more efficient processing of rapidly changing temporal information, which is relevant for speech. The volumetric results showed the asymmetries favouring the left hemisphere for both HG and PT of control subjects. The functional specialization of the left cerebral hemisphere for language functions in most of these individuals has received sufficient confirmation. There is also much neuroanatomical evidence suggesting that structural differences between the two hemispheres exist. Foundas et al, 1994 was among the first to attempt to relate the PT asymmetry directly to language lateralization, by means of IAT. While MR morphometry was used to measure the PT length, they found that when language is lateralized to left hemisphere, the left PT was longer than the right PT. Our measurement of PT volumetry supports these results and 82% of our control subjects showed higher PT volume in the language dominant hemisphere. Although it is well known that PT is larger in left hemisphere than right, little has been reported on HG in this regard. Musiek & Reeves, 1990 reported an asymmetrical length of HG (left>right) in normal

subjects in their postmortem study. Moreover it was found that PT was included in highly organized and interconnecting language system which includes dorsolateral prefrontal cortex and inferior parietal lobule.

Another grey matter structure we included in the present study was insula, which lies deep into the anterior sylvain fissure and functionally it is richly connected with language areas. Chee et al, 2004 reported in a functional neuroimaging study that amongst the regions showing language dependent increments in activation, the left insula showed greater activation in subjects with equal proficiency in both Chinese and English languages.

However the measured insular volumes in our control subjects were comparable on both sides. Only slight volume differences were observed in right handed subjects. More reliable with our obtained volumetric measures, the VBM results revealed interhemispheric differences favouring left hemisphere in grey matter concentration for right handed controls and favouring right hemisphere for left handed controls. Analysis of grey matter volume using optimized VBM correctly identified the regional atrophy of temporal grey matter structures in patients with TLE. Our automated VBM results confirmed the findings from the manual brain volumetric method previously described (Keller et al., 2002a). Our findings are also compatible with a number of earlier MRI-based volumetric and VBM studies in which grey matter concentration and volume in total (Hermann et al., 2003),) which was found to be reduced in TLE with MTS cases.

The gold standard for in vivo quantitative assessment of brain atrophy is manual delineation of selected grey matter structures. However, because of difficulty in defining accurate anatomical margins, labour intensiveness, and wide inter- and intrarater variability, ROI based morphometry method cannot provide comprehensive assessments of the entire brain, and results are difficult to replicate and compare between groups. So our results are not compared with ROI based manual volumetry. In this study, we also tested for any

intrahemispheric differences between right and left PT, HG and insula in TLE group. A small group (9%) of MTS cases had right speech representation, which can be due to an early injury to the left hemisphere that caused language functions to reorganize to the right hemisphere. Some of the earlier studies suggested modification of language lateralization in the case of early injury, the left sided injuries need to have happened before approximately at the age of five years old and quite large areas within primary speech zones need to have suffered the damage (Bracch et al, 1964). Studies on aphasic patients (Rasmussen and Milner, 1977) also showed that following left hemisphere damage, speech functions can reorganize to the right hemisphere. No significant intrahemispheric insular volume differences were found in MTS cases. We expected a relationship between insula asymmetry and functional lateralization but failed to be observed. Also it should be noted that VBM failed to detect any grey matter concentration differences for insula when compared against control subjects.

Together these findings suggest that VBM is sensitive to morphologically based differences between the two hemispheres. So far as the VBM findings, we conclude that intrahemispheric insular differences in both RTLE and LTLE do not relate directly to language lateralization. VBM in TLE has been limited to few studies (Keller et al., 2001; Woermann et al., 1999) and has shown conflicting results. In the first attempt, this technique was unable to identify any pathology (Woermann et al., 1999) when comparing TLE patients to healthy controls.

We correlated our VBM volume measurements with structural integrity of white matter language pathways. White matter abnormalities demonstrated with DTI and volumetry by means of VBM revealed significant correlation between reduced grey matter volume (PT & HG) and FA of ArcF and ILF in TLE patients. Moreover whole brain analysis of volumetric differences between TLE and controls subjects revealed significant reduction in total intracranial volume. This information can provide more reliable measure of language

lateralization in these subjects. Although MTS is observed in most TLE patients, some patients do not demonstrate evidence of significant correlation between reduced volumetry and FA, particularly for UF and IFOF. Some of our non-lesional TLE patients have subtle pathological features of MTS that could not be detected with VBM based analysis. Our finding of reduced FA –VBM correlations was in agreement with other two studies which reported abnormal grey matter volume differences in temporal lobe epilepsy (Concha et al., 2009). The percentage of FA reduction in the other group of TLE patients (6.9%) was not as large as that of patients with unilateral MTS (20%) reported by our study. As opposed to previous reports (Du et al., 2012), we did not observe volume difference of any subcortical gray matter in dysplastic tumour patient group which again may be explained by the relatively small sample size.

However the combined observations from our study demonstrated that white matter abnormalities in TLE and potential gray matter atrophy in temporal areas support the idea that DTI-VBM analysis plays a fundamental role in determining degree functional lateralization in TLE subjects. It was clearly understood from the study that morphological asymmetries of PT and HG may be predetermined and more resistant to change and the morphological asymmetry of the insula may be related to user-dependent factors. Therefore asymmetries in these two regions appear to bear a stronger relationship to language lateralization than the insula.

The present study has few limitations.

- a) Our findings relate to a relatively small sample of patients and require confirmation in larger group of patients.
- b) TLE patients and healthy controls did not much differ in age ($p > 0.1$), while controls had higher educational level than patients ($p < .001$). Even if we cannot exclude an

influence of this age factor on fMRI language tasks, education level did not have effects on frontal or temporal lobe activation in VG or SeT tasks.

- c) Looking for concordance of fMRI lateralization results with Wada test was not done. In our institution, the Wada test is only rarely performed in TLE patients for language lateralization because of a) invasiveness and b) the need for eloquent language area mapping which is better done using fMRI.
- d) The pre-surgical language lateralization findings obtained by the various imaging techniques were not correlated with post surgical language outcome measures.

CHAPTER 6

SUMMARY AND CONCLUSIONS

6.1 Major findings

- a) Mean functional laterality indices were significantly higher in right handed than left handed subjects.
- b) LTLE patients did not have a significantly altered intra or inter hemispheric distribution of language related activation patterns relative to controls or RTLE.
- c) BOLD HRF signal changes on VG and SeT tasks were correlated with fibre tract asymmetries significantly in controls and TLE subjects. Our study confirms that these tasks more generally, the expressive paradigms allow the determination of the overall hemispheric language lateralization, as well as lateralization within key regions known for their essential role in language processing, in brain of epilepsy patients.
- d) Language laterality scores was significantly correlated with relative fibre density (ArcF, ILF) and grey matter volumes of PT and HG in controls as well as in TLE subjects. No significant correlations were found for insular volume in both subject groups.
- e) The degree of structural abnormality correlated well with degree of functional abnormality in terms of fibre tract asymmetry indices and fMRI laterality indices.
- f) In the absence of fMRI language tasks, the presurgical lateralization of language function may be done using diffusion tractography & volumetry of specific cortical structures such as PT and HG.
- g) A strong degree of asymmetry was specifically found for major language tracts, ArcF (dorsal) and ILF (ventral). This data reflects that regional brain function indeed corresponds to higher structural connectivity.

- h) Even though no obvious changes in inter- or intrahemispheric laterality of language related activation were seen in TLE cases during any of the fMRI language paradigms the study provided evidence that, temporal lobe pathology in TLE patients was strongly related to subtle changes in the language connectivity network and corresponding volume changes in cortical grey matter structures.
- i) Tractography based statistics revealed leftward asymmetric clusters in the arcuate fasciculus and inferior longitudinal fasciculus were differentially related to activation asymmetries in these functional tasks. Frontal and temporal activation asymmetries during visual verb generation were positively related to the strength of specific microstructural white matter asymmetries in the arcuate fasciculus. In contrast, microstructural inferior longitudinal fasciculus asymmetries were related to temporal activation asymmetries during semantic and syntactic tasks.

6.2 Major implications of these findings

These findings suggest that white matter asymmetries may indeed be one of the factors underlying functional hemispheric asymmetries. Moreover, they also showed that specific localized white matter asymmetries might be of greater relevance for functional activation asymmetries than microstructural features of whole pathways.

The study also established that in TLE patients with atypical representations for language, the use of multiple language tasks increases the likelihood of accurate lateralization of the cerebral hemispheres for language functions.

In a clinical setting, the assessment of functional hemispheric language lateralization is an important part of the presurgical evaluation of patients with epilepsy in the proximity of the presumed location of language areas. As per the discussions, the major findings of the study strongly point out that functional right-sided language lateralization should not automatically be interpreted as an absence of language processing in the left hemisphere.

Even in cases of right-sided hemispheric language lateralization, careful consideration of the language white matter tracts should be taken during epilepsy surgery of the left hemisphere to reduce the risk of language deficits postoperatively.

This study confirms the importance of presurgical fMRI in predicting language outcome after ATL and highlights the clinical relevance of decreased language lateralization in LTLE. Decreased left lateralization seems to be an effective compensatory mechanism which protects language functions by moving them away from interictal and ictal epileptic activity before ATL, and protects from postsurgical naming deficits after surgery. The use of more than one fMRI task eliciting frontal as well as anterior temporal activations such as the VG and SeT tasks are strongly advised, when studying both LTLE and RTLE patients.

Pathways connecting BOLD-derived clusters were analyzed within specific cortical Areas: Broca's, with the pars triangularis, the pars opercularis, Geschwind's and Wernicke's area. The grey matter and white matter structural asymmetry reflects the degree of functional lateralization in different subjects.

In summary, the study has combined functional MRI experimental tasks deterministic tractography and VBM based volumetric approach to study the structure-function-anatomical correlates of relationship of language functions in normal healthy controls and TLE subjects.

6.3 Conclusion

Based on the observations, we concluded that there exist a strong one to one correlation between fMRI lateralization indices with grey matter volumes of specific areas and specific white matter structural connectivity measures for determining language lateralization. The dissertation demonstrated that the combination of these techniques can provide unique information which was not available with a single modality. Imaging the white matter tracts using diffusion based tractography and grey matter structural correlates can be combined with fMRI, using blood-oxygenated level dependent signal changes for

noninvasively exploring the in vivo structure–function relationship in the human brain. This information can be used in presurgical planning of language function TLE patients. The findings can help assist neurosurgeons in the surgical planning of intractable TLE patients who are at risk of developing postoperative language deficits.

6.4 Future directions

Unfortunately due to the time constraints, the study was conducted only in a small number of subjects but we achieved robust language related structural and functional activation results. For more refined assessment of language lateralization in epilepsy, we need to answer some questions in future research based on studies on larger population,

- a) While it has been shown in temporal lobe epilepsy patients that white matter alterations sub-serving language function can occur, it will be interesting to find whether the extent of abnormality is very extensive at the very beginning of the disease or gradually becomes widespread due to uncontrolled seizures later in the disease course?
- b) Do these white matter changes actually account for relative reorganization in language functions? In order to answer this, it is essential to compare the presurgical results with the post surgical outcomes.
- c) Determination of other structural and functional substrates of epilepsy patients can be studied by means of newer advanced imaging techniques like DSI (Diffusion Spectrum Imaging) ,HARDI (High Angular Resolution Diffusion Imaging),Resting state functional MRI and related functional connectivity studies.
- d) The advances in MRI techniques such as, a higher magnetic field strength (3T or 7T) and stronger diffusion gradients could generate more detailed structural and functional images to make possible the detection of minimal alterations in the brain of epilepsy patients.

- e) Finally it is essential to explore how these neuroimaging data & biomarkers can be compiled to make better predictors of surgical outcome and newer pharmaceutical targets that influences patient management.

Bibliography

Adcock, J.E., Wise, R.G., Oxbury, J.M., Oxbury, S.M. and Matthews, P.M., 2003. Quantitative fMRI assessment of the differences in lateralization of language-related brain activation in patients with temporal lobe epilepsy. *Neuroimage*, 18(2), pp.423-438.

Alexander, A.L., Lee, J.E., Lazar, M. and Field, A.S., 2007. Diffusion tensor imaging of the brain. *Neurotherapeutics*, 4(3), pp.316-329.

Anderson, A.W. and Gore, J.C., 1994. Analysis and correction of motion artifacts in diffusion weighted imaging. *Magnetic resonance in medicine*, 32(3), pp.379-387

Arfanakis, K., Haughton, V.M., Carew, J.D., Rogers, B.P., Dempsey, R.J. and Meyerand, M.E., 2002. Diffusion tensor MR imaging in diffuse axonal injury. *American Journal of Neuroradiology*, 23(5), pp.794-802.

Ashburner, J. and Friston, K.J., 2000. Voxel-based morphometry—the methods. *Neuroimage*, 11(6), pp.805-821.

Ashburner, J., Csernansk, J.G., Davatzikos, C., Fox, N.C., Frisoni, G.B. and Thompson, P.M., 2003. Computer-assisted imaging to assess brain structure in healthy and diseased brains. *The Lancet Neurology*, 2(2), pp.79-88.

Baciu, M., Le Bas, J.F., Segebarth, C. and Benabid, A.L., 2003. Presurgical fMRI evaluation of cerebral reorganization and motor deficit in patients with tumors and vascular malformations. *European journal of radiology*, 46(2), pp.139-146.

Baldo, J.V., Paulraj, S.R., Curran, B.C., Dronkers, N.F., 2015. Impaired reasoning and problem-solving in individuals with language impairment due to aphasia or language delay. *Front. Psychol.* 6. doi:10.3389/fpsyg.2015.01523.

Baldo, J.V., Paulraj, S.R., Curran, B.C., Dronkers, N.F., 2015. Impaired reasoning and problem-solving in individuals with language impairment due to aphasia or language delay. *Front. Psychol.* 6. doi:10.3389/fpsyg.2015.01523

Basser, P.J. and Jones, D.K., 2002. Diffusion-tensor MRI: theory, experimental design and data analysis—a technical review. *NMR in Biomedicine*, 15(7-8), pp.456-467.

Basser, P.J., Mattiello, J. and LeBihan, D., 1994. MR diffusion tensor spectroscopy and imaging. *Biophysical journal*, 66(1), p.259.

Beaulieu, C. and Allen, P.S., 1994. Determinants of anisotropic water diffusion in nerves. *Magnetic resonance in medicine*, 31(4), pp.394-400.

Beaulieu, C., 2002. The basis of anisotropic water diffusion in the nervous system—a technical review. *NMR in Biomedicine*, 15(7-8), pp.435-455.

Beaulieu, C., 2002. The basis of anisotropic water diffusion in the nervous system—a technical review. *NMR in Biomedicine*, 15(7-8), pp.435-455.

Behrens, T.E.J., Woolrich, M.W., Jenkinson, M., Johansen-Berg, H., Nunes, R.G., Clare, S., Matthews, P.M., Brady, J.M. and Smith, S.M., 2003. Characterization and propagation of uncertainty in diffusion-weighted MR imaging. *Magnetic resonance in medicine*, 50(5), pp.1077-1088.

Bell, M.L., Rao, S., So, E.L., Trenerry, M., Kazemi, N., Matt Stead, S., Cascino, G., Marsh, R., Meyer, F.B., Watson, R.E. and Giannini, C., 2009. Epilepsy surgery outcomes in temporal lobe epilepsy with a normal MRI. *Epilepsia*, 50(9), pp.2053-2060.

Benke, T., Köylü, B., Visani, P., Karner, E., Brenneis, C., Bartha, L., Trinkla, E., Trieb, T., Felber, S., Bauer, G. and Chemelli, A., 2006. Language lateralization in temporal lobe epilepsy: a comparison between fMRI and the Wada Test. *Epilepsia*, 47(8), pp.1308-1319.

Berg, A.T., Shinnar, S., Testa, F.M., Levy, S.R., Smith, S.N. and Beckerman, B., 2004. Mortality in childhood-onset epilepsy. *Archives of pediatrics & adolescent medicine*, 158(12), pp.1147-1152.

Berkovic, S.F., Andermann, F., Olivier, A., Ethier, R., Melanson, D., Robitaille, Y., Kuzniecky, R., Peters, T. and Feindel, W., 1991. Hippocampal sclerosis in temporal lobe epilepsy demonstrated by magnetic resonance imaging. *Annals of neurology*, 29(2), pp.175-182.

Bernasconi, N., Bernasconi, A., Caramanos, Z., Antel, S.B., Andermann, F. and Arnold, D.L., 2003. Mesial temporal damage in temporal lobe epilepsy: a volumetric MRI study of the hippocampus, amygdala and parahippocampal region. *Brain*, 126(2), pp.462-469.

Billingsley, R.L., McAndrews, M.P., Crawley, A.P. and Mikulis, D.J., 2001. Functional MRI of phonological and semantic processing in temporal lobe epilepsy. *Brain*, 124(6), pp.1218-1227.

Bizzi, A., 2009. Presurgical mapping of verbal language in brain tumors with functional MR imaging and MR tractography. *Neuroimaging Clinics of North America*, 19(4), pp.573-596.

Bonelli, S.B., Thompson, P.J., Yogarajah, M., Vollmar, C., Powell, R.H.W., Symms, M.R., McEvoy, A.W., Micallef, C., Koepp, M.J., Duncan, J.S., 2012. Imaging language networks before and after anterior temporal lobe resection: Results of a longitudinal fMRI study. *Epilepsia* 53, 639–650. doi:10.1111/j.1528-1167.2012.03433.x.

Bonelli, S.B., Thompson, P.J., Yogarajah, M., Vollmar, C., Powell, R.H.W., Symms, M.R., McEvoy, A.W., Micallef, C., Koepp, M.J., Duncan, J.S., 2012. Imaging language networks before and after anterior temporal lobe resection: Results of a

longitudinal fMRI study. *Epilepsia* 53, 639–650. doi:10.1111/j.1528-1167.2012.03433.x

Branch, C., Milner, B. and Rasmussen, T., 1964. Intracarotid Sodium Amytal for the Lateralization of Cerebral Speech Dominance: Observations in 123 Patients*. *Journal of neurosurgery*, 21(5), pp.399-405.

Brandstack, N., Kurki, T. and Tenovuo, O., 2013. Quantitative diffusion-tensor tractography of long association tracts in patients with traumatic brain injury without associated findings at routine MR imaging. *Radiology*, 267(1), pp.231-239.

Brázdil, M., Zákopčan, J., Kuba, R., Fanfrdlová, Z. and Rektor, I., 2003. Atypical hemispheric language dominance in left temporal lobe epilepsy as a result of the reorganization of language functions. *Epilepsy & Behavior*, 4(4), pp.414-419.

Briellmann, R.S., Newton, M.R., Wellard, R.M. and Jackson, G.D., 2001. Hippocampal sclerosis following brief generalized seizures in adulthood. *Neurology*, 57(2), pp.315-317.

Brown, R., 1828. XXVII. A brief account of microscopical observations made in the months of June, July and August 1827, on the particles contained in the pollen of plants; and on the general existence of active molecules in organic and inorganic bodies. *The Philosophical Magazine, or Annals of Chemistry, Mathematics, Astronomy, Natural History and General Science*, 4(21), pp.161-173.

Bruton, C.J., Stevens, J.R. and Frith, C.D., 1994. Epilepsy, psychosis, and schizophrenia Clinical and neuropathologic correlations. *Neurology*, 44(1), pp.34-34.

Büchel, C., Raedler, T., Sommer, M., Sach, M., Weiller, C. and Koch, M.A., 2004. White matter asymmetry in the human brain: a diffusion tensor MRI study. *Cerebral cortex*, 14(9), pp.945-951.

Burgerman, R.S., Sperling, M.R., French, J.A., Saykin, A.J. and O'Connor, M.J., 1995. Comparison of mesial versus neocortical onset temporal lobe seizures: neurodiagnostic findings and surgical outcome. *Epilepsia*, 36(7), pp.662-670.

Camfield, C.S., Camfield, P.R., Gordon, K., Wirrell, E. and Dooley, J.M., 1996. Incidence of epilepsy in childhood and adolescence: a population-based study in Nova Scotia from 1977 to 1985. *Epilepsia*, 37(1), pp.19-23.

Cao, Y. and Philp, J., 2006. Interactional context and willingness to communicate: A comparison of behavior in whole class, group and dyadic interaction. *System*, 34(4), pp.480-493.

Carpentier, A., Pugh, K.R., Westerveld, M., Studholme, C., Skrinjar, O., Thompson, J.L., Spencer, D.D. and Constable, R.T., 2001. Functional MRI of language processing: dependence on input modality and temporal lobe epilepsy. *Epilepsia*, 42(10), pp.1241-1254.

Carr, H.Y. and Purcell, E.M., 1954. Effects of diffusion on free precession in nuclear magnetic resonance experiments. *Physical review*, 94(3), p.630.

Catani, M., Allin, M.P., Husain, M., Pugliese, L., Mesulam, M.M., Murray, R.M. and Jones, D.K., 2007. Symmetries in human brain language pathways correlate with verbal recall. *Proceedings of the National Academy of Sciences*, 104(43), pp.17163-17168.

Catani, M., Howard, R.J., Pajevic, S. and Jones, D.K., 2002. Virtual in vivo interactive dissection of white matter fasciculi in the human brain. *Neuroimage*, 17(1), pp.77-94.

Chee, M.W.L., Zheng, H., Goh, J.O.S., Park, D. and Sutton, B.P., 2011. Brain structure in young and old East Asians and Westerners: comparisons of structural volume and cortical thickness. *Journal of Cognitive Neuroscience*, 23(5), pp.1065-1079.

Clusmann, H., Kral, T., Fackeldey, E., Blümcke, I., Helmstaedter, C., Von Oertzen, J., Urbach, H. and Schramm, J., 2004. Lesional mesial temporal lobe epilepsy and limited resections: prognostic factors and outcome. *Journal of Neurology, Neurosurgery & Psychiatry*, 75(11), pp.1589-1596.

Concha, L., Beaulieu, C., Collins, D.L. and Gross, D.W., 2009. White-matter diffusion abnormalities in temporal-lobe epilepsy with and without mesial temporal sclerosis. *Journal of Neurology, Neurosurgery & Psychiatry*, 80(3), pp.312-319.

Connelly, A., Jackson, G.D., Duncan, J.S., King, M.D. and Gadian, D.G., 1994. Magnetic resonance spectroscopy in temporal lobe epilepsy. *Neurology*, 44(8), pp.1411-1411.

Cooper, R., Winter, A.L., Crow, H.J. and Walter, W.G., 1965. Comparison of subcortical, cortical and scalp activity using chronically indwelling electrodes in man. *Electroencephalography and clinical neurophysiology*, 18(3), pp.217-228.

D'Esposito, M., Zarahn, E., Aguirre, G.K. and Rypma, B., 1999. The effect of normal aging on the coupling of neural activity to the bold hemodynamic response. *Neuroimage*, 10(1), pp.6-14.

Diehl, B., Busch, R.M., Duncan, J.S., Piao, Z., Tkach, J., Lüders, H.O., 2008. Abnormalities in diffusion tensor imaging of the uncinate fasciculus relate to reduced memory in temporal lobe epilepsy. *Epilepsia* 49, 1409–1418. doi:10.1111/j.1528-1167.2008.01596.x.

Diehl, B., Busch, R.M., Duncan, J.S., Piao, Z., Tkach, J., Lüders, H.O., 2008. Abnormalities in diffusion tensor imaging of the uncinate fasciculus relate to reduced memory in temporal lobe epilepsy. *Epilepsia* 49, 1409–1418. doi:10.1111/j.1528-1167.2008.01596.x.

Dodson, W.E., 2004. Definitions and classifications of epilepsy. *The treatment of epilepsy*, pp.3-20.

Dorsaint-Pierre, R., Penhune, V.B., Watkins, K.E., Neelin, P., Lerch, J.P., Bouffard, M. and Zatorre, R.J., 2006. Asymmetries of the planum temporale and Heschl's gyrus: relationship to language lateralization. *Brain*, 129(5), pp.1164-1176.

Dorsaint-Pierre, R., Penhune, V.B., Watkins, K.E., Neelin, P., Lerch, J.P., Bouffard, M. and Zatorre, R.J., 2006. Asymmetries of the planum temporale and Heschl's gyrus: relationship to language lateralization. *Brain*, 129(5), pp.1164-1176.

Dreifuss, S., Vingerhoets, F.J.G., Lazeyras, F., Andino, S.G., Spinelli, L., Delavelle, J. and Seeck, M., 2001. Volumetric measurements of subcortical nuclei in patients with temporal lobe epilepsy. *Neurology*, 57(9), pp.1636-1641.

Dronkers, N.F. and Larsen, J., 2001. Neuroanatomy of the classical syndromes of aphasia.

Du, M.Y., Wu, Q.Z., Yue, Q., Li, J., Liao, Y., Kuang, W.H., Huang, X.Q., Chan, R.C., Mechelli, A. and Gong, Q.Y., 2012. Voxelwise meta-analysis of gray matter reduction in major depressive disorder. *Progress in Neuro-Psychopharmacology and Biological Psychiatry*, 36(1), pp.11-16.

Duffau, H., 2008. The anatomo-functional connectivity of language revisited: new insights provided by electrostimulation and tractography. *Neuropsychologia*, 46(4), pp.927-934.

Duncan, J., 2009. The current status of neuroimaging for epilepsy. *Current opinion in neurology*, 22(2), pp.179-184.

Dupont, S., Tanguy, M.L., Clemenceau, S., Adam, C., Hazemann, P. and Baulac, M., 2006. Long-term Prognosis and Psychosocial Outcomes after Surgery for MTLE. *Epilepsia*, 47(12), pp.2115-2124.

Earle, K.M., Baldwin, M. and Penfield, W., 1953. Incisural sclerosis and temporal lobe seizures produced by hippocampal herniation at birth. *AMA Archives of Neurology & Psychiatry*, 69(1), pp.27-42.

Einstein, A., 1905. Does the inertia of a body depend upon its energy-content. *Annalen der Physik*, 18(13), pp.639-641.

Engel, J., 1996. Excitation and inhibition in epilepsy. *Canadian Journal of Neurological Sciences/Journal Canadien des Sciences Neurologiques*, 23(03), pp.167-174.

Engel, J., 2006. ILAE classification of epilepsy syndromes. *Epilepsy research*, 70, pp.5-10.

Eriksson, S., Malmgren, K., Rydenhag, B., Jönsson, L., Uvebrant, P. and Nordborg, C., 1999. Surgical treatment of epilepsy-clinical, radiological and histopathological findings in 139 children and adults. *Acta neurologica scandinavica*, 99(1), pp.8-15.

Eriksson, S., Rugg-Gunn, F.J., Symms, M.R., Barker, G.J. and Duncan, J.S., 2001. Diffusion tensor imaging in patients with epilepsy and malformations of cortical development. *Brain*, 124(3), pp.617-626.

Erlichman, M., 1989. Electroencephalographic (EEG) video monitoring. *Health technology assessment reports*, (4), pp.1-14.

Formisano, E. and Goebel, R., 2003. Tracking cognitive processes with functional MRI mental chronometry. *Current opinion in neurobiology*, 13(2), pp.174-181.

Forsgren, L., 2004. Epidemiology and prognosis of epilepsy and its treatment. *The treatment of epilepsy*, pp.21-42.

Foundas, A.L., Leonard, C.M., Gilmore, R., Fennell, E. and Heilman, K.M., 1994. Planum temporale asymmetry and language dominance. *Neuropsychologia*, 32(10), pp.1225-1231.

Foundas, A.L., Leonard, C.M., Gilmore, R.L., Fennell, E.B. and Heilman, K.M., 1996. Pars triangularis asymmetry and language dominance. *Proceedings of the National Academy of Sciences*, 93(2), pp.719-722.

Frahm, J., Merboldt, K.D. and Hänicke, W., 1988. Direct FLASH MR imaging of magnetic field inhomogeneities by gradient compensation. *Magnetic resonance in medicine*, 6(4), pp.474-480.

Friederici, A.D., 2002. Towards a neural basis of auditory sentence processing. *Trends in cognitive sciences*, 6(2), pp.78-84.

Fuerst, D., Shah, J., Kupsky, W.J., Johnson, R., Shah, A., Hayman–Abello, B., Ergh, T., Poore, Q., Canady, A. and Watson, C., 2001. Volumetric MRI, pathological, and neuropsychological progression in hippocampal sclerosis. *Neurology*, 57(2), pp.184-188.

Fuerst, D., Shah, J., Kupsky, W.J., Johnson, R., Shah, A., Hayman–Abello, B., Ergh, T., Poore, Q., Canady, A. and Watson, C., 2001. Volumetric MRI, pathological, and neuropsychological progression in hippocampal sclerosis. *Neurology*, 57(2), pp.184-188.

Gabr, M., Lüders, H., Dinner, D., Morris, H. and Wyllie, E., 1989. Speech manifestations in lateralization of temporal lobe seizures. *Annals of neurology*, 25(1), pp.82-87.

Gati, J.S., Menon, R.S., Uğurbil, K. and Rutt, B.K., 1997. Experimental determination of the BOLD field strength dependence in vessels and tissue. *Magnetic resonance in medicine*, 38(2), pp.296-302.

Geschwind, N. and Levitsky, W., 1968. Human brain: left-right asymmetries in temporal speech region. *Science*, 161(3837), pp.186-187.

Geschwind, N. and Levitsky, W., 1968. Human brain: left-right asymmetries in temporal speech region. *Science*, 161(3837), pp.186-187.

Geschwind, N. and Sherwin, I., 1967. Language-induced epilepsy. *Archives of Neurology*, 16(1), p.25.

Good, C.D., Johnsrude, I., Ashburner, J., Henson, R.N., Friston, K.J. and Frackowiak, R.S., 2001. Cerebral asymmetry and the effects of sex and handedness on brain structure: a voxel-based morphometric analysis of 465 normal adult human brains. *Neuroimage*, 14(3), pp.685-700.

Good, C.D., Johnsrude, I.S., Ashburner, J., Henson, R.N., Friston, K.J. and Frackowiak, R.S., 2002, June. A voxel-based morphometric study of ageing in 465 normal adult human brains. In *Biomedical Imaging, 2002. 5th IEEE EMBS International Summer School on* (pp. 16-pp). IEEE.

Govindan, R.M., Makki, M.I., Sundaram, S.K., Juhász, C. and Chugani, H.T., 2008. Diffusion tensor analysis of temporal and extra-temporal lobe tracts in temporal lobe epilepsy. *Epilepsy research*, 80(1), pp.30-41.

Hagberg, R.C., Safi, H.J., Sabik, J., Conte, J. and Block, J.E., 2004. Improved intraoperative management of anastomotic bleeding during aortic reconstruction: results of a randomized controlled trial. *The American Surgeon*, 70(4), p.307.

Hagmann, P., Cammoun, L., Martuzzi, R., Maeder, P., Clarke, S., Thiran, J.P. and Meuli, R., 2006. Hand preference and sex shape the architecture of language networks. *Human brain mapping*, 27(10), pp.828-835.

Hahn, E.L., 1950. Spin echoes. *Physical review*, 80(4), p.580.

Hamberger, M.J., Seidel, W.T., 2009. Localization of cortical dysfunction based on auditory and visual naming performance. *J. Int. Neuropsychol. Soc. JINS* 15, 529–535. doi:10.1017/S1355617709090754.

Hauser, W.A. and Lee, J.R., 2002. Do seizures beget seizures?. *Progress in brain research*, 135, pp.215-219.

Hauser, W.A., 1992. Seizure disorders: the changes with age. *Epilepsia*, 33(s4), pp.6-14.

Hermann, R., Knip, M., Veijola, R., Simell, O., Laine, A.P., Åkerblom, H.K., Groop, P.H., Forsblom, C., Pettersson-Fernholm, K., Ilonen, J. and FinnDiane Study Group, 2003. Temporal changes in the frequencies of HLA genotypes in patients with type 1 diabetes—indication of an increased environmental pressure?. *Diabetologia*, 46(3), pp.420-425.

Hetherington, H., Kuzniecky, R., Pan, J., Mason, G., Morawetz, R., Harris, C., Faught, E., Vaughan, T. and Pohost, G., 1995. Proton nuclear magnetic resonance spectroscopic imaging of human temporal lobe epilepsy at 4.1 T. *Annals of neurology*, 38(3), pp.396-404.

Hickok, G. and Poeppel, D., 2007. The cortical organization of speech processing. *Nature Reviews Neuroscience*, 8(5), pp.393-402.

Hickok, G., 2009. The functional neuroanatomy of language. *Physics of life reviews*, 6(3), pp.121-143.

Houser, C.R., 1990. Granule cell dispersion in the dentate gyrus of humans with temporal lobe epilepsy. *Brain research*, 535(2), pp.195-204.

Huettel, S.A., Song, A.W. and McCarthy, G., 2004. *Functional magnetic resonance imaging* (Vol. 1). Sunderland: Sinauer Associates.

Hutsler, J. and Galuske, R.A., 2003. Hemispheric asymmetries in cerebral cortical networks. *Trends in neurosciences*, 26(8), pp.429-435.

Jack Jr, C.R., Sharbrough, F.W., Twomey, C.K., Cascino, G.D., Hirschorn, K.A., Marsh, W.R., Zinsmeister, A.R. and Scheithauer, B., 1990. Temporal lobe seizures: lateralization with MR volume measurements of the hippocampal formation. *Radiology*, 175(2), pp.423-429.

Jackson, J.H., 1899. On certain relations of the cerebrum and cerebellum (on rigidity of hemiplegia and on paralysis agitans). *Brain*, 22(4), pp.621-630.

James, W., 1890. Origin of Right-handedness. *Science*, pp.275-275.

Jezzard, P. and Balaban, R.S., 1995. Correction for geometric distortion in echo planar images from B0 field variations. *Magnetic resonance in medicine*, 34(1), pp.65-73.

Johansen-Berg, H. and Behrens, T.E., 2006. Just pretty pictures? What diffusion tractography can add in clinical neuroscience. *Current opinion in neurology*, 19(4), p.379.

Jokeit, H., Okujava, M. and Woermann, F.G., 2001. Carbamazepine reduces memory induced activation of mesial temporal lobe structures: a pharmacological fMRI-study. *BMC neurology*, 1(1), p.1.

Kälviäinen, R. and Salmenperä, T., 2002. Do recurrent seizures cause neuronal damage? A series of studies with MRI volumetry in adults with partial epilepsy. *Progress in brain research*, 135, pp.279-295.

Keller, S.S. and Roberts, N., 2008. Voxel-based morphometry of temporal lobe epilepsy: An introduction and review of the literature. *Epilepsia*, 49(5), pp.741-757.

Keller, S.S., Wiesmann, U.C., Mackay, C.E., Denby, C.E., Webb, J. and Roberts, N., 2002. Voxel based morphometry of grey matter abnormalities in patients with

medically intractable temporal lobe epilepsy: effects of side of seizure onset and epilepsy duration. *Journal of Neurology, Neurosurgery & Psychiatry*, 73(6), pp.648-655.

Kesavadas, C., Thomas, B., Sujesh, S., Ashalata, R., Abraham, M., Gupta, A.K. and Radhakrishnan, K., 2007. Real-time functional MR imaging (fMRI) for presurgical evaluation of paediatric epilepsy. *Pediatric radiology*, 37(10), pp.964-974.

King, D., Bronen, R.A., Spencer, D.D. and Spencer, S.S., 1997. Topographic distribution of seizure onset and hippocampal atrophy: relationship between MRI and depth EEG. *Electroencephalography and clinical neurophysiology*, 103(6), pp.692-697.

Kovelman, I., Baker, S.A. and Petitto, L.A., 2008. Bilingual and monolingual brains compared: a functional magnetic resonance imaging investigation of syntactic processing and a possible “neural signature” of bilingualism. *Journal of cognitive neuroscience*, 20(1), pp.153-169.

Kwan, P. and Brodie, M.J., 2000. Early identification of refractory epilepsy. *New England Journal of Medicine*, 342(5), pp.314-319.

Labudda, K., Mertens, M., Janszky, J., Bien, C.G. and Woermann, F.G., 2012. Atypical language lateralisation associated with right fronto-temporal grey matter increases—a combined fMRI and VBM study in left-sided mesial temporal lobe epilepsy patients. *Neuroimage*, 59(1), pp.728-737.

Le Bihan, D. and Van Zijl, P., 2002. From the diffusion coefficient to the diffusion tensor. *NMR in Biomedicine*, 15(7-8), pp.431-434.

Le Bihan, D., Mangin, J.F., Poupon, C., Clark, C.A., Pappata, S., Molko, N. and Chabriat, H., 2001. Diffusion tensor imaging: concepts and applications. *Journal of magnetic resonance imaging*, 13(4), pp.534-546.

Loring, D.W., Meador, K.J., Lee, G.P., Murro, A.M., Smith, J.R., Flanigin, H.F., Gallagher, B.B. and King, D.W., 1990. Cerebral language lateralization: evidence from intracarotid amobarbital testing. *Neuropsychologia*, 28(8), pp.831-838.

Mabbott, D.J., Rovet, J., Noseworthy, M.D., Smith, M.L. and Rockel, C., 2009. The relations between white matter and declarative memory in older children and adolescents. *Brain research*, 1294, pp.80-90.

Mahdavi, A., Houshmand, S., Oghabian, M.A., Zarei, M., Mahdavi, A., Shoar, M.H. and Ghanaati, H., 2011. Developing optimized fMRI protocol for clinical use: comparison of different language paradigms. *Journal of Magnetic Resonance Imaging*, 34(2), pp.413-419.

Mansfield, P., 1982. *Nmr imaging in biomedicine: Supplement 2 advances in magnetic resonance* (Vol. 2). Elsevier.

Mathern, G.W., Adelson, P.D., Cahan, L.D. and Leite, J.P., 2002. Hippocampal neuron damage in human epilepsy: Meyer's hypothesis revisited. *Progress in brain research*, 135, pp.237-251.

McKhann, G.M., Schoenfeld-McNeill, J., Born, D.E., Haglund, M.M. and Ojemann, G.A., 2000. Intraoperative hippocampal electrocorticography to predict the extent of hippocampal resection in temporal lobe epilepsy surgery. *Journal of neurosurgery*, 93(1), pp.44-52.

Mechelli, A., Crinion, J.T., Noppeney, U., O'Doherty, J., Ashburner, J., Frackowiak, R.S. and Price, C.J., 2004. Neurolinguistics: structural plasticity in the bilingual brain. *Nature*, 431(7010), pp.757-757.

Mori, S. and van Zijl, P., 2002. Fiber tracking: principles and strategies—a technical review. *NMR in Biomedicine*, 15(7-8), pp.468-480.

Mori, S., Crain, B.J., Chacko, V.P. and Van Zijl, P., 1999. Three-dimensional tracking of axonal projections in the brain by magnetic resonance imaging. *Annals of neurology*, 45(2), pp.265-269.

Mori, S., Crain, B.J., Chacko, V.P. and Van Zijl, P., 1999. Three-dimensional tracking of axonal projections in the brain by magnetic resonance imaging. *Annals of neurology*, 45(2), pp.265-269.

Mori, S., Frederiksen, K., van Zijl, P., Stieltjes, B., Kraut, M.A., Solaiyappan, M. and Pomper, M.G., 2002. Brain white matter anatomy of tumor patients evaluated with diffusion tensor imaging. *Annals of neurology*, 51(3), pp.377-380.

Moseley, M.E., Cohen, Y., Mintorovitch, J., Chileuitt, L., Shimizu, H., Kucharczyk, J., Wendland, M.F. and Weinstein, P.R., 1990. Early detection of regional cerebral ischemia in cats: comparison of diffusion-and T2-weighted MRI and spectroscopy. *Magnetic resonance in medicine*, 14(2), pp.330-346.

Mosso, A., Ye Olde.1881. Neuroimaging.

Mueller, S.G., Laxer, K.D., Barakos, J., Cheong, I., Garcia, P. and Weiner, M.W., 2009. Widespread neocortical abnormalities in temporal lobe epilepsy with and without mesial sclerosis. *Neuroimage*, 46(2), pp.353-359.

Mueller, S.G., Laxer, K.D., Cashdollar, N., Buckley, S., Paul, C. and Weiner, M.W., 2006. Voxel-based Optimized Morphometry (VBM) of Gray and White Matter in Temporal Lobe Epilepsy (TLE) with and without Mesial Temporal Sclerosis. *Epilepsia*, 47(5), pp.900-907.

Musiek, F.E. and Reeves, A.G., 1990. Asymmetries of the auditory areas of the cerebrum. *J Am Acad Audiol*, 1(4), pp.240-245.

Muthusami, P., James, J., Thomas, B., Kapilamoorthy, T.R. and Kesavadas, C., 2014. Diffusion tensor imaging and tractography of the human language pathways: Moving into the clinical realm. *Journal of Magnetic Resonance Imaging*, 40(5), pp.1041-1053.

Neil, J.J., Shiran, S.I., McKinstry, R.C., Schefft, G.L., Snyder, A.Z., Almlie, C.R., Akbudak, E., Aronovitz, J.A., Miller, J.P., Lee, B.C. and Conturo, T.E., 1998. Normal brain in human newborns: apparent diffusion coefficient and diffusion anisotropy measured by using diffusion tensor MR imaging. *Radiology*, 209(1), pp.57-66

Nilsson, L., Farahmand, B.Y., Persson, P.G., Thiblin, I. and Tomson, T., 1999. Risk factors for sudden unexpected death in epilepsy: a case control study. *The Lancet*, 353(9156), pp.888-893.

Ojemann, G.A., 2003. The neurobiology of language and verbal memory: observations from awake neurosurgery. *Int. J. Psychophysiol., The Progress of Psychophysiology at the Beginning of the Twenty-First Century. 11th World Congress of Psychophysiology. The Olympics of the Brain. Celebrating the 20th Anniversary of the International Organization of Psychophysiology.* 48, 141–146. doi:10.1016/S0167-8760(03)00051-5.

Olney, J.W., de Gubareff, T. and Labruyere, J., 1983. Seizure-related brain damage induced by cholinergic agents.

Parker, G.J., Haroon, H.A. and Wheeler-Kingshott, C.A., 2003. A framework for a streamline-based probabilistic index of connectivity (PICO) using a structural interpretation of MRI diffusion measurements. *Journal of Magnetic Resonance Imaging*, 18(2), pp.242-254.

Parker, G.J., Luzzi, S., Alexander, D.C., Wheeler-Kingshott, C.A., Ciccarelli, O. and Ralph, M.A.L., 2005. Lateralization of ventral and dorsal auditory-language pathways in the human brain. *Neuroimage*, 24(3), pp.656-666.

Penfield, W. and Jasper, H., 1954. Epilepsy and the functional anatomy of the human brain.

Penfield, W., 1952. Ablation of abnormal cortex in cerebral palsy. *Journal of neurology, neurosurgery, and psychiatry*, 15(2), p.73.

Pierpaoli, C., Jezzard, P., Basser, P.J., Barnett, A. and Di Chiro, G., 1996. Diffusion tensor MR imaging of the human brain. *Radiology*, 201(3), pp.637-648.

Pillai, J. and Sperling, M.R., 2006. Interictal EEG and the diagnosis of epilepsy. *Epilepsia*, 47(s1), pp.14-22.

Poline, J.B., Worsley, K.J., Holmes, A.P., Frackowiak, R.S.J. and Friston, K.J., 1995. Estimating smoothness in statistical parametric maps: variability of p values. *Journal of computer assisted tomography*, 19(5), pp.788-796.

Powell, H.R., Parker, G.J., Alexander, D.C., Symms, M.R., Boulby, P.A., Wheeler-Kingshott, C.A., Barker, G.J., Koepp, M.J. and Duncan, J.S., 2007. Abnormalities of language networks in temporal lobe epilepsy. *Neuroimage*, 36(1), pp.209-221.

Powell, H.R., Parker, G.J., Alexander, D.C., Symms, M.R., Boulby, P.A., Wheeler-Kingshott, C.A., Barker, G.J., Noppeney, U., Koepp, M.J. and Duncan, J.S., 2006. Hemispheric asymmetries in language-related pathways: a combined functional MRI and tractography study. *Neuroimage*, 32(1), pp.388-399.

Price, C.J., 2010. The anatomy of language: a review of 100 fMRI studies published in 2009. *Annals of the New York Academy of Sciences*, 1191(1), pp.62-88.

Quesney, L.F., 1986. Clinical and EEG features of complex partial seizures of temporal lobe origin. *Epilepsia*, 27(s2), pp.S27-S45.

Radhakrishnan, A., James, J.S., Kesavadas, C., Thomas, B., Bahuleyan, B., Abraham, M. and Radhakrishnan, K., 2011. Utility of diffusion tensor imaging tractography in decision making for extratemporal resective epilepsy surgery. *Epilepsy research*, 97(1), pp.52-63.

Radhakrishnan, K., So, E.L., Silbert, P.L., Jack, C.R., Cascino, G.D., Sharbrough, F.W. and O'Brien, P.C., 1998. Predictors of outcome of anterior temporal lobectomy for intractable epilepsy A multivariate study. *Neurology*, 51(2), pp.465-471.

Rahman, M.M. and Talukder, A.H.I., 2008, November. A theoretical approach for familiarization with techniques of interleaved Echo-Planar imaging for Functional Magnetic Resonance Imaging and their features. In *Electrical Engineering, Computing Science and Automatic Control, 2008. CCE 2008. 5th International Conference on* (pp. 143-148). IEEE.

Raichle, M.E., 1987. Circulatory and metabolic correlates of brain function in normal humans. *Comprehensive Physiology*.

Raichle, M.E., Grubb, R.L., Gado, M.H., Eichling, J.O. and Ter-Pogossian, M.M., 1976. Correlation between regional cerebral blood flow and oxidative metabolism: in vivo studies in man. *Archives of Neurology*, 33(8), pp.523-526.

Rasmussen, T. and Milner, B., 1977. The role of early left-brain injury in determining lateralization of cerebral speech functions. *Annals of the New York Academy of Sciences*, 299(1), pp.355-369.

Richardson, F.M. and Price, C.J., 2009. Structural MRI studies of language function in the undamaged brain. *Brain Structure and Function*, 213(6), pp.511-523.

Richardson, M.P., Strange, B.A., Thompson, P.J., Baxendale, S.A., Duncan, J.S. and Dolan, R.J., 2004. Pre-operative verbal memory fMRI predicts post-operative memory decline after left temporal lobe resection. *Brain*, 127(11), pp.2419-2426.

Rodrigo, S., Oppenheim, C., Chassoux, F., Hodel, J., De Vanssay, A., Baudoin-Chial, S., Devaux, B. and Meder, J.F., 2008. Language lateralization in temporal lobe epilepsy using functional MRI and probabilistic tractography. *Epilepsia*, 49(8), pp.1367-1376.

Rodrigo, S., Oppenheim, C., Chassoux, F., Hodel, J., De Vanssay, A., Baudoin-Chial, S., Devaux, B. and Meder, J.F., 2008. Language lateralization in temporal lobe epilepsy using functional MRI and probabilistic tractography. *Epilepsia*, 49(8), pp.1367-1376.

Rojiani, A.M., Emery, J.A., Anderson, K.J. and Massey, J.K., 1996. Distribution of heterotopic neurons in normal hemispheric white matter: a morphometric analysis. *Journal of Neuropathology & Experimental Neurology*, 55(2), pp.178-183.

Rosazza, C., Ghielmetti, F., Minati, L., Vitali, P., Giovagnoli, A.R., Deleo, F., Didato, G., Parente, A., Marras, C., Bruzzone, M.G., D'Incerti, L., Spreafico, R., Villani, F., 2013. Preoperative language lateralization in temporal lobe epilepsy (TLE) predicts peri-ictal, pre- and post-operative language performance: An fMRI study. *NeuroImage Clin.* 3, 73–83. doi:10.1016/j.nicl.2013.07.001.

Rosenow, F. and Lüders, H., 2001. Presurgical evaluation of epilepsy. *Brain*, 124(9), pp.1683-1700.

Roy, C.S. and Sherrington, C.S., 1890. On the regulation of the blood-supply of the brain. *The Journal of physiology*, 11(1-2), p.85.

Sabsevitz, D.S., Swanson, S.J., Hammeke, T.A., Spanaki, M.V., Possing, E.T., Morris, G., Mueller, W.M. and Binder, J.R., 2003. Use of preoperative functional neuroimaging to predict language deficits from epilepsy surgery. *Neurology*, 60(11), pp.1788-1792.

Sandok, E.K., O'Brien, T.J., Jack, C.R. and So, E.L., 2000. Significance of cerebellar atrophy in intractable temporal lobe epilepsy: a quantitative MRI study. *Epilepsia*, 41(10), pp.1315-1320.

Schwarz, M., Pauli, E., 2009. Postoperative speech processing in temporal lobe epilepsy: functional relationship between object naming, semantics and phonology. *Epilepsy Behav.* EB 16, 629–633. doi:10.1016/j.yebeh.2009.09.016.

Scott, C.A., Fish, D.R., Smith, S.J.M., Free, S.L., Stevens, J.M., Thompson, P.J., Duncan, J.S., Shorvon, S.D. and Harkness, W.F.J., 1999. Presurgical evaluation of

patients with epilepsy and normal MRI: role of scalp video-EEG telemetry. *Journal of Neurology, Neurosurgery & Psychiatry*, 66(1), pp.69-71.

Smits, M., Visch-Brink, E., Schraa-Tam, C.K., Koudstaal, P.J. and van der Lugt, A., 2006. Functional MR Imaging of Language Processing: An Overview of Easy-to-Implement Paradigms for Patient Care and Clinical Research 1. *Radiographics*, 26(suppl_1), pp.S145-S158.

Sotak, C.H., 2002. The role of diffusion tensor imaging in the evaluation of ischemic brain injury—a review. *NMR in Biomedicine*, 15(7-8), pp.561-569.

Spencer, D.D., Spencer, S.S., Mattson, R.H., Williamson, P.D. and Novelly, R.A., 1984. Access to the posterior medial temporal lobe structures in the surgical treatment of temporal lobe epilepsy. *Neurosurgery*, 15(5), pp.667-671.

Springer, J.A., Binder, J.R., Hammeke, T.A., Swanson, S.J., Frost, J.A., Bellgowan, P.S., Brewer, C.C., Perry, H.M., Morris, G.L., Mueller, W.M., 1999. Language dominance in neurologically normal and epilepsy subjects: a functional MRI study. *Brain J. Neurol.* 122 (Pt 11), 2033–2046.

Stejskal, E.O. and Tanner, J.E., 1965. Spin diffusion measurements: spin echoes in the presence of a time-dependent field gradient. *The journal of chemical physics*, 42(1), pp.288-292.

Stippich, C., Rapps, N., Dreyhaupt, J., Durst, A., Kress, B., Nennig, E., Tronnier, V.M. and Sartor, K., 2007. Localizing and Lateralizing Language in Patients with Brain Tumors: Feasibility of Routine Preoperative Functional MR Imaging in 81 Consecutive Patients 1. *Radiology*, 243(3), pp.828-836.

Sumanaweera, T.S., Glover, G.H., Binford, T.O. and Adler, J.R., 1993. MR susceptibility misregistration correction. *Medical Imaging, IEEE Transactions on*, 12(2), pp.251-259.

Szaflarski, J.P., Binder, J.R., Possing, E.T., McKiernan, K.A., Ward, B.D. and Hammeke, T.A., 2002. Language lateralization in left-handed and ambidextrous people fMRI data. *Neurology*, 59(2), pp.238-244.

Tanner, J.E., 1970. Use of the stimulated echo in NMR diffusion studies. *The Journal of Chemical Physics*, 52(5), pp.2523-2526.

Tassi, L., Meroni, A., Deleo, F., Villani, F., Mai, R., Russo, G.L., Colombo, N., Avanzini, G., Falcone, C., Bramerio, M. and Citterio, A., 2009. Temporal lobe epilepsy: neuropathological and clinical correlations in 243 surgically treated patients. *Epileptic Disorders*, 11(4), pp.281-292.

Ter-Pogossian, M.M., Eichling, J.O., Davis, D.O. and Welch, M.J., 1970. The measure in vivo of regional cerebral oxygen utilization by means of oxyhemoglobin labeled with radioactive oxygen-15. *Journal of Clinical Investigation*, 49(2), p.381.

Thiel, A., Herholz, K., Koyuncu, A., Ghaemi, M., Kracht, L.W., Habedank, B. and Heiss, W.D., 2001. Plasticity of language networks in patients with brain tumors: a positron emission tomography activation study. *Annals of neurology*, 50(5), pp.620-629.

Thivard, L., Lehericy, S., Krainik, A., Adam, C., Dormont, D., Chiras, J., Baulac, M. and Dupont, S., 2005. Diffusion tensor imaging in medial temporal lobe epilepsy with hippocampal sclerosis. *Neuroimage*, 28(3), pp.682-690.

Tuch, D.S., Reese, T.G., Wiegell, M.R. and Wedeen, V.J., 2003. Diffusion MRI of complex neural architecture. *Neuron*, 40(5), pp.885-895.

Tuch, D.S., Reese, T.G., Wiegell, M.R., Makris, N., Belliveau, J.W. and Wedeen, V.J., 2002. High angular resolution diffusion imaging reveals intravoxel white matter fiber heterogeneity. *Magnetic Resonance in Medicine*, 48(4), pp.577-582.

Turner, R., Howseman, A., Rees, G.E., Josephs, O. and Friston, K., 1998. Functional magnetic resonance imaging of the human brain: data acquisition and analysis. *Experimental Brain Research*, 123(1-2), pp.5-12.

Turner, R., Jezzard, P., Wen, H., Kwong, K.K., Le Bihan, D., Zeffiro, T. and Balaban, R.S., 1993. Functional mapping of the human visual cortex at 4 and 1.5 tesla using deoxygenation contrast EPI. *Magnetic resonance in medicine*, 29(2), pp.277-279.

Van Paesschen, W., Connelly, A., King, M.D., Jackson, G.D. and Duncan, J.S., 1997. The spectrum of hippocampal sclerosis: a quantitative magnetic resonance imaging study. *Annals of neurology*, 41(1), pp.41-51.

Velíšek, L. and Moshe, S.L., 2003. Temporal lobe epileptogenesis and epilepsy in the developing brain: bridging the gap between the laboratory and the clinic. Progression, but in what direction?. *Epilepsia*, 44(s12), pp.51-59.

Veltman, D.J., Mechelli, A., Friston, K.J. and Price, C.J., 2002. The importance of distributed sampling in blocked functional magnetic resonance imaging designs. *Neuroimage*, 17(3), pp.1203-1206.

Vernooij, M.W., Smits, M., Wielopolski, P.A., Houston, G.C., Krestin, G.P. and van der Lugt, A., 2007. Fiber density asymmetry of the arcuate fasciculus in relation to functional hemispheric language lateralization in both right- and left-handed healthy subjects: a combined fMRI and DTI study. *Neuroimage*, 35(3), pp.1064-1076.

Von Oertzen, J., Urbach, H., Jungbluth, S., Kurthen, M., Reuber, M., Fernandez, G. and Elger, C.E., 2002. Standard magnetic resonance imaging is inadequate for patients with refractory focal epilepsy. *Journal of Neurology, Neurosurgery & Psychiatry*, 73(6), pp.643-647.

Wada, J. and Rasmussen, T., 1960. Intracarotid injection of sodium amytal for the lateralization of cerebral speech dominance: experimental and clinical observations. *Journal of Neurosurgery*, 17(2), pp.266-282.

Wada, J.A., Clarke, R. and Hamm, A., 1975. Cerebral hemispheric asymmetry in humans: Cortical speech zones in 100 adult and 100 infant brains. *Archives of Neurology*, 32(4), pp.239-246.

Waldvogel, D., van Gelderen, P., Muellbacher, W., Ziemann, U., Immisch, I. and Hallett, M., 2000. The relative metabolic demand of inhibition and excitation. *Nature*, 406(6799), pp.995-998.

Wesbey, G.E., Higgins, C.B., McNamara, M.T., Engelstad, B.L., Lipton, M.J., Sievers, R., Ehman, R.L., Lovin, J. and Brasch, R.C., 1984. Effect of gadolinium-DTPA on the magnetic relaxation times of normal and infarcted myocardium. *Radiology*, 153(1), pp.165-169.

Wiebe, S., Blume, W.T., Girvin, J.P. and Eliasziw, M., 2001. A randomized, controlled trial of surgery for temporal-lobe epilepsy. *New England Journal of Medicine*, 345(5), pp.311-318.

Wiebe, S., Blume, W.T., Girvin, J.P., Eliasziw, M., Effectiveness and Efficiency of Surgery for Temporal Lobe Epilepsy Study Group, 2001. A randomized, controlled trial of surgery for temporal-lobe epilepsy. *N. Engl. J. Med.* 345, 311–318. doi:10.1056/NEJM200108023450501.

Wieser, H.G., Ortega, M., Friedman, A. and Yonekawa, Y., 2003. Long-term seizure outcomes following amygdalohippocampectomy. *Journal of neurosurgery*, 98(4), pp.751-763.

Wieshmann, U.C., 2003. Clinical application of neuroimaging in epilepsy. *Journal of Neurology, Neurosurgery & Psychiatry*, 74(4), pp.466-470.

Wirestam, R., Greitz, D., Thomsen, C., Brockstedt, S., Olsson, M.B. and Ståhlberg, F., 1996. Theoretical and experimental evaluation of phase-dispersion effects caused by brain motion in diffusion and perfusion MR imaging. *Journal of Magnetic Resonance Imaging*, 6(2), pp.348-355.

Woermann, F.G., Jokeit, H., Luerding, R., Freitag, H., Schulz, R., Guertler, S., Okujava, M., Wolf, P., Tuxhorn, I. and Ebner, A., 2003. Language lateralization by Wada test and fMRI in 100 patients with epilepsy. *Neurology*, 61(5), pp.699-701.

Yasargil, M.G., Teddy, P.J. and Roth, P., 1985. Selective amygdalo-hippocampectomy operative anatomy and surgical technique. In *Advances and technical standards in neurosurgery* (pp. 93-123). Springer Vienna.

Yogarajah, M., Focke, N.K., Bonelli, S.B., Thompson, P., Vollmar, C., McEvoy, A.W., Alexander, D.C., Symms, M.R., Koepp, M.J. and Duncan, J.S., 2010. The structural plasticity of white matter networks following anterior temporal lobe resection. *Brain*, 133(8), pp.2348-2364.

Yoo, S.Y., Chang, K.H., Song, I.C., Han, M.H., Kwon, B.J., Lee, S.H., Yu, I.K. and Chun, C.K., 2002. Apparent diffusion coefficient value of the hippocampus in patients with hippocampal sclerosis and in healthy volunteers. *American journal of neuroradiology*, 23(5), pp.809-812.

LIST OF PUBLICATIONS

Journal Publications

James, Jija S., Sheela R. Kumari, Ruma Madhu Sreedharan, Bejoy Thomas, Ashalatha Radhkrishnan, and Chandrasekharan Kesavadas. “Analyzing Functional, Structural, and Anatomical Correlation of Hemispheric Language Lateralization in Healthy Subjects Using Functional MRI, Diffusion Tensor Imaging, and Voxel-Based Morphometry.” *Neurology India* 63, no. 1 (February 2015): 49–57. doi:10.4103/0028-3886.152634.

James, Jija S., Ashalatha Radhkrishnan, Bejoy Thomas, Mini Madhusoodanan, Chandrashekharan Kesavadas, Mathew Abraham, Ramshekhar Menon, Chaturbhuj Rathore, and George Vilanilam. “Diffusion Tensor Imaging Tractography of Meyer’s Loop in Planning Resective Surgery for Drug-Resistant Temporal Lobe Epilepsy.” *Epilepsy Research* 110 (February 2015): 95–104. doi:10.1016/j.eplesyres.2014.11.020.

James, Jija S., Pg Rajesh, Anuvitha Vs Chandran, and Chandrasekharan Kesavadas. “fMRI Paradigm Designing and Post-Processing Tools.” *The Indian Journal of Radiology & Imaging* 24, no. 1 (January 2014): 13–21. doi:10.4103/0971-3026.130686.

Sreedharan, Ruma Madhu, Amitha C. Menon, **Jija S. James**, Chandrasekharan Kesavadas, and Sanjeev V. Thomas. “Arcuate Fasciculus Laterality by Diffusion Tensor Imaging Correlates with Language Laterality by Functional MRI in Preadolescent Children.” *Neuroradiology* 57, no. 3 (March 2015): 291–97. doi:10.1007/s00234-014-1469-1.

Muthusami, Prakash, **Jija James**, Bejoy Thomas, T. R. Kapilamoorthy, and Chandrasekharan Kesavadas. “Diffusion Tensor Imaging and Tractography of the Human Language Pathways: Moving into the Clinical Realm.” *Journal of Magnetic*

Resonance Imaging: JMRI 40, no. 5 (November 2014): 1041–53. doi:10.1002/jmri.24528.

Radhakrishnan, Ashalatha, **Jija S. James**, Chandrasekharan Kesavadas, Bejoy Thomas, Biji Bahuleyan, Mathew Abraham, and Kurupath Radhakrishnan. “Utility of Diffusion Tensor Imaging Tractography in Decision Making for Extratemporal Resective Epilepsy Surgery.” *Epilepsy Research* 97, no. 1–2 (November 2011): 52–63. doi:10.1016/j.epilepsyres.2011.07.003.

Varghese, Tinu, R. Sheelakumari, **Jija S. James**, and Ps Mathuranath. “A Review of Neuroimaging Biomarkers of Alzheimer’s Disease.” *Neurology Asia* 18, no. 3 (2013): 239–48.

Book Chapter

James JS, Kesavadas C. Functional magnetic resonance imaging of language in patients with epilepsy. In: Kar BK, editor. *Cognition and brain development: Converging evidence from various methodologies*. 1st ed. Washington: American Psychological Association; 2013. p.289-310. ISBN:978-1-4338-1271-2

Conference Proceedings

Jija S James,Sheela Kumari et al,“Different volumetric analysis techniques based on structural Magnetic Resonance Imaging data to quantify whole or subcortical brain structures volume” ,**RSNA 2012**

Jija S James, Ruma Madhu Sreedharan et al,“Correlation between Functional Magnetic Resonance Imaging (fMRI) and Diffusion Tensor Imaging (DTI) Reveals Language Laterality in Temporal Lobe Epilepsy Patients Compared to Normal Volunteers” ,**RSNA 2012**

Ashish Gupta, N.Sivakumaran, Ashalatha R, C.Kesavadas,Sujesh S,Mini M, Anakha G, **Jija S James** et al, “Statistical Parametric Mapping of EEG correlated fMRI data

to detect Epileptic foci “, (**BSSI 2012**). In proceeding of: Biomedical Systems, Signals and Images

C.Kesavadas, **Jija S James** et al,“Functional and structural correlation of hemispheric language lateralization assessed by functional MRI (fMRI), Diffusion tensor imaging (DTI) and Voxel based Morphometry (VBM)”, **ISMRM 2013**